A STUDY ON THE PERFORMANCE OF A PORTABLE SINGLE-DUCT PROPANE AIR CONDITIONER AND WAYS OF REDUCING THE AMOUNT OF REFRIGERANT

A Thesis submitted by

Jeri Tangalajuk Siang

Master, Master Teknik (M.T)
Bachelor, Sarjana Teknik (S.T)

For the award of

Doctor of Philosophy

2021

ABSTRACT

The use of environmentally-friendly refrigerants is important for keeping the environment free from ozone-depleting substances and helping minimize global warming threats. Propane (R290) is one of the environmentally-friendly refrigerants. It is a flammable hydrocarbon gas without ozone depletion potential and its contribution to global warming is negligible. Many countries have developed a safety standard to regulate products that use flammable refrigerants.

There are many types of air conditioners to meet the increased demand for cooling, and one of these is the portable air conditioner. Portable air conditioners are designed to be moved wherever the system is needed and are compact system so all components are constructed in a single package located inside the conditioned room. There are two types of portable air conditioners: single-duct and double-ducts. A single-duct system utilizes the conditioned room air to absorb the condenser's heat and releases the heat to the outside of the room through the duct. A double-duct portable air conditioner has an extra duct to bring outside air to the condenser instead of utilizing air within the conditioned room. This study focuses on single-duct portable air conditioners.

This study was conducted with two aims in mind. First, to compare the performance of a single-duct portable air conditioner with the non-portable air conditioner. Second, to investigate ways of reducing the amount of refrigerant within a single-duct portable air conditioner. It is important to minimize the refrigerant within the air conditioner to increase safety due to the flammability of the refrigerant.

From the assessment of the effects of refrigerant charge and room temperature on the performance of a selected portable air conditioner, it was found that there are more similarities than differences between the two systems. Similar to non-portable air conditioners, an increase in room temperature increases: refrigerant temperature at the inlet of all main parts of the system, refrigerant mass flow rate, work done by the compressor, and maximum pressure. In other words, an increase in room temperature decreases the level of sub-cooling and coefficient of performance (COP). The main differences in the effect of increased room temperature are: a decrease in maximum refrigerant velocity of the portable air conditioner at the overcharge condition and a slight increase in the cooling capacity of the portable air conditioner. Similar to non-portable air conditioners, an increase in refrigerant charge increases: the refrigerant density at the outlet of the compressor, the level of sub-cooling, refrigerant mass flow rate, and work done by of the compressor. The main differences in the effect of an increase in refrigerant charge between portable and non-portable air conditioners are: an insignificant change in refrigerant temperature at the evaporator inlet for the portable air conditioner, and a decrease in refrigerant temperature at the evaporator inlet for non-portable air conditioners; a continuous increase in cooling capacity and COP for the portable air conditioner, and both cooling capacity and COP reach their maximum for non-portable air conditioners.

This study found a few ways to decrease the refrigerant charge in the system: using a capillary tube with a smaller diameter, reducing the coil diameter of the capillary tube, reducing evaporator pressure, and increasing condenser pressure. In this research it was also discovered that, integrating the capillary tube and liquid line and replacing them with a single capillary tube, decreases the refrigerant charge.

CERTIFICATION OF THESIS

This Thesis is the work of ***Jeri Tangalajuk Siang*** except where otherwise acknowledged. The work is original and has not previously been submitted for any other award, except where acknowledged.

Principal Supervisor: Dr Ahmad Sharifian-Barforoush

Associate Supervisor: Assoc Prof Andrew Wandel

Student and Supervisors signatures of endorsement are held at the University.

STATEMENT OF CONTRIBUTION

The majority of the authorship of the papers presented as a Thesis by Publication undertaken by ***Jeri Tangalajuk Siang***.

Principal Supervisor: Dr Ahmad Sharifian-Barforoush

Associate Supervisor: Assoc Prof Andrew Wandel

ACKNOWLEDGEMENTS

My academic journey at the University of Southern Queensland (USQ) has been a challenging but rewarding learning experience. I would like to express my sincere gratitude to a number of people for their guidance and assistance.

First, I am extremely grateful to my supervisors Dr. Ahmad Sharifian-Barforoush and Associate Professor Andrew Wandel who provided unparalleled help with patience and encouragement, continuously guiding me, and assisting me to reach my PhD goal. Without their invaluable discussion, suggestions, and assistance, it would have been impossible for me to complete the PhD program.

Thank you to Dr. Ahmad Sharifian-Borforoush who contributed to the published papers as a joint author. His support in each of the published papers in this Thesis is invaluable for me to produce the good research papers.

I would like to acknowledge the USQ English Language Center staff. They showed me how to use English in writing, speaking, and listening for the first time. Also, the USQ Library staff, who always helped by providing me with the books and articles which supported my research. I would also like to thank the technical and administrative support staff at USQ's Faculty of Health, Engineering and Sciences.

Thank you to Sandra Cochran for proofreading my thesis. Without her invaluable help, it would be impossible for me to write this Thesis in academic level of a Thesis.

Thank you to Indonesian Higher Degree Education which provided me with a scholarship. Without the scholarship, I would never have been able to go to Australia to do my PhD research. I would also like to thank Atma Jaya Makassar for its support during my PhD program.

Finally, my special gratitude goes to my family who was always beside me offering unconditional love: my wife Milka, my daughter Jesica and my son Fredly. My endless love goes to my father, my mother, and to my sisters (Nona and Tutti) for their life-long support.

LIST OF PUBLICATIONS

Journal papers

Siang, J.T. and Sharifian, A., 2017. Performance of a single-duct portable propane air conditioning system under different refrigerant charge levels. *Heat Transfer—Asian Research*, 46(8), pp.1246-1261.

Sharifian, A. and Siang, J.T., 2015. Impacts of room temperature on the performance of a portable propane air conditioner. *International Journal of Air-Conditioning and Refrigeration*, 23(02), p.1550015.

Conference papers

Siang, J.T. and Sharifian, A., 2018, August. Effect of inlet pressure, size and wind speed of an evaporator on amount of refrigerant charge and performance of a portable propane air conditioner. In *2018 4th International Conference on Science and Technology (ICST)* (pp. 1-6). IEEE.

Siang, J.T. and Sharifian, A., 2017. Extending the capillary tube of a propane air-conditioner to reduce the refrigerant charge. *Energy Procedia*, 110, pp.229-234.

Siang, J.T. and Sharifian, A., 2013. Reducing the mass of the refrigerant in the capillary tube of a propane air-conditioner. In *Proceedings of the 14th Asian Congress of Fluid Mechanics (14 ACFM)* (Vol. 2, pp. 850-857). Publishing House for Science and Technology.

Journal paper submitted

Siang, J.T. and Sharifian, A. Effects of inlet pressure on the performance and size of the condenser of a portable propane air-conditioner, *Journal of Thermal Science and Technology*

TABLE OF CONTENTS

LIST OF TABLES

LIST OF FIGURES

CHAPTER 1 INTRODUCTION

Global warming is the increase in the average temperature of the Earth's atmosphere. This increase is due to the rise in heat from the sun's radiation trapped in the Earth's atmosphere (Christina Nunez, 2019). The Earth's temperature is currently higher than in pre-industrial times (IPCC, 2018). In 2005, the average global temperature was 0.9ºC higher compared to the temperature in 1906 (National Geographic, 2020). Global warming is expected to cause extreme weather events, polar ice melting, rise in sea levels and ocean acidification, and profound and widespread effects on the Earth's ecosystems. Some effects have already been experienced. Sea level has risen 3.2 mm compared to its level in 1910 (Willis et al., 2018). In 2018, 3500 people in Alaska moved to another place due to coastal erosion, and 1200 people on Carteret Island (Papua New Guinea) moved to other places to live (West, 2019). Some regions and cities around the world, such as Southern Vietnam, Southern Thailand, Shanghai in China, and Mumbai in India, are expected to go underwater before 2050 (Lu and Flavelle, 2019). Another consequence of rising global temperature is the relocation of some animals. The penguin population in Antarctica has fallen by 90% or more since 1980s (Welch, 2018). Some animals such as Speyeria Atlantis butterflies and foxes that live in low temperature environments have moved to find new cooler places to live (Jakuboski, 2012; WWF, 2020).

The increase in heat trapped in the Earth's atmosphere is caused by the rise in gases in the atmosphere which have the ability to reflect the heat back to the Earth. These gases, known as greenhouse gases, form a blanket around the Earth's atmosphere (National Geographic, 2019). Greenhouse gases are important for living things on the Earth because, without them, the average temperature of the Earth's surface would be 18ºC (Ma and Tipping, 1998). Natural greenhouse gases are H_2O (water

vapour), CO_2 (carbon dioxide), CH_4 (methane), N_2O (nitrous oxide), and O_3 (ozone). Greenhouse gases come from activities such as industry and manufacturing, refrigeration and transportation. Some activities within these sectors produce non-natural greenhouse gases such as CFC, HCHC, HFC, halons, perfluorocarbons (PFCs), nitrogen trifluoride (NF_3) and sulphur hexafluoride (SF_6) (NOAA, 2020). An increase in the greenhouse gases in the atmosphere strengthens the insulation of solar radiation heat and increases the average temperature of the atmosphere.

Burning fossil and synthetic chemical gases for human needs also produces greenhouse gases. Carbon dioxide (CO_2) has the highest percentage of greenhouse gasses in the atmosphere. In 2017, the concentration of CO_2 was 405.5 ppm; an increase of 146% compared to the pre-industrial era. Methane is the second most important greenhouse gas (WMO, 2019), contributing to 17% of radiative forcing. Radiative forcing is the comparison of sun radiation entering the atmosphere with outgoing infra-red radiation (NOAA, 2020a). Atmospheric methane in the atmosphere is composed of 40% natural and 60% from human activities. The concentration of methane in 2018 was 1869 ppb which is an increase of 259% compared to the pre-industrial era.

Ozone depletion is a crucial negative impact of using synthetic refrigerants. The most negative impact of ozone depletion is the increase in UVB radiation reaching the Earth's surface (EPA, 2018; Wuebbles, 2020). Ozone depletion increases UVB radiation which also causes the development of cataracts, skin cancer and clouding of the eye's lens (EPA, 2018; Wuebbles, 2020). Ozone depletion is caused by chlorine and bromine. Chlorine and bromine are radicals released into the stratosphere in response to ultraviolet radiation, causing serious damage to ozone molecules. According to the US Environmental Protection Agency (EPA, 2018), one

atom of chlorine is able to break 100,000 ozone molecules. The increase in chlorine and bromide atoms in the stratosphere destroys the ozone molecules, and consequently the ozone layer thickness decreases. The Dobson unit is used to measure ozone layer thickness. One Dobson unit (DU) is 0.01 mm thickness of an ozone molecule at standard temperature and pressure (STP) (NASA, 2018). A Dobson unit contains 2.69×10^{16} ozone molecules per cm^2. The normal ozone layer is 300 DU. If the thickness of the ozone layer is less than 100 DU, scientists define it as an ozone hole. According to the measurement of ozone above the Antarctic by NASA, the thicknesses of ozone on 17 September 1979, 7 October 1989, 9 October 2006, and 1 October 2010 were 194 DU, 108 DU, 82 DU, and 118 DU, respectively.

Global warming and ozone depletion are two environmental issues directly related to air conditioning and the refrigeration sector (Department of Agriculture, Water and Environment, 2020). This is due to the leakage of refrigerant from the air conditioning system that has potential effects on global warming and ozone depletion (WHO, 2015).

CFCs are important man-made greenhouse gases that contribute to global warming. The CFC that is used as refrigerant is known as R_{12}. While its concentration in the atmosphere has decreased since the implementation of the Montreal Protocol in 1987, there has been an increase in the concentration of other refrigerants such as HCFCs and HFCs. The most common HCFC refrigerant, and still in use today, is $HCFC_{22}$ (R_{22}). As HCFCs are Class II Ozone Depletion Potential (ODP) (ODP less than 0.2), they were not the priority for phasing down. This refrigerant has a Global Warming Potential (GWP) of 1810. GWP is the potential of a substance to trap solar radiation energy in the atmosphere compared to CO_2. The HFC group of refrigerants

includes R_{32}, R_{134a}, R_{404A}, R_{407C} and R_{410A} with GWP of 677, 1300, 3922, 1774 and 2088, respectively (GHG Protocol, 2014).

Refrigerant CFCs are the worst ozone depleting gases. However, after the phasing out of refrigerant CFCs, the only group of ozone depleting refrigerant is HCFC. The existing HCFC refrigerant R_{22} has an ODP of 0.055. ODP is defined as the ability of a substance to destroy an ozone molecule compared to CFC_{11}.

The World Meteorological Organization (WMO) held the first world climate conference in February 1979, and in 1988, the WMO and the United Nations Environment Programme (UNEP) established the Intergovernmental Panel on Climate Change (IPCC). The IPCC works to evaluate climate science and bring climate science information to policy makers. The IPCC produces regular basic scientific assessments on climate change every few years and its reports are the key point of international climate change negotiation. The Kyoto Protocol is the United Nations Framework Convention on Climate Change (UNFCCC) and was established in 1992. UNFCCC works on the reduction of greenhouse gas emission. The reduction of six greenhouse gases is the focus of the Kyoto Protocol. These gases are carbon dioxide (CO_2), methane (CH_4), nitrous oxide (N_2O), hydrofluorocarbons (HFCs), perfluorocarbons (PFCs) and sulphur hexafluoride (SF_6). In 2015, the European Union legislated to control fluorinate gases (F-gases) that include HFCs. The legislation aims to limit the total amount of F-gases' sales by 2030, ban the use of F-gases in new equipment such as fridges and air conditioning, prevent F-gases' emission from existing equipment, and recover the gases at the end of equipment's life. Australia banned the import of HFCs in 2018 to implement the Montreal Protocol amendment in Kigali, Rwanda (held from 10 – 14 October 2016) (Australian Department of Agriculture, Water and the Environment, 2019). This

agreement includes the phase-down of 85% of HFCs in developed countries by 2036, and 80% by 2045 in most developing countries.

The Montreal Protocol was ratified to protect the ozone layer and has significantly reduced ozone depleting substances. In the refrigeration and air conditioning sectors, CFCs and HCFCs are the ozone depleting substances on the phase-down list. CFCs are now completely phased-out while HCFCs will be completely phased-out by 2040 (UNIDO, 2009).

The improved condition of the atmosphere and ozone layer is the basis of seeking alternative environmentally-friendly refrigerants. Environmentally-friendly refrigerants, such as ammonia, carbon dioxide and hydrocarbons, are naturally-occurring substances. Before the discovery of the negative impacts of synthetic refrigerants on the environment, synthetic refrigerants were chosen as working fluid as they are non-toxic, non-flammable and require moderate operating pressure (Pearson, 2003). After realising the negative impact of synthetic refrigerants on the environment, the use of natural refrigerant increased, and harmful synthetic refrigerants are no longer produced.

Carbon dioxide (R_{744}) is one of the natural alternative refrigerants which is non-ozone depleting and has low global warming potential compared to other refrigerants (Emani and Mandal, 2018). R_{744} is also a non-toxic and non-flammable refrigerant. However, the operating temperature of this R_{744} is high (Refprop, 2002). For air conditioning temperatures -5–40°C, R_{744}operates at 2–7 MPa (Dai et al., 2018). This disadvantage of R_{744} is that it increases the cost of the design. As the CO_2 operates at high pressure, the cost of electrical consumption also is a problem (Doiphode et al., 2019).

The next common natural refrigerant is ammonia (R_{717}). Ammonia's performance is excellent. It has good solubility in oil lubricants and is low priced (Emani and Mandal, 2018). Ammonia is also non-ozone depleting and has no global warming potential. However, it is flammable, is a toxic substance, and is not compatible with copper. When blood concentration exceeds the normal level, ammonia becomes toxic to the body, leading to seizure and coma (Hjelle, 2014; Padappayil and Borger, 2020). The disadvantages of ammonia make it unsuitable for commercial and domestic refrigeration and air conditioning systems.

Hydrocarbons are another alternative natural refrigerant. Hydrocarbons such as propane (R_{290}) and isobutene (R_{600a}) are environmentally-friendly. They are non-ozone depleting and have negligible global warming potential. Hydrocarbons are suitable for use in existing air conditioning systems without modification. R_{290} is a suitable replacement for R_{22} systems. The mixture of R_{290} – R_{600a} is compatible with R_{12} systems (Zhou et al., 2019; Emani and Mandal, 2018). Hydrocarbons also have good performance compared to the old synthetic refrigerants. Compared to the existing R_{22} refrigeration system, R_{290} systems have better COP but less cooling capacity (Liu at al., 2018). Besides the higher COP, the discharge compressor temperature of R_{290} is lower than R_{22} (El-Sayed et al., 2018).

Propane has similar thermodynamic properties to those of R_{22}. It could be retrofitted into a R_{22} system. Compared to R_{22}, R_{290} has a larger liquid molar volume (Macline-cross and Leonardi, 1997). The advantages of larger liquid molar volume are higher COP and lower refrigerant leakage (Macline-cross and Leonardi, 1996).

There are some drawbacks to propane as it is classified as a flammable refrigerant (Storslett, 2018). Propane now is popular in small air conditioning systems, but it is

risky to use in big air conditioning systems. For maintenance, propane air conditioning systems need specific expertise as they must be free from leakage.

R_{290} has been used as a refrigerant in split air conditioning systems, window air conditioning systems, chillers, and portable air conditioning systems. There is no difficulty in applying R_{290} as its thermodynamic properties are similar to those of the old synthetic refrigerants. However, it is important to minimize the R_{290} mass in the air conditioning system to reduce its flammability risk. For chillers, it is less dangerous when R_{290} is applied because refrigerant circulation is located outside the conditioned room while the circulating fluid in the room is cooled by water. Portable propane air conditioning systems are small and have to be leak-proof systems. The pipe joints of the portable pipe air conditioning system are welded.

There is a key difference between the working condition of a non-portable and portable air conditioning system. Split type air conditioning systems consist of two units, indoor and outdoor units. A portable air conditioning system is a compact unit located in the conditioned room. There are two types of portable air conditioning systems. The first one includes two ducts which use outdoor air as a heat sink and as heat deliverance. Outdoor air enters the first duct and flows over the condenser and discharges the hot air through the second duct to the outside. The second type of portable air conditioner system is coupled with a single condenser air duct. In this type, the air within the conditioned room flows directly over the condenser and then is discharged outside through the single-duct. Therefore, the temperature of the inlet air over the condenser is similar to the conditioned room temperature. There is limited research on the portable air-conditioner.

1.1 Update on recent legislation

Most countries have relaxed legislation regarding maximum air conditioner hydrocarbon refrigerant charge, or continue to impose the older limit of 150 grams

Globally, the International Electrotechnical Commission (IEC) increased the limit of hydrocarbon charge from 150g to 500g in 2019 which has been applied in European countries (Hydrocarbon 21, 2020). In Australia and New Zealand, the new standard (AS/NZS 60335.2.89:2020) is an "identical adoption" of IEC 60335-2-89, Edition 3.0, that increased the limit of 150g propane charge to 500g. This standard supersedes the early version of 2010 (Accelerate, 2020). UL is an accredited standards developer in the US and Canada. Since 2011, Canada's UL Standard for Refrigerating Units has specified a charge limit of 300 grams (UL Laboratories, 2017). In the USA, the limit of hydrocarbon charge is still 150g based on an EPA decision in 2011 (Cooling Post, 2020)

1.2 Update on recent studies

There have been many new studies into different types of non-portable air conditioners that support the similarities and differences between portable and non-portable air-conditioners reported in this work. The most notable studies are the work of Shen and Fricke (2020) and Devecioglu et al. (2017) on window type and split-type air conditioners, respectively. These report that the increase in room temperature decreases COP. Hu et al., (2018) also found that an increase in charge increases sub-cooling for cold storage refrigeration systems. Tanaka et al. (2018) found that the increase in room temperature decreases the COP. These results are all in line with previous studies on non-portable air conditioners and the results reported in this work for portable air-conditioners.

There are a few recent studies that consider dissimilarities between portable and non-portable air conditioners reported in the present study. Jawale et al., 2018 found that an increase in room temperature decreases the compressor work of window-type air conditioners. Saravanan et al. (2019) and Deymi-Dashtebayaz et al. (2018) found that cooling capacity and COP have maximum values when refrigerant charge increases for split type air conditioners.

The only study that is inconsistent with previous outcomes for non-portable air conditioners is a study by Tanaka et al. (2018) on a split-type air conditioner. They found that an increase in the temperature of air flows over the evaporator decreases the mass flow rate of the refrigerant. Such a performance is similar to that reported in this work for portable air-conditioners but is inconsistent with previous studies on non-portable air conditioners.

The only recent study on portable air conditioners was carried by Yoon et al (2019) and is outside the scope of this study. They studied the effect of spraying the condensate water from the evaporator on the condenser. They found this decreases the temperature of the condenser and power consumption and increases cooling capacity.

1.3 Aim and objective of studies

Contrary to existing air conditioning systems that utilize outdoor air to absorb heat from the condenser, the single-duct portable air conditioning system utilizes indoor air. The effect of such a difference is unknown thus, the present research aims to fill the research gap and analyse its performance and compare it with common types of air conditioning systems. As propane is a flammable refrigerant, it is also imperative to study ways of reducing the refrigerant charge within the system.

This study was divided into six research works as follows:

1. The first aim was to reduce the refrigerant in the capillary tube without sacrificing the performance of the air conditioning system. The outcomes of the work were presented in the paper entitled “Reducing the mass of refrigerant in the capillary tube of a propane air conditioner”. The research gap of this work is the effect of the coil diameter of the capillary tube on the propane mass within the helical capillary tube of an air conditioner. The objective of the paper was to calculate the refrigerant for different diameters of capillary tubes using MATLAB script. The shape of the capillary tube was straight and coiled with different coil diameters
2. The next aim of the work was to find a way to reduce the mass of the refrigerant within the air conditioning system by extending the capillary tube to replace the existing capillary tube and liquid line. In a portable propane air conditioning system, the distance between the outlet of the condenser and the inlet of the evaporator is unchanged. The capillary tube and liquid line are located in this area. The length of the extending capillary tube is equal to the total length of existing capillary tube and liquid line. The outlet refrigerant condition of the condenser and the inlet refrigerant condition of the evaporator were the criterions to calculate the diameter of the extending capillary tube. This work was in the paper entitle “Extending the capillary tube of the propane air conditioner to reduce the refrigerant charge”. This research focuses to fill the research gap of the effect of replacing the liquid line and existing capillary tube with a single capillary tube on the refrigerant mass of the air conditioner. The objectives of the paper were to calculate the mass within the existing capillary tube and liquid

line, calculating the mass within the new single capillary tube and comparing it with the refrigerant mass within the existing capillary tube and liquid line. Calculations were carried out with developing a MATLAB script

3. The next aim was to analyse the refrigerant charge and cooling capacity of a single-duct portable propane air conditioning system by modifying the inlet pressure of the evaporator, resizing the evaporator pipe, and varying the air speed over the evaporator. The relevant paper is entitled “Effect of inlet pressure, size and wind speed of an evaporator on amount of refrigerant charge and performance of a portable propane air conditioner”. The inlet pressure of the evaporator, the size of the evaporator and wind speed over the evaporator affected the amount of refrigerant within the evaporator and the performance of standard air conditioners. The inlet pressure of the evaporator of an air conditioner affects the evaporator temperature and refrigerant properties. This research focuses to fill the research gap of the effect of variation of evaporator inlet pressure variation, size of the evaporator, and airspeed over the evaporator of a portable propane air conditioner on the refrigerant mass and performance of the air conditioner. This paper had three objectives. The first objective was to determine the cooling capacity, refrigerant mass, and specific heat transfer rate of the evaporator as the inlet pressure of the evaporator changes. The next objective was to assess the effects of resizing the evaporator pipe and calculate the cooling capacity, refrigerant mass, and specific heat transfer rate. The last objective was to analyse the effect of wind speed over the evaporator on refrigerant mass, heat transfer rate and specific heat transfer rate. A MATLAB script was developed to carry out the calculation

4. The next work aimed to assess and quantify the effect of increasing inlet pressure on the capacity of the condenser and on required mass of refrigerant within the condenser of a single-duct portable air-conditioner. This was discussed in the paper entitled “Effect of inlet pressure on the performance and size of the condenser of the portable propane air-conditioner”. The inlet pressure of the condenser influences the performance, size and amount of refrigerant in the condenser of standard air conditioners. A different condenser inlet pressure results in a different condenser temperature, different refrigerant properties and a different amount of heat transferred from the condenser. This research focuses on filling the research gap of the effect of variation of inlet pressure of the condenser on the performance and size of the portable propane air conditioner. The objective of this paper was to evaluate and compare condenser capacity at standard size to the condensers with shortened pipes. A MATLAB script was developed to assess the performance of the air conditioner of a standard and modified condenser. Heat transfer, density of refrigerant, refrigerant mass in the condenser and the specific capacity of the condenser and evaporator were obtained with MATLAB calculation
5. The aim of the next work was to analyse the performance of a portable propane air conditioner with variation of room temperature. This aim was discussed in the paper entitled “Impacts of room temperature on the performance of a portable propane air conditioner”. The variation in room temperature sets the temperature difference between the evaporator and room temperature changes; and also changes the condenser and room temperature difference. The effect of room temperature variation was

expected to have a major effect on the air conditioner's performance. This research focuses on filling the research gap of the effect of variation of room temperature on the performance of the portable propane air conditioner. The objective of this research was to analyse the effect of room temperature variation on refrigerant temperature, refrigerant density, cooling capacity, COP, maximum velocity, specific cooling capacity, useful work of the compressor and maximum pressure

6. The experimental research aimed to compare the performance of a single-duct portable propane air conditioning system with non-portable air conditioning system. The experimental result was discussed in the paper entitled "Performance of a single-duct portable propane air conditioning system under different charge levels". The effects of mass of refrigerant on the performance of the air conditioning system had been studied previously. However, there was a research gap on the single-duct portable propane air conditioning system. This research focuses on filling the research gap on the effect of variation of refrigerant charge on the performance of the portable propane air conditioner. The objective of the paper was to analyse the effect of refrigerant charge level on refrigerant temperature, refrigerant density, cooling capacity, useful work of the condenser, COP, maximum velocity, specific cooling capacity, and maximum pressure.

1.4 Summary

Global warming and ozone depletion are two environmental problems which are related to air conditioning systems. Global warming has a negative impact on living things, such as inappropriate conditions of life due to an increase in global

temperature. Ozone depletion causes much solar radiation reaching the Earth's atmosphere and affecting the health of living things. In the air conditioning sector, CFCs, HCFCs and HFCs are the refrigerants with the potential to increase global warming and ozone depletion. CFCs have been completely phased out, HCFCs and HFCs are in process of being phased-down to avoid worsening global warming and ozone depletion. Avoiding the use of CFCs and HCFCs, and to controlling the use of HFCs is supported by legislation around the world.

As the use of hazardous synthetic refrigerant is controlled, the use of alternative environmentally-friendly refrigerant substitutes is a must. Natural refrigerants such as CO_2, NH_3 and HCs are good candidates for replacing old hazardous refrigerants. Natural refrigerants are environmentally-friendly refrigerants as they are non-ozone depleting and possess negligible global warming potential. As CO_2 and NH_3 are expensive to implement, HCs are the best potential future alternative refrigerant. The properties of HCs are similar to those of synthetic refrigerants. The only drawback of HCs is their flammability. One HC refrigerant is propane which is now familiar in small air conditioning systems. One of the small air conditioning systems is the portable air conditioning system. There are two types of portable air conditioning systems: single- and double-duct portable air conditioning systems. Research on portable air conditioning systems is limited.

The aims of the present research were to develop a better understanding of single-duct portable propane air conditioners, analyse their performance, compare their performance with the common type of the air conditioner, and study possible ways to reduce the mass of refrigerant in the system.

The following chapters present six research studies. Four chapters contain the computational work: three conference papers and one journal article. The experimental work is published in journal articles. The writer is the first and corresponding author for all publications except for the journal article in Chapter 6 where he is the second and corresponding author.

The main parts of the thesis begin with minimizing the refrigerant charge within the air conditioning system in Chapters 2 – 5. These chapters are followed by the experimental work on the effect of room temperature and refrigerant charge on the performance of the portable air conditioning system and its comparison to the non-portable air conditioning system in Chapters 6 and 7. Chapter 2 contains the model of the capillary tube; focussing on obtaining a minimum charge within the capillary tube without changing the refrigerant inlet and outlet conditions of capillary tube. Another method of reducing the refrigerant charge where the capillary tube is involved, is to replace the existing capillary tube and liquid line with an extended capillary tube. The length of the extended capillary tube is equal to the existing capillary tube combined with the length of the liquid line. The next technique is to reduce the refrigerant within the air conditioning system is to modify the evaporator condition which is discussed in Chapter 4. Modification of the evaporator condition includes inlet pressure and air speed over the evaporator to find the reduction of refrigerant charge within the evaporator. Another possible way to reduce the refrigerant charge within the air conditioner is to modify the condition of the condenser which is discussed in Chapter 5. Room temperature and the amount of refrigerant charge are two important variables that affect the performance of the air conditioning system. It is important to understand the performance of the portable air conditioning system under the room temperature and refrigerant charge. Chapters 6

and 7 contain the experiment study to analyse the performance of the portable air conditioner and comparison with common air conditioning systems. Chapter 6 discusses the effect of room temperature on the performance of the portable air conditioner. Chapter 7 discusses the effect of variation of refrigerant charge on the performance of the portable air conditioning system.

CHAPTER 2 REDUCING THE MASS OF REFRIGERANT IN THE CAPILLARY TUBE OF A PROPANE AIR CONDITIONER

Minimizing the refrigerant charge is possible by modifying the size and condition of the main parts of the air conditioning system such as capillary tube, evaporator and the condenser. The capillary tube contains a small amount of refrigerant charge as the size of the capillary tube is small. The shape and diameter of the capillary tube determines the refrigerant mass within it. This chapter provides the computational study for reducing the refrigerant charge within the capillary tube. The way to change the refrigerant mass within the capillary tube is to change the diameter of the capillary tube and change the shape of the capillary tube from straight to coiled. The main part of this Chapter was published in Proceedings of the 14th Asian Congress of Fluid Mechanics (14 ACFM), October 15 – 19 2013, Hanoi-Halong Vietnam.

2.1 Introduction

The use of synthetic materials, which are found to be detrimental to the environment, is being avoided. Most industrial sectors have begun to set up targets to reduce the use of synthetic materials. In the refrigeration and air-conditioning sector, the use of hazardous synthetic refrigerant has begun to be reduced and they are currently in the process of being phased out. Two most prominent examples of synthetic refrigerants are R_{12} and R_{22} which are very effective in the process of absorption and release of heat; however, they have very significant impacts on the destruction of the ozone layer, which leads to the global warming. In order to replace harmful synthetic refrigerants, many researchers have been looking for less harmful alternatives. It was found that some natural materials, such as hydrocarbons, are capable of being used

as refrigerant and they have only a negligible impact on the global warming (Park and Jung, 2007). One drawback of hydrocarbons is their inherent flammability. For this reason, the mass of hydrocarbons in all components of air-conditioning and refrigeration systems, such as in the capillary tube should be minimized to reduce the associated risks.

In recent years, many research works have been conducted on the characteristics of the flow in the capillary tube, both experimentally and theoretically. The relationship between the length and diameter of straight capillary tubes, and the stability and pressure fluctuations of the refrigerant at the inlet was evaluated by Zhou and Zhang (2010). They found that the stability of the fluid pressure in parallel joint capillary tubes is steadier than that in single capillary tubes. They also observed that the mass flow rate in the coiled capillary tube tends to increase with the increase in the diameter of the coil. Park and Jung (2007) gave the relationship between the inlet pressure and length of capillary tubes at the same mass flow rate through the straight and coiled capillary tubes. They found that smaller diameter capillary tubes require shorter tubes under the same operating conditions. Zhou and Zhang (2010) found that any changes in the condensation pressure of air-conditioners can affect the refrigerant mass flow rate through their capillary tubes. Mass flow rate increases with increasing condensing pressure and decreases with increasing length of the capillary tube. The previous studies have not investigated the effect of coil diameter on the propane mass within helical capillary tubes.

Reducing the diameter of the capillary tube is expected to increase the velocity of the refrigerant. Previous studies have shown that a high velocity refrigerant causes several issues such as noise, erosion of the inner surfaces of the tube, or pressure surge and liquid hammer during rapid closing of liquid line solenoid valve

(American Standard Inc., 2002; Copeland, 2000). In the absence of a solenoid valve, the maximum velocity is recommended to be less than 20 m/s (Copeland, 2000). If the velocity exceeds this value, it should remain subsonic, because a supersonic refrigerant leads to shock waves that damage the system. Acoustic sound of propane is 220 m/s at 4.4°*C* which is well above the recommended value of 20 m/s (McQuay, 2003).

This study quantifies the influence of the geometry and shape of capillary tubes on the existing mass of the propane in the capillary tube under the same operating conditions such as inlet and outlet pressures and temperatures, and mass flow rate. The operating conditions were measured on a commercial split air-conditioner and were used as inputs to a parametric script, which performs the required calculations. The presented results also include the length of the capillary tubes and velocity profile.

2.2 Model Description

A parametric MATLAB script has been developed to model the capillary tubes. In this study, the performances of sixteen capillary tubes have been investigated. The inside diameters of the capillary tubes were 1.6 mm, 1.8 mm, 2.0 mm, and 2.2 mm in two variations, with straight or spiral shape. In the cases of coiled capillary tubes, the coil diameters were 0.02 m, 0.04 m, 0.06 m. The capillary tubes are assumed to be made of copper, and the wall roughness is set to be 0.003 mm (Fox et al, 2010).

The mass flow rate and inlet and outlet pressure and temperature of the capillary tube were measured on a commercial propane air-conditioner, (Delonghi portable 2.85 kW propane air-conditioner) available in our laboratory. The uncertainties of the measurement of Coriolis mass flow meter, pressure transducers, and type J

thermocouples are ±0.00138 kg/s, ±25 kPa, and ±1ºC, respectively. The capillary tube of the air-conditioner is nearly straight, and its inside diameter is 2.0 mm. The tube inlet pressure and temperature were measured to be 838.5 kPa and 13.97°C at the room temperature of 11.4°C and when steady state conditions were reached. The inlet refrigerant was in a sub-cooled state. The tube outlet pressure and temperature were measured to be 430.9 kPa and -3.49°C, respectively. Using a Coriolis mass flow metre, the mass flow rate of the refrigerant was 0.02043 kg/s at the room temperature.

The homogenous model has been chosen to model the refrigerant flow within the capillary tube. As the two-phase flow within the capillary tube is in a high velocity condition, the two-phase flow is accepted to be homogenous (Zhow and Zhang, 2006). The flow in the capillary tubes is considered to be one-dimensional, steady, and adiabatic. Thermodynamic data such as enthalpy, density and viscosity of propane was obtained from Reprop 6.02 thermodynamic data base (NIST, 2000) and was set in the script. After defining the geometry of the capillary tube in the code, it calculates the inlet flow properties based on the input pressure and enthalpy.

Refrigeration and air conditioning systems are designed and manufactured to work in a wide range of conditions. At the design point of operation, the refrigerant enters the capillary tube in a sub-cooled state (Farzad, 1990). However, the condition of the fluid that flows into a capillary tube can be in a slightly saturated state due to changes in the ambient temperature (Fernando, 2007; Jahn, 2010). The parametric code is capable of recognizing whether the inlet flow is in the sub-cooled or two-phase saturated state. In the case of saturated flow, the quality of the inlet flow is calculated prior to calculating the inlet properties. In practice, it is not convenient to measure the pressure and temperature of the flow in the beginning and at the end of

the capillary tube due to its small diameter. The measured pressures and temperatures were the properties of the flow from the condenser and to the evaporator. Therefore, the script calculates the minor head loss due to the contraction at the entrance of the capillary tubes according to the following formula,

$$h_L = k_{cont} \frac{{V_{in}}^2}{2} \tag{2.1}$$

The minor head loss coefficient (k_{cont}) for sudden contractions in circular ducts depends on the area ratio of the exit to the inlet and is obtained from reference (Fox et al., 2010). The value is determined to be 0.5 for the tubes with the diameter of 1.6, 1.8, and 2 mm and is 0.48 for the 2.2 mm capillary tube. The corresponding pressure loss is calculated using the following formula,

$$\Delta p = \rho_{ave} \times h_L \tag{2.2}$$

It should be noted that the outlet properties of the contraction are not yet known. In order to calculate the average values in formula (2.2), initially the outlet properties are assumed to be equal to the inlet properties. The pressure after the contraction is calculated as,

$$P_e = P_{in} - \Delta P \tag{2.3}$$

The outlet diameter and mass flow rate are known; by assuming the outlet density is equal to that at the inlet, the outlet velocity can be determined using the following formula,

$$\mathrm{V} = \frac{\dot{\mathrm{m}}}{\rho \times \mathrm{S}} \tag{2.4}$$

The outlet enthalpy can be computed by the first law of thermodynamics as follows (Çengel and Boles, 2006),

$$h_e = h_i + \frac{V_{in}^2}{2} - \frac{V_e^2}{2} \tag{2.5}$$

The outlet density of the propane can be derived from the properties table, using the obtained values of the outlet pressure and enthalpy. After updating the outlet velocity from formula (2.4), the code compares it with that obtained at the previous step. The script terminates the calculation if the change of the outlet velocity is less than or equal to a predetermined value (0.001%), otherwise it reiterates the calculation based on the updated outlet properties. The iteration is terminated if the change in the outlet velocity between two consecutive steps becomes less than the predetermined value.

The capillary tubes are divided into equal segments of ΔL (initially 0.1 mm). The first segment is adjacent to the contraction and its inlet pressure and enthalpy are assumed to be equal to those at the outlet of the contraction. The outlet properties of the segment are initially assumed to be equal to those at the inlet. With this assumption and after calculation of the average properties, the flow Reynolds number is determined using the following formula,

$$Re = \frac{4 \times \dot{m}}{\pi \times \mu_{ave} \times d_i} \tag{2.6}$$

The refrigerant flow within the capillary tube is not assumed laminar. In the case of a laminar flow (Re<2300) at the entrance o the capillary tube, the flow might be laminar as the minor head loss should be calculated based on the refrigerant entrance velocity. The major head loss coefficient is calculated as follows (Fernando, 2007);

$$f_{laminar} = \frac{64}{Re} \tag{2.7}$$

Traditionally, the Colebrook equation is used to determine the major head loss coefficients for turbulent flows. However, previous studies of two-phase flows show

that more accurate results can be achieved using the Churchill formula (Zhou and Zhang, 2006), which is expressed as follows,

$$f = 8\left[\left(\frac{8}{Re_D}\right)^{12} + \frac{1}{(A+B)^{1.5}}\right]^{1/12} \quad (2.8a)$$

$$A = \left\{2.457 \times \ln\left[\frac{1}{(7/Re_D)^{0.9} + 0.27\times\frac{\varepsilon}{D}}\right]\right\}^{16} \quad (2.8b)$$

$$B = \left(\frac{37530}{Re_D}\right)^{16} \quad (2.8c)$$

In the case of coiled capillary tubes, the minor head loss coefficient of a 360° coil is assumed to be twice of that of a 180° bend (Munson, 2002),

$$K_{180°bend} = 1.5 \quad (2.9)$$

Therefore:

$$K_{coil} = 3 \quad (2.10)$$

The minor head loss coefficient of each segment can be found as follows,

$$K_{segment} = K_{coil} \times \frac{\Delta L}{\pi \times D} \quad (2.11)$$

Where *D* is the coil diameter. In the case of the straight capillary tubes, the minor head loss coefficient is assumed to be zero. The total head loss is calculated as,

$$h_L = \left(f \times \frac{\Delta L}{D} + K_{segment}\right) \times \frac{V_{ave}^2}{2} \quad (2.12)$$

The pressure loss, outlet pressure, and outlet enthalpy are calculated using formulas (2.2), (2.3), and (2.5), respectively. Based on the new outlet properties, the average values of density, velocity, and viscosity of the propane are updated, and then the calculations are reiterated until the change of the outlet velocity becomes less than or equal to the pre-set value of 0.001%.

After acquiring the pre-set value and prior to proceeding to the next segment, the pressure loss due to the expansion at the end of the capillary tube is calculated using the outlet properties of the last segment and the following formula,

$$\Delta P = \rho_{ave} \times k_{exp} \times \frac{V_e^2}{2} \quad (2.13)$$

The minor loss coefficient of the sudden expansion is obtained from reference (Fox, Pritchard and McDonald 2010) and is 0.98, 0.96, 0.94, and 0.9 for capillary tubes with the diameter of 1.6 mm, 1.8 mm, 2.0 mm, and 2.2 mm, respectively. It should be noted that in the formula (2.13), V_e represents the exit velocity from the capillary tube, not the exit velocity from the last segment.

The calculation is terminated when the value of the pressure loss due to the sudden expansion equals or exceeds the difference between the outlet pressure of the segment and the exit pressure of the capillary tube.

2.3 Results

The code is validated with the experimental results available in the literature. In an experimental work by Zhou and Zhang (2010), the coiled capillary tube had an inside diameter of 1.4 mm, and coil diameter of 0.04 m. The inlet refrigerant was in a sub-cooled state at a pressure and temperature of 1.58 MPa and 313 K. The refrigerant entered the capillary tube with a mass flow rate of 28.74 kg/h and left at a pressure of 0.8 MPa. The exact locations of the pressure gauge and thermometer were not reported, therefore the distance between the instruments and the inlet and outlet of the capillary tube are assumed to be zero. Ignoring these distances is expected to deliver a longer capillary tube. The calculated length is 0.38 *m*, which is 15.2% longer than the actual length (0.33 m). This level of error is assumed to be acceptable in this study.

The script is run for the sixteen capillary tubes. The inlet and outlet conditions are the same as the measured values at the inlet and outlet of the capillary tube of the split air-conditioner at an ambient temperature of 11.4°C. In the experiments, the

inlet propane was in the sub-cooled state at a pressure and temperature of 838.5 kPa and 12.97°C, respectively. The outlet propane was in a saturated state at a temperature of −3.49°C.

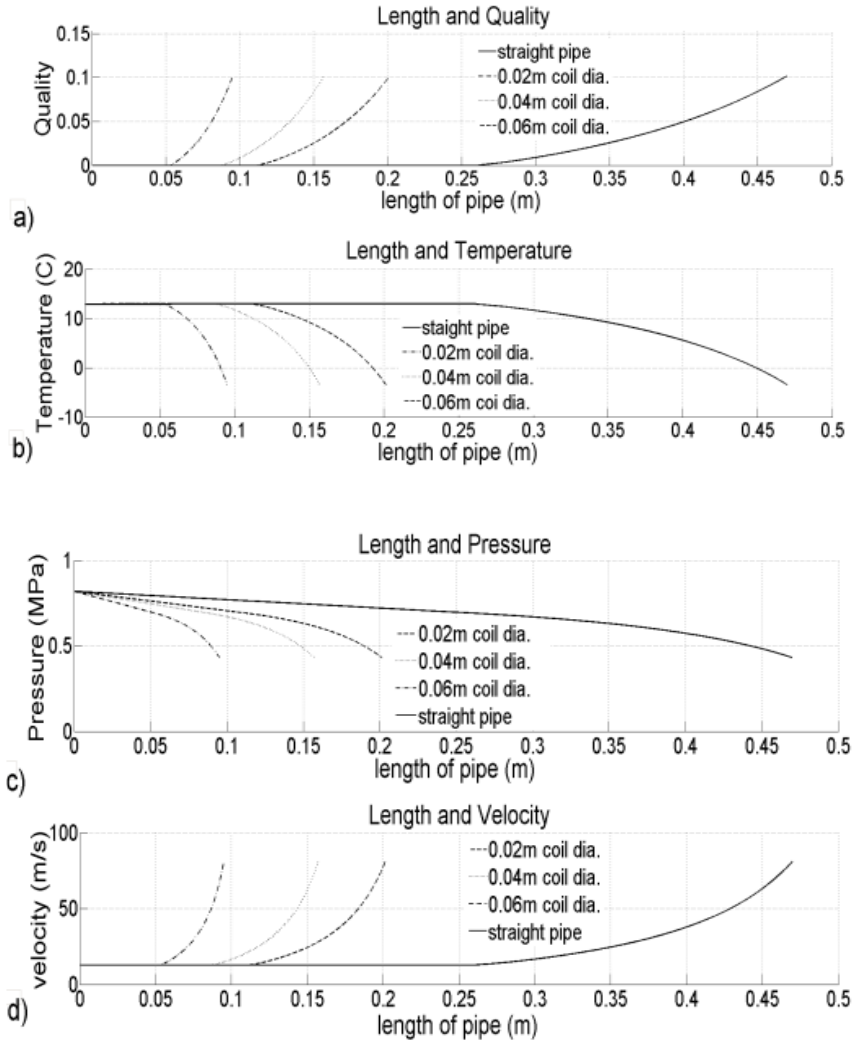

Figure 2-1 Characteristic of the flow through the straight and coiled capillary tube with inside diameter of 2 mm, a) quality, b) temperature, c) pressure, and d) velocity

Figure 2-1 shows the results for the capillary tubes with the inside diameter of 2 mm. Figure 2-1a indicates that in the all cases, propane remains in a state of sub-cooled for a considerable length of the capillary tube. These lengths are 261.3 mm, 112.2 mm, 87.4 mm, and 52.8 mm for the straight tube, and the tubes with coil diameters of 0.06 m, 0.04 m, and 0.02 m, respectively. The temperature increases along the tube in the sub-cooled state due to the viscous friction (and minor head loss in the

case of the coiled tubes) between the refrigerant and the tube wall, but the changes are small, and less than 0.02°C (Figure 2-1b). The temperature drops sharply in the all cases when the refrigerant reaches the saturated state, as it is expected.

Contrary to the increase of temperature in the sub-cooled state, the pressure drops from the entrance of the capillary tube to the exit, and the slope of the curve increases as the refrigerant moves along the tube (Figure 2-1c). The maximum rate of pressure fall occurs for the helical capillary tube with the coil diameter of 0.02 m, and consequently has the shortest length among the capillary tubes with the inside diameter of 2 mm. As the coil diameter increases, the rate of pressure fall decreases. The longest tube is the straight capillary tube.

Figure 2-1d shows the variation of the refrigerant velocity along the capillary tubes with the inner diameter of 2 mm. According to the Figure, the velocity of the refrigerant is virtually constant in the sub-cooled condition. The velocity dramatically increases at the saturated state, and the rate increases as the vapour quality increases. The exit velocity is the same in the all cases with the diameter of 2 mm, as the mass flow rate and the exit conditions are essentially identical among the cases. The length of the capillary tube which corresponds to the refrigerant velocity above 20 m/s is a maximum for the straight capillary tube and a minimum for the helical capillary tube with a coil diameter of 0.02 m. In the order of increasing coil diameter, this length is calculated to be 29.5 mm, 48.3 mm, 62.0 mm and 145.5 mm (the straight capillary tube).

Similar trends are observed for the capillary tubes with different inside diameter. The results are presented in Table 2-1, which lists the required length, the mass of the propane in the capillary tube, and the exit velocity of the refrigerant for all modelled

cases. According to the Table, the first and second shortest capillary tubes are the capillary tubes with the diameter of 1.6 mm and the coil diameter of 0.02 m and 0.04 m with corresponding lengths of 34.4 mm and 53.8 mm, respectively. It is interesting to note that the capillary tube with the diameter of 1.8 mm and coil diameter of 0.02 m has a length of 59.0 mm which is 7 mm shorter than the length of the capillary tube with the diameter of 1.6 mm and coil diameter of 0.06 m. A similar trend can be seen for the capillary tube with the diameter of 2 mm and coil diameter of 0.02 m which is 28.7% shorter than that of the straight capillary tube with the diameter of 1.6 mm ((133.2-95)/133.2). The longest capillary tube is the straight capillary tube with the diameter of 2.2 mm (785.4 mm) which is about 22 times longer than the shortest capillary tube (34.4 mm).

Table 2-1: The required length of the capillary tube, mass of the propane in the capillary tube, velocity and quality of the propane at the exit of the capillary tube for all modelled cases

Shape	Coil diam. (m)	Pipe diam. (mm)	Length (mm)	Mass (g)	Outlet quality (%)	Outlet velocity (m/s)
Straight	-	1.6	133.2	0.102	9.27	116.96
Straight	-	1.8	262.9	0.262	9.81	96.96
Straight	-	2.0	470.0	0.586	10.17	80.99
Straight	-	2.2	785.4	1.200	10.42	68.30
Coiled	0.02	1.6	34.4	0.026	9.27	116.96
Coiled	0.02	1.8	59.0	0.058	9.81	96.96
Coiled	0.02	2.0	95.0	0.118	10.17	80.99
Coiled	0.02	2.2	143.8	0.219	10.42	68.30
Coiled	0.04	1.6	53.8	0.041	9.27	116.96
Coiled	0.04	1.8	96.0	0.096	9.81	96.96
Coiled	0.04	2.0	156.9	0.196	10.17	80.99
Coiled	0.04	2.2	242.1	0.369	10.42	68.30
Coiled	0.06	1.6	66.0	0.050	9.27	116.96
Coiled	0.06	1.8	120.2	0.119	9.81	96.96
Coiled	0.06	2.0	201.3	0.251	10.17	80.99
Coiled	0.06	2.2	314.0	0.479	10.42	68.30

Table 2-1 also list the mass of the refrigerant filling the tubes. It should be noted that the mass of propane is proportional to the volume of capillary tubes, and not necessarily to their length. For example, the mass of the propane filling the capillary tube with the diameter of 1.6 mm, coil diameter of 0.06 m, and length of 66 mm is 0.050g which is 0.008g less than 0.058g contained in the shorter capillary tube with the length of 59 mm, diameter of 1.8 mm, and coil diameter of 0.02 m. The minimum mass of propane is 0.036g which is for the capillary tube with the diameter of 1.6 mm and coil diameter of 0.02 m. The straight capillary tube with the diameter of 2.2 mm requires the maximum mass of propane (1.2g).

The exit conditions and mass flow rate of the refrigerant remain unchanged among all the cases modelled; thus, the exit velocity depends only on the inner diameter of the capillary tubes and not on their shape. The maximum exit velocity of 116.96 m/s reached in the capillary tubes with the diameter of 1.6 mm, and the minimum exit velocity of 68.30 m/s occurs in the capillary tubes with the diameter of 2.2 mm. According to Table 2-1, the exit velocity of the refrigerant exceeds the maximum recommended value of 20 m/s in all the cases modelled.

Table 2-2 presents the length of the portion of the capillary tube that contains propane with velocities above the recommended value of 20 m/s. According to the results, this length decreases as the inside diameter, or the coil diameter decreases. The shortest length containing high velocity propane is 17.9 mm, and is for the capillary tube with the inside diameter of 1.6 mm and the coil diameter of 0.02 m. The straight capillary tube with the inside diameter of 2.2 mm has the longest portion (196.6 mm) among all the cases modelled

Table 2-2: Shape, coil diameter, pipe diameter, length of capillary tube where the velocity of refrigerant exceeds 20 m/s

Shape	Coil diameter (m)	Pipe diameter (mm)	Length of the portion of the capillary tube containing propane with velocity above 20 m/s(mm)
Straight	-	1.6	68.4
Straight	-	1.8	102.3
Straight	-	2.0	145.5
Straight	-	2.2	196.6
Coiled	0.02	1.6	17.9
Coiled	0.02	1.8	23.2
Coiled	0.02	2.0	29.5
Coiled	0.02	2.2	35.9
Coiled	0.04	1.6	27.6
Coiled	0.04	1.8	37.2
Coiled	0.04	2.0	48.3
Coiled	0.04	2.2	60.1
Coiled	0.06	1.6	34.2
Coiled	0.06	1.8	47.0
Coiled	0.06	2.0	62.0
Coiled	0.06	2.2	78.0

2.4 Discussion

The split air-conditioner in our laboratory includes a straight capillary tube. Its modelling is not able to validate the main part of the script assigned to the calculation of minor losses. Therefore, the existing experimental data available in the literature are used to validate the accuracy of the code. The obtained results show an error of about 15%. This level of error is acceptable due to uncertainty in the roughness of the tube wall interior that changes with time, and due to neglecting of minor head losses at the connections of the pressure gauges and thermocouples.

The results indicate that a decrease in the diameter of the capillary tube leads to a significant decrease in the mass of the propane in the tube. For example, for a straight capillary tube with the inside diameter of 1.6 mm, the present mass is 0.102

grams which is about 11 times less than that of a straight capillary tube with inside diameter of 2.2 mm (1.2g).

The results show that both techniques of reducing the diameter of a capillary tube and reducing the coil diameter are capable to decrease the mass of propane required for filling the capillary tube. The contribution of the minor losses (reducing the coil diameter) to the total head loss of the capillary tube is significant. For example, the required mass of propane filling the capillary tube with the diameter of 1.6 mm and coil diameter of 0.02 m is 0.026g, which is about 3.9 times less than that of the straight capillary tube with the same diameter. One possible reason for the importance of minor head losses in the propane capillary tubes compared to other similar applications is the lower viscosity of propane respect to the viscosity of other common fluids. The viscosity of sub-cooled propane at $20°C$ is 102.9×10^{-6} $Pa.s$ (NIST 2000), which is about 10 times less than the viscosity of water at the same temperature (1010×10^{-6} $Pa.s$ (Fox et al, 2010)). The viscosity has a significant impact on the major loss but no effect on the minor losses.

The outlet velocity of the refrigerant is greater than the inlet velocity for all the cases calculated. The outlet propane has a lower temperature than the inlet which tends to increase the density, but as the pressure falls simultaneously, the overall effect is the reduction of the density of the refrigerant. The lower density leads to a higher outlet velocity (see Figure 2-1d). The results also indicate that the outlet velocity exceeds the recommended value of 20 m/s in the all cases. However, the length of the portion of the capillary tube containing the high velocity propane decreases with the reduction of the inside diameter or coil diameter (see Table 2-2). The length is only 17.9 mm for the capillary tube with the inside diameter of 1.6 mm and the coil diameter of 0.02 m but increases to about 196.6 mm for the straight capillary tube

with the inside diameter of 2.2 mm. This provides an additional benefit of the small diameter tubes when the system includes high velocity refrigerants.

A couple of issues need to be addressed prior to adoption of using coiled capillary tubes with small diameter. Table 2-1 shows that a significant decrease of about 98% ((1.2-0.026)/1.2) of the mass of the propane in the capillary tube can be achieved by reducing the coil and inside diameters, without any adverse effect on the cooling capacity of the split air-conditioner. However, it should be noted that for a small air-conditioner such as the one in this study, the absolute value of mass savings is not significant and is only 1.174g (1.2-0.026). Another decisive issue is the distance between the outlet of the condenser and the inlet to the evaporator which cannot be shortened in some cases. A liquid line with a relatively large diameter compared to that of the capillary tube passes the refrigerant from the capillary tube to the evaporator. As a result, any reduction in the length of the capillary tube may lead to the increase of the length of the liquid line which in turn actually increases the mass of the propane in the system.

One way to reduce the mass of refrigerant within the air conditioning system is to reduce the size of the capillary tube and change the shape of the capillary tube. In Chapter 2, the dimensions and shape of the capillary tube were varied to find the minimum mass of refrigerant within the capillary tube. It was found that the minimum charge was in the tube with the smallest diameter. The research considered two types of the capillary tube: straight and coiled. The diameter of the straight capillary tube and the diameter of the coiled capillary tube were changed to analyze the change in mass and the velocity of the refrigerant.

Table 2-3: The results of the papers for inlet temperature of the main parts, maximum pressure and maximum velocity

	T_1	T_2	T_3	T_4	P_{max}	V_{max}
Increase room temp	in	in	in	in	in	dec[1*]
Increase refrigerant charge	const[6*]	dec	const[5*]	const[6*]	in[9*]	in
Extending capillary tube	-	-	const	const	const	dec
Increase evap inlet pressure	-	-	in	in	-	-
Increase evap wind speed	-	-	-	-	-	-
Shorten evap pipe length	-	-	-	-	-	-
Increase capillary tube diameter	-	-	-	-	-	dec
Increase capillary tube coil diameter	-	-	-	-	-	const
Increase cond inlet pressure	-	in	in	-	in	-
Shorten cond pipe length	-	-	-	-	-	-

in : increase
dec : decrease
const : constant
T_1 : inlet temperature of compressor
T_2 : inlet temperature of condenser
T_3 : inlet temperature of capillary tube
T_4 : inlet temperature of evaporator
P_{max} : maximum pressure
V_{max} : maximum velocity
1* : increase at higher charge
5* : decrease at high temperature
6* : increase at high temperature
9* : constant at high room temperature

It was found that by decreasing the diameter of the capillary tube, the velocity of refrigerant increased. An increase in the refrigerant velocity increased the friction force of the refrigerant and the capillary tube wall. The higher friction force in the capillary tube is beneficial to the shorter capillary tube for the same outlet pressure. The effect of decreasing the diameter of the capillary tube is increasing the major loss from the pipe. Another way to reduce the length of the capillary tube is to increase the minor loss of the refrigerant. In this research, the minor loss of the capillary tube was changed by changing the diameter of coil. It was found that, by

decreasing the diameter of the coiled capillary tube, the minor loss increased which also increased the pressure loss along the capillary tube. Tables 2-3, 2-4 and 2-5 show the outcomes of these papers.

Table 2-4: The results of the papers for density of refrigerant at inlet of main parts, compressor work and condenser capacity

	ρ_1	ρ_2	ρ_3	ρ_4	W_{comp}	Cond cap
Increase room temp	in	in	dec	dec	in	-
Increase refrigerant charge	const	in[7*]	const	const	in	-
Extending capillary Tube	-	-	-	-	-	-
Increase evap inlet pressure	-	-	-	-	-	-
Increase evap wind speed	-	-	-	-	-	-
Shorten evap pipe length	-	-	-	-	-	-
Increase capillary tube diameter	-	-	-	-	-	-
Increase capillary tube coil diameter	-	-	-	-	-	in
Increase cond inlet pressure	-	-	-	-	-	dec

ρ_1 : inlet density of compressor
ρ_2 : inlet density of condenser
ρ_3 : inlet density of capillary tube
ρ_4 : inlet density of evaporator
W_{comp} : useful compressor work
Cond cap : condenser capacity
7* : constant at high temperature
- : no change

Table 2-5: The results of the papers for refrigerant mass flow rate, cooling capacity, sub-cooling, specific capacity and refrigerant charge

	m	Cooling	COP	Sub Cooling	SC	Charge
Increase room temp	in[2*]	in[3*]	dec	dec	in[4*]	-
Increase refrigerant charge	in	In	in	in[8*]	dec	-
Extending capillary tube	-	-	-	const	in	dec
Increase evap inlet pressure	-	dec	in	const	dec	in
Increase evap wind speed	-	in	-	const	in	dec
Shorten evap pipe length	-	dec	-	-	in	dec
Increase capillary tube diameter	-	-	-	-	dec	in
Increase capillary tube coil diameter	-	-	-	-	dec	in
Increase cond inlet pressure	-	in	in	-	dec	in
Shorten cond pipe length	-	dec	dec	-	in	dec

2* : at overcharged, first increase to a certain value and then decrease at further increase in room temperature
3* : at high charge, constant at low room temperature and decrease at high room temperature
4* : constant at standard charge, first increase and than decrease after certain value at high charge
8* : constant at average room temperature
m : mass flow rate
Cooling : cooling capacity
SC : specific capacity

2.5 Conclusion

In order to reduce the risk associated with the use of flammable refrigerants, a numerical code has been developed to quantify the effect of two potential techniques in reducing the mass of the propane in the capillary tube. The two techniques are reducing the inner diameter of the capillary tube and reducing the coil diameter. It has been found that both techniques are effective and capable of reducing a high percentage of the required propane. The first technique has the disadvantage of increasing the velocity of the refrigerant to a level that may exceed the recommended value. However, the first method reduces the length of the portion of the tube

containing the high velocity refrigerant. As the viscosity of propane is relatively small compared to common fluids, the second technique is also effective and doesn't have the disadvantage of the first approach. Care needs to be taken in applying these techniques if the distance between condenser and evaporator cannot be bridged by the new short capillary tubes. In those cases, reducing the size of the capillary tube leads to a longer liquid line which may actually increase the mass of the propane in the air-conditioner.

There is another method for capillary tube modification. The next chapter discusses the way to reduce the refrigerant within the air conditioning system by modifying the capillary tube and liquid line into a single extended capillary tube. Capillary tube and liquid line are located between the condenser and evaporator.

CHAPTER 3 EXTENDING THE CAPILLARY TUBE OF THE PROPANE AIR CONDITIONER TO REDUCE THE REFRIGERANT CHARGE

This chapter discusses the computational work of changing the combination of capillary tube and liquid line into a single extended capillary tube to reduce the refrigerant charge. The length of the new extended capillary tube equals the length of the existing capillary tube combined with the length of the liquid line. The diameter of the liquid line is similar to the diameter of the evaporator. Because the diameter of the liquid line is larger than the capillary tube, the mass of the refrigerant within the liquid line is more than the mass within the capillary tube. Replacing the capillary tube and liquid line with a single extended capillary tube allows a decrease in the refrigerant charge. The technique of combining the capillary tube and liquid line is discussed in this chapter. This Chapter was adopted from the paper that was published in Energy Procedia, Volume 110, March 2017, pages 229 – 234.

3.1 Introduction

Synthetic refrigerants are being phased out, and their production will be banned entirely by 2030 due to their global warming and ozone depletion impacts (UNEP, 2003). Hydrocarbons such as propane are used as replacement of synthetic refrigerants due to their negligible global warming, near zero ozone depletion potentials, and their similar thermodynamic properties. However, the amount of propane in the system should be limited due to its flammability.

In regard to the use of hydrocarbon refrigerants, several technical committees, which are responsible for standards development, have been trying to include the additional safety measures in recent years. The maximum allowable amount of hydrocarbon refrigerants in a system is specified according to room floor area, installation height and lower flammability limit of the refrigerant. A formula that is well accepted by

most standards suggests a maximum of approximately 300 grams hydrocarbon refrigerants for portable factory sealed single package air conditioners (Corberan et al., 2011). During last decade, some amendments have been proposed for more restrictive regulations (Kataoka and Usami, 2012).

Most previous research focused on decreasing the amount of charge in components with the maximum charge of the system. The results show that a significant mass reduction can be achieved by (a) using miniature heat exchangers (Fernando et al., 2004), (b) increasing the condensing temperature (Fernando et al., 2007). The length of the capillary tube is expected to have only a negligible impact on the required charge of the system, as capillary tubes contain only a small fraction of the refrigerant charge (Siang and Sharifian, 2013). For this reason, the research in this area has been very limited.

In a previous work (Siang and Sharifian, 2013), it has been shown that reducing the inside diameter of capillary tubes significantly reduces the refrigerant charge in the tube; however, this technique has a negative impact on the overall life of the capillary tube and the noise level by increasing the maximum velocity of the refrigerant. An alternative approach is to use a shorter and helical capillary tube to lower the maximum velocity. This method is effective but not practical if the distance between the outlet of the condenser and the inlet of the evaporator cannot be reduced. Here, shortening the length of capillary tubes extends the length of the tube between the outlet of the capillary tube and the inlet of the evaporator (liquid line). The liquid line has a larger diameter compared to the capillary tube; consequently, this arrangement may actually increase the overall refrigerant charge of the system. In such cases, it is suggested to both extend the capillary tube and eliminate or shorten the liquid line.

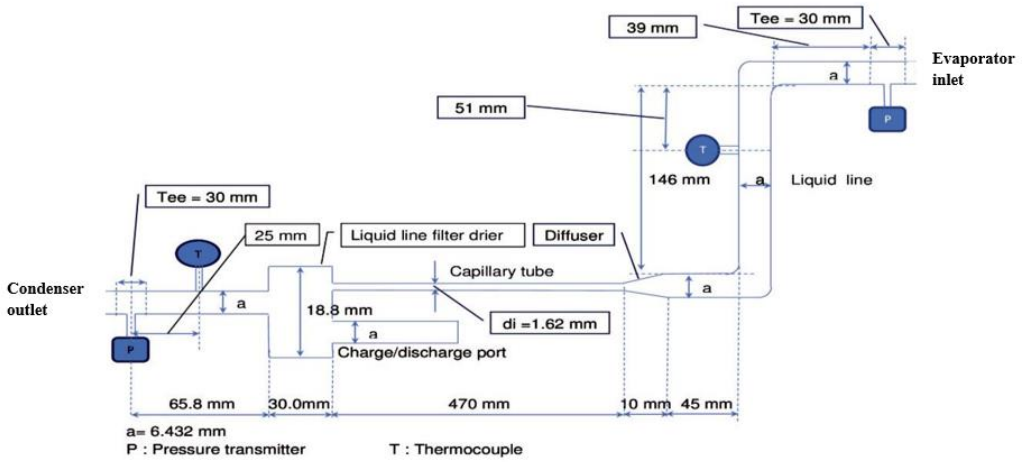

Figure 3-1. Schematic of the original capillary tube and instrumentation (not to be scaled)

In the proposed technique, the length of the new capillary tube equals the sum of the length of the original capillary tube and the length of the liquid line. However, in this work, the length of the new capillary tube equals the sum of the original capillary tube and the part of the liquid line which is located between the diffuser and downstream pressure transducer (see Figure 3-1). This provides an opportunity to compare the computational results with the experimental data. The diameter of the proposed capillary tube is chosen in such a way that the pressure loss remains unchanged in the two cases. This is necessary because increasing the pressure loss can increase the size of the required compressor, which may lead to an increase in the overall refrigerant charge of the system.

3.2 Methodology

The approach in this study incorporates computational and experimental methods. First, a script was developed to model the capillary tube and liquid line, and then its accuracy was assessed by comparing the computational results with those of experiments. At the next step, the model was used to estimate the mass of propane in the capillary tube and liquid line. It should be noted that the experimental setup in the present study does not provide an explicit measure of the mass of the refrigerant

in the system. Therefore, the accuracy of the code was validated based on the measured outlet pressures.

The following assumptions were made for simplicity of the script. The flow in the capillary tubes and liquid line was assumed to be one dimensional, steady, and adiabatic. Thermodynamic data such as enthalpy, density and viscosity of propane were obtained from Reprop 6.02 thermodynamic data base (McLinden et al., 1998) and were set in the script. After defining the geometry of the capillary tube in the code, the inlet flow properties were calculated based on the inlet pressure and temperature. It should be noted that the refrigerant is in a state of saturation except at the entrance of the capillary tube where the refrigerant is in a sub-cooled state. The calculation in the saturation condition is based on the average properties of the liquid and vapour.

The Colebrook equation is frequently used to determine major head loss coefficient for turbulent flow. In spite of this, previous studies on two phase flows suggest that a more accurate result might be obtained through the use of Churchill formula (Zhou and Zhang, 2006), which is defined as follows,

$$f = 8\left[\left(\frac{8}{Re_D}\right)^{12} + \frac{1}{(A+B)^{1.5}}\right]^{1/12}, \qquad A = \left\{2.457 \times ln\left[\frac{1}{(7/Re_D)^{0.9}+0.27\times\frac{e}{D}}\right]\right\}^{16},$$
$$B = \left(\frac{37530}{Re_D}\right)^{16} \tag{3.1}$$

Where e denotes roughness (m), D stands for diameter (m), and f and Re_D represents friction factor and Reynolds number, respectively. The properties of refrigerant using McAdams method can be calculated as,

$$\frac{1}{\varphi} = \frac{x}{\varphi_v} + \frac{(1-x)}{\varphi_l} \tag{3.2}$$

Where φ can denote quality (x), viscosity (μ), specific enthalpy (h), thermal conductivity (k), or density (ρ). The subscripts l and v refer to liquid and vapour states, respectively.

In this work, initially both McAdams and Colebrook formulas were used to determine the accuracy, and then the Colebrook formula which shows better results than other method was used for the rest of the study.

The capillary tube was initially divided into equal segments of 0.7 mm. The first segment was next to the pressure transducer behind the capillary tube (see Figure 3-1). It should be stressed that there is a 2.5 cm gap between the pressure transducer and thermocouple due to technical restrictions. The effect of this gap was ignored in this work, and the measured temperature was assumed to be the inlet temperature of the refrigerant. The final results confirm that the change of temperature in this distance is very small, thus the effect is very minor. The outlet pressure and enthalpy of the segment were initially assumed to be equivalent to those of the inlet properties which were obtained from the measured values. After calculating the average properties, the flow Reynolds number was calculated based on the inside diameter of the tube. All minor head loss coefficients with the exception of the filter were obtained from the reference (Fox et al., 2010). According to the reference, the minor head loss coefficients were found to be 0.5 for sudden contraction, 0.95 for the sudden expansion at the inlet of the filter, 0.79 for the expansion at the inlet of the diffuser, and 0.3 for the elbow. The outlet enthalpy was computed using the first law of thermodynamics. More details of the script can be found in our previous work (Siang and Sharifian, 2013).

The capillary tube and liquid line of the propane air-conditioner modelled in this work are those of a 2.85 kW portable air-conditioner. The length of the nearly straight capillary tube and liquid line are 0.47 m, and 0.30 m, respectively. The capillary tube and liquid line are made of copper with a mean surface roughness of 0.003 mm (Fox et al., 2010), and have nominal internal diameters of 1.620 mm, and 6.432 mm, respectively.

The measuring instruments include a Coriolis mass flow meter at the inlet of the condenser, two piezoresistive pressure transducers, and two J-type thermocouples at the inlet and outlet of the capillary tube (see Figure 3-1). The second thermocouple and pressure transducer are located on the downstream side in the middle of the liquid line at distances of 170 mm and 295 mm from the end of the capillary tube, respectively. As will be seen later, the gap between the thermocouple and pressure transducer does not cause a significant error due to marginal changes of pressure and temperature in the liquid line.

3.3 Results

The experimental setup in the present study does not provide an explicit measure of the mass of the refrigerant in the system. Therefore, the accuracy of the code was validated based on the measured outlet pressure of the refrigerant at the location of the second pressure transducer in the middle of the liquid line. Table 3-1 summaries and compares the computational results with the experimental data for five cases. The first and third cases were performed with a charge of 390g propane at two ambient temperatures of 35.5°C and 20.5°C, respectively, while the other three case studies were conducted with 367.1g charge at three ambient temperatures of 20.5°C, 26.5°C, and 35.5°C. It should be noted that the ambient temperature was maintained

constant with an error of ±0.5°C error. For example, in the first case in which the desired temperature was 35.5°C, the temperature varied between 35°C and 36°C but was on 35.97°C throughout most of the experiment.

Table 3-1: Experimental and computational results for different propane charges and ambient temperatures

Case	1	2	3	4	5
Measured ambient temperature (˚C)	35.5±0.5	20.5 ±0.5	20.5 ±0.5	26.5±0.5	35.5±0.5
Measured total charge (gram)	390	367.1	390	367.1	367.1
Measured inlet pressure (MPa)	1.596	1.116	1.273	1.302	1.564
Measured mass flow rate (kg/s)	0.014316	0.011527	0.014156	0.011302	0.013104
Measured inlet temperature (˚C)	35.97	21.15	21.4	26.75	35.84
Measured pressure loss (MPa)	0.968	0.641	0.752	0.748	0.946
Calculated pressure loss (MPa), Colebrook	0.968	0.590	0.899	0.573	0.804
Calculated pressure loss (MPa), McAdams	N/A	0.641	N/A	0.429	0.780
Relative error (%), Colebrook	0.00	-7.96	19.55	-23.40	15.01
Measured outlet pressure (MPa)	0.627	0.475	0.522	0.554	0.618
Calculated outlet pressure (MPa), Colebrook	0.627	0.526	0.374	0.729	0.760
Calculated outlet pressure (MPa), McAdams	N/A	0.475	N/A	0.873	0.784
Relative error (%), McAdams	N/A	0.00	N/A	42.65	17.55
Diameterof extended capillary tube (mm)	1.7	1.7	1.7	1.7	1.7
Charge in extended capillary tube (gram)	2.011	2.135	2.117	2.112	2.027
Charge in existing system (gram)	5.574	6.087	5.851	6.098	5.728
Decrease of propane charge (%)	63.92	64.93	63.81	65.36	64.62

Due to lack of sufficient information regarding the head loss coefficients for the filter and charge/discharge ports, the experimental results of the first case were used to estimate their overall minor head loss coefficient by Colebrook's equation. The results show a minor loss coefficient of 10.42 provides the best outcomes with zero error for the first case. This value leads to a relative error of −7.96% for the second case, 19.55% for the third case, −23.40% for the fourth case, and 15.01% for the fifth case. The results of the second experiment were used to determine the coefficient of minor loss by McAdams technique. It was found that a value of 2.54 produces zero error in calculation of pressure. However, using this value does not produce any results (cases 1 and 3), or presents a relative error greater than that of Colebrook equation (cases 4 and 5). Comparing the accuracy of the two computational approaches, Colebrook method was selected for the rest of this study.

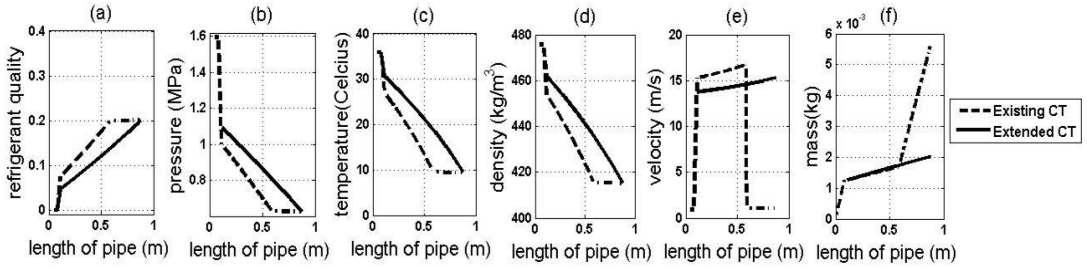

Figure 3-2. changes of refrigerant properties along the existing and proposed extended capillary tubes at ambient temperature of 35.5ºC +-0.5ºC and charge of 390 g, a)quality, b)pressure, c)temperature, d)density, e) velocity, and f) mass.

In the second step, the script was run for the existing capillary tube and liquid line at the inlet pressure of 1.60 MPa and inlet temperature of 35.97°C (sub-cooled condition) (case 1). The flow characteristic and mass of refrigerant in the system were determined and the results are presented in Table 3-1 and Figure 3-2. It should be noted that the presented results are only for the length between the two pressure transducers, and not along the entire length of the capillary tube and liquid line. Consequently, it is expected that the computational results underestimate the reduction of the refrigerant charge (if any) but still makes the point.

Figure 3-2a shows that the refrigerant remains in sub-cooled state along the pipe before entering the filter of the original capillary tube. In this distance, the changes of pressure, density, temperature, and velocity are negligible (Figures 3-2b, 3-2c, 3-2d and 3-2e). At the filter, the minor losses were calculated using equation 4, assuming zero length filter. Nevertheless, Figure 3-2 includes the length of the filter, assuming a linear variation of properties along the filter.

From the entrance to the end of the filter, the quality increases from zero to 0.08, pressure drops from 1.60 MPa to 1.00 MPa, temperature falls from 35.97°C to 27.04°C, density decreases from 475.73 kg/m^3 to 453.94 kg/m^3, and the velocity increases from 0.93 m/s to 15.30 m/s. The properties continue to change along the capillary tube, and the refrigerant reaches a quality of 0.20, pressure of 633.8 kPa, temperature of 9.81°C, density of 416.16 kg/m^3, and velocity of 16.69 m/s at the inlet to the diffuser. The change of the quality, pressure, temperature, and density are insignificant along the diffuser and liquid line, but the velocity drops to 1.06 m/s.

In the third step, the extended capillary tube was modelled. The length of the extended capillary tube is 0.77 m which is the sum of the lengths of the original capillary tube and the part of the liquid line located between the two pressure transducers. The diameter of the new capillary tube was adjusted (using trial and error method) until the outlet pressure of the extended capillary tube equalled that of the original configuration. The new diameter is 1.70 mm.

The results show that the refrigerant experiences similar property changes to those of the original case along the entrance and filter before entering the capillary tube. As the new capillary tube has a larger diameter, the entrance velocity decreases to 13.75 from 15.30 m/s of the original case. The change of the properties is approximately

linear along the new capillary tube, and the properties at the end of the elongated capillary tube are the same as those of the previous case, except for the velocity which is 15.31 m/s, far greater than the original case (1.06 m/s). It should be noted that the velocities along the path where previously the original capillary tube were located are smaller for the extended capillary tube. Conversely, the velocities along the length where the liquid line were situated are much higher than that of the original case. It is interesting to see that the maximum velocity in the case of the extended capillary tube (15.31 m/s) is less than that of the original case (16.69 m/s).

Figure 3-2f shows the mass of the refrigerant from the entrance of the capillary tube. According to the Figure, the rate of the increase of the mass between the upstream pressure transducer and the entrance of the capillary tube, where the refrigerant is in a sub-cooled state, is sharp and the accumulated mass reaches a value of 1.25g in both cases. The rate of increase of the mass along the rest of the original capillary tube is moderate and decreases slightly as the quality increases. At the exit of the original capillary tube, the total mass of refrigerant reaches a value of 1.67g. For the case of the extended capillary tube at the same distance, the total mass reaches to a value of 1.73g which is 3.2% greater than that of the original case. The sudden increase of the mass in the liquid line is due to its larger diameter than that of the extended capillary tube. The total mass accumulated in the original capillary tube and the liquid line is 5.57g, whereas the total mass in the extended capillary tube is 2.01g, representing a decrease of 63.9%.

In the fourth step, the script was run for the existing and extended capillary tube for remaining cases (cases 2 to 5), and the results are presented in Table 3-1. The results demonstrate similar characteristics to those in case 1. The overall decrease in the

refrigerant charge is 64.93%, 63.81%, 65.36% and 64.62% for the cases 2 to 5, respectively.

3.4 Discussion

It was found that McAdams method does not always yield a result. Further investigation showed that the calculated pressure drop throughout the tube was high, and the calculated pressure became less than the minimum pressure that was embedded in the script (0.05 MPa). The formula (3.2) is re arranged and presented as follows,

$$\rho = \frac{\rho_v}{x+(1-x)\frac{\rho_v}{\rho_f}} \tag{3.3}$$

As the ratio of ρ_v/ρ_f is usually small, the density can be approximated as ρ_v/x. For example, when the quality of refrigerant is 0.5, the density is approximately twice of ρ_g which is lower than that of Colebrook method, in which the density is the average of ρ_v and ρ_f. The low-density results in high velocity, which in turn increases the calculated pressure drop.

The results show that in both original and proposed extended capillary tubes, the changes in the temperature, density, and velocity of the refrigerant along the tube are insignificant prior to entering the capillary tube. The refrigerant undergoes significant changes along the capillary tubes, but in the case of the original tube, the rates of the change decreases inside the liquid line. The main difference between the two tubes is associated with the rate of the change in the properties of the refrigerant. In the case of the extended tube, the rates at which the properties change are smaller due to its larger diameter. The accumulated mass of the refrigerant in the original capillary tube is slightly less than that of the extended capillary tube along the same length due to its smaller diameter. Nevertheless, due to the smaller diameter of the

extended capillary tube compared to the liquid line, the total mass of the refrigerant becomes smaller than that of the original case. At the operational conditions of this study, the total mass of refrigerant was reduced by 63.9%. The actual value of the reduction is expected to be higher if the entire liquid line was modelled. It should be noted that the total mass of the refrigerant in the air-conditioner experiences only a small decrease. In the conditions that this work was carried out, the total mass of the refrigerant decreases from 390g to 386.44g, representing a reduction of 0.9%.

One interesting point is the decrease of the maximum refrigerant velocity in the extended capillary tube compared to that of the original tube. In the original case, the velocity increases along the capillary tube as the quality of the refrigerant increases. The maximum velocity occurs at the exit of the capillary tube before entering the liquid line which has a larger diameter. The velocity increases continuously along the extended tube which has a constant diameter. Subsequently, the maximum velocity occurs at the end of the capillary tube. In comparison, the maximum velocity of the refrigerant in the extended capillary tube is 8.3% ((16.69-15.31)/16.69) less than that of the original case, which offers an additional advantage over the existing configuration.

Reducing the mass of refrigerant can also be carried out by replacing the existing capillary tube and liquid line with a single capillary tube. There are two formulas that were compared in this work: the Colebrook equation and McAdams equation. The results show that Colebrook's formula obtains a better calculation result. Replacing the existing capillary tube and liquid line with a single capillary tube has the benefit of a smaller refrigerant mass within the capillary tube and lower maximum velocity which can extend the life of the capillary tube.

3.5 Conclusion

The computational results support the concept of substituting the capillary tube and liquid line of propane air-conditioners with a larger diameter and longer capillary tube which causes an equivalent head loss. The results show that such a technique is effective in reducing the mass of propane. In addition, another benefit of using the elongated capillary tube and removal of the liquid line is a reasonable decrease in the maximum velocity of refrigerant.

The next modification can be made at the evaporator section. As the evaporator is a heat exchanger which contains more mass of refrigerant compared to the capillary tube, it is important to find a way of decreasing the refrigerant mass within the evaporator for safer use of a flammable refrigerant such as propane. The technique of reducing the refrigerant mass within the evaporator is discussed in the next chapter.

CHAPTER 4 EFFECT OF INLET PRESSURE, SIZE AND WIND SPEED OF AN EVAPORATOR ON AMOUNT OF REFRIGERANT CHARGE AND PERFORMANCE OF A PORTABLE PROPANE AIR CONDITIONER

The evaporator is one of the main parts of an air conditioning system, and it contains much refrigerant. This chapter discusses the computational technique used to evaluate the possible ways of reducing refrigerant mass within the evaporator. To explore possible changes in refrigerant mass within the evaporator, some conditions such as the inlet pressure and speed of air over the evaporator were varied. The main part of this Chapter was published in IEEE Xplore for the 4th International Conference on Science and Technology, 2018.

4.1 Introduction

Many synthetic refrigerants have drawbacks, such as ozone depletion potential and global warming impact, (Gartshore, 1995). Due to these drawbacks, non-environmentally friendly synthetic refrigerants are planned to be phased out by 2030 (UNEP, 2003).

In the refrigeration and air-conditioning sector, some synthetic refrigerants have been developed to replace the harmful synthetic refrigerants. However, these refrigerants such as R404a, R407C and R410A (called transitional refrigerants) still have high global warming potential (IPCC, 1994). The transitional refrigerants generally have low ozone depletion potential and good thermodynamic performance, as they are non-azeotropic mixtures, and can replace refrigerants such as R22. However, they are associated with another problem when there is leakage in the system.

Hydrocarbons are also alternative substances for replacing the harmful synthetic refrigerants because of their negligible ozone depletion and global warming impact (Park et al., 2007). Hydrocarbons have good thermodynamic properties and a much lighter density compared to the existing synthetic refrigerants, leading to lower refrigerant charging for the same cooling capacity (Gartshore, 1995). A drawback of hydrocarbons is their flammability. One way to improve safety is to use the lowest amount of refrigerant possible for an identical cooling capacity as coefficient of performance does not decrease.

One hydrocarbon refrigerant currently used in air-conditioning systems is propane. Propane refrigeration systems show a better coefficient of performance but lower cooling capacity in comparison to R22 (Park et al., 2007). Hydrocarbon refrigerants are flammable and there have been many attempts to find a reliable way to reduce the amount of refrigerant in the air conditioning systems.

However, only a very limited number of studies have focused on single-duct portable air-conditioners. Unlike non-portable air-conditioners, the condenser and evaporator of a single-duct portable air-conditioner are at the same room temperature. But, both operate on the same thermodynamic cycle. Therefore, only some research results on non-portable systems can be applied to the portable air conditioning system (Sharifian and Siang, 2015).

The evaporator is one of the main components of any air-conditioning system in which the cooling process occurs and it contains the second highest amount of refrigerant after the condenser (Corberan et al., 2008). This research focuses on ways that the amount of propane within the evaporator can be reduced, and the impacts of those techniques on the overall performance of portable propane air conditioners.

The techniques investigated are the effect of the inlet pressure of the evaporator, the effect of shortening the length of evaporator pipe and the effect of wind speed on the evaporator. This research is mainly carried out computationally with some experimental work to validate the developed script.

As propane is a flammable refrigerant, many studies on the cooling capacity of hydrocarbon air-conditioning systems have been carried out to identify best operating conditions which support the safety of propane use. One way to support the safe use of propane as a refrigerant is to reduce the internal volume of the heat exchanger (evaporator and condenser) (Poggi et al., 2008; Siang and Sharifian, 2013). Jain and Mishra, 2011, in their simulation study, found that the cooling capacity of evaporators increase with a decrease in inlet pressure (Jain et al., 2011). Fernando et al., 2004, in their experimental research regarding propane heat pumps, found that, optimum charge of heat pump decreased with a decrease in the evaporator temperature without any adverse effect on the coefficient of performance of the system. The effect of an increase in refrigeration temperature on refrigerant condition at the evaporator outlet was explained in the research of Fernando et al., 2004. They found that an increase in evaporation temperature slightly decreases superheat at the evaporator outlet. Mastrullo et al., 2014 found the same result of the research by Fernando et al., 2004. Cheng et al., 2014 found that an increase in the evaporation temperature decreases the cooling capacity. The increase in evaporation pressure/temperature decreases the heat transfer at the evaporator (Mastrullo et al., 2014). Vaitkus, 2012 found that an increase in evaporation pressure increases compressor current. Very low pressure of refrigerant at the evaporator has a negative impact on cooling performance because the ready appearance of frost at the evaporator (Teng et al., 2012). Fatouh et al., 2010 found that cooling capacity, COP

and evaporator pressure increase with an increase in the evaporator air volume flow rate (Fatouh et al., 2010). The effect of evaporator design on the performance of heat pumps was carried out by Blanco Castro et al., 2005. They found that a smaller volume of heat exchanger gives a higher COP but has a lower heat transfer coefficient.

4.2 Methodology

This work focuses predominately on computational modelling, and experiments are only used to validate the accuracy of the model. Experimental and computational details are given in this section.

4.3 Experimental Setup

The air-conditioner used in this research is a single-duct portable propane air conditioner. The cooling capacity of the air conditioner is 2.85 kW, 300g charge. Charging of the air conditioner was carried out by a professional technician with a special charging machine (SkillsTech Australia). A straight capillary tube used as an expansion device has a 0.47 m length, 3 mm outside diameter and 1.62 mm inside diameter. The condenser and evaporator heat exchangers are fin and tube models with brass pipe and aluminium fins. The condenser pipe length is 17.28 m with 6.43 mm and 7.14 mm inside and outside diameter, respectively. The condenser fins are aluminium with 0.15 mm thickness, height 320 mm. The width of the fin is 85 mm for four sets of coils. The evaporator pipe length is 12.6 m with the same outside and inside diameter as the condenser. The height and width of the evaporator fins are 250 mm and 40 mm, respectively. The thickness of the evaporator fins is similar to the condenser fins. The inlet and outlet pipe diameter of the evaporator is similar to

the condenser pipe. The material of the condenser pipe and its fins are the same as the evaporator pipe and its fins.

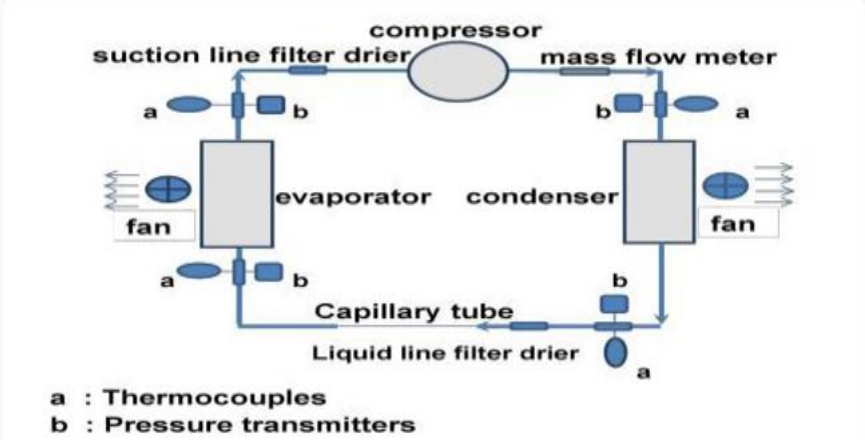

Figure 4-1 Schematic diagram of the air-conditioner and experimental setup

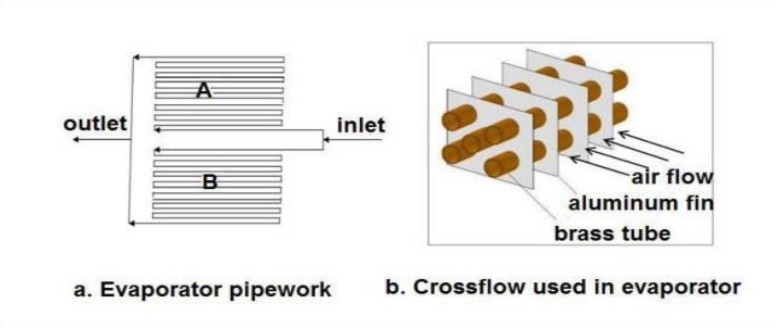

Figure 4-2. Diagram of pipe and cross flow arrangement used in the evaporator

To obtain data from the evaporator, a Coriolis Flowmeter (SIEMENS SITRANS FC430), two pressure transmitters (WIKA A-10 type) and two type J thermocouples were integrated to the air conditioning system. The mass flow meter was installed inline after the compressor to make sure that the passing fluid flows were in a superheated condition. Thermocouples and pressure transducers were installed at the inlet and outlet of the evaporator. A digital vane anemometer (Lutron LM-8000) was used to measure the wind speed in the vicinity of the evaporator coil. Ambient temperature was measured using a separate K-type thermocouple. All of the instruments, except for the anemometer, were connected to the data logger

(LabVIEW version 12) and all data were recorded by the computer. A schematic diagram of the air-conditioner system used in this research can be seen in Figure 4-1. The pipe work of the evaporator and cross flow arrangement used in the evaporator can be seen in Figure 4-2.

4.4 Computational Work

A formula to calculate heat transfer from surroundings to the evaporator is (Incropera, 1996):

$$q = (T_{amb} - T) \times (h_{air} + h_r) \times A_{t\times} \left(1 - \frac{(N \times A_f)}{A_t \times (1 - \eta_f)}\right) \qquad (4.1)$$

Where T represents propane temperature (°C), T_{amb} ambient temperature (°C), h_{air} convective heat transfer coefficient of air (W/m^2K), h_r radiative heat transfer coefficient (W/m^2K), A_t total area of fins and pipes (m^2), N number of fins, A_f area of one fin (m^2), and η_f fin efficiency. The convective heat transfer coefficient is determined as follows (Incropera, 1996):

$$h_{air} = \frac{Nu_{air} \times k_{air}}{H_f} \qquad (4.2)$$

Where Nu_{air} represents Nusselt number of air, k_{air} thermal conductivity of air (W/m K), and H_f height of fin (m). In the case of turbulent flow, Nusselt number is calculated as (Incropera, 1996):

$$Nu_{air} = (0.037 \times Re^{0.8} - 871) \times Pr^{(1/3)} \qquad (4.3)$$

and in the case of laminar flow, Nusselt number is calculated as (Incropera, 1996):

$$Nu_{air} = 0.664 \times Re^{0.5} \times Pr^{(1/3)} \qquad (4.4)$$

Where Pr represents the Prandtl number of air, and the Reynolds number of air (Re) blowing on the evaporator is based on the fin width (Incropera, 1996). The fin efficiency is calculated as:

$$\eta_f = \frac{\tanh m \times L_c}{m \times L_c} \quad (4.5)$$

Where Lc is the corrected fin length and can be calculated as:

$$L_c = H_f + \frac{t_f}{2} \quad (4.6)$$

Where t_f represents the thickness of the fin. The parameter m in formula 4.5 can be calculated as:

$$m = \left(\frac{h_{air} \times P}{k_{air} \times A_f}\right)^{1/2} \quad (4.7)$$

Where P represents the perimeter of the fin (m). The convective heat transfer coefficient, fin perimeter, and fin area can be calculated as:

$$h_{air} = \frac{Nu_{air} \times k}{w_f} \quad (4.8)$$

$$P = 2H_f + 2t_f \quad (4.9)$$

$$A_f = 2\, H_f \times w_f - \frac{\pi}{4} do^2 \quad (4.10)$$

Where W_f, and d_0 represent fin width, and outside diameter of the pipe, respectively. There are no fins at the bendings, or at the connecting pipes between the evaporator and thermocouples. At these sections, Nusselt number is calculated as follows (Cengel, 2004):

$$Nu_{air} = \left\{0.6 + \frac{0.387 \times Ra^{1/6}}{\left[1+(0.559/Pr)^{9/16}\right]^2}\right\}^2 \quad (4.11)$$

Where Rayleigh number (Ra) is defined as follows:

$$Ra = \frac{g \times \beta \times (T - T_{amb})}{v^2} \quad (4.12)$$

and g and ν represent the gravity (m/s^2) and kinematic viscosity (m^2/s), respectively. The coefficient of volume expansion (β) is:

$$\beta = \frac{1}{T_f} \quad (4.13)$$

T_f is the film temperature and is the average of wall and room temperatures.

The convective heat transfer coefficient of air at the locations where no fins are deployed is defined as (Cengel, 2004):

$$h_{air} = \frac{Nu_{air} \times k_{air}}{d_o} \quad (4.14)$$

The radiative heat transfer coefficient (h_r) can be calculated as:

$$h_r = 4 \times \sigma \times \in \times T_m^{\,3} \quad (4.15)$$

Where σ, ε and T_m represent the Stefan-Boltzmann constant (5.6703×10^{-8} W/m^{2}K^4), emissivity and mean temperature, respectively. The emissivity of copper is assumed to be 0.5 (Incropera, 1996).

The outlet enthalpy (h_{out}) at the steady state is estimated using the energy conservation equation as follows (Cengel, 2006):

$$h_{out} = h_{in} - \frac{q}{\dot{m}} + \left(\frac{V_{in}^{\,2} - V_{out}^{\,2}}{2}\right) \quad (4.16)$$

Where h_{out} represents the outlet enthalpy (J/kg), h_{in} inlet enthalpy (J/kg), $\dot{m}$ is mass flow rate (kg/s), V_{in} inlet velocity of refrigerant (m/s), and V_{out} outlet velocity (m/s) of refrigerant. As the outlet velocity is not initially known, the script uses a loop and reiterates the calculation until the outlet enthalpy and velocity satisfies formula 4.16.

The pressure losses (ΔP) is calculated as follows (Fox, 2004):

$$\Delta P = h_l \times \rho_f \quad (4.17)$$

The density of the refrigerant is represented by ρ_f, and total loss (h_l) is calculated using the following formula (Fox, 2004):

$$h_l = \frac{L \times f_{ref} \times V_{ave}^{\,2}}{2 \times d_i} \quad (4.18)$$

Where L represents the length of segment (m), f_{ref} friction factor, V_{ave} average velocity of the refrigerant at the inlet and outlet of the segment (m/s), and d_i the inside diameter of the segment (m). The friction factor (f_{ref}) is calculated based on

Colebrook equation. The equivalent lengths of minor loss of 180-degree bends and T-junctions are assumed to be 14 and 20 times that of the pipe diameter (Fox, 2004). Properties of fluid are calculated based on Refprop 6.0 (McLinden et al., 1998).

The evaporator was divided into 150 segments in the bending pipe of the evaporator and 215 segments in the straight sections of each coil. The inlet of each segment was assumed to be the outlet of the previous segment. For the calculation of each segment, average properties of refrigerant at the inlet and outlet of the segment were used. In the first iteration, outlet properties were the same as the inlet properties, but the script iterates the calculation until the change of outlet properties becomes negligible (in order of 10^{-14}).

The formulas used for calculation on condenser were the same as the formulas used for calculation on the evaporator. The condenser was divided into 168 segments in the straight sections of each coil. At bending sections, the number of segments was the same with the evaporator's.

The capillary tube was a straight brass capillary tube. It was divided into 700 segments. The pressure drops within the capillary tube and thermodynamic process were calculated using the same formulas as evaporator's. The heat transfer process between the capillary tube and its surrounds was assumed as natural convection as the capillary tube was covered by a transparent hose and there no air motion around the tube.

The compression process within the compressor was assumed as isentropic compression process. In this case, compressor work was calculated using the formula:

$$w_{comp} = \dot{m}(h_{out\_comp} - h_{in\_comp}) \quad (4.19)$$

4.5 Validation

4.5.1 Evaporator

Figure 4-3 shows that the difference between the computational results and measured data of the evaporator's outlet pressure is reasonable. At 20°C room temperature, the calculated pressure was 4.1% higher than that from measured pressure at 261g charge, and is 7.7% higher than that from measured pressure at 390g charge. The calculated pressure at 32°C room temperature was 3.1% higher than that from measured pressure at 261g charge, and 4.3% higher than that from measured pressure at 390g charge. At 35°C room temperature the calculated pressure was 2.9% higher than the measured pressure at 261g charge, and 4.2% higher than measured pressure at charge of 390g.

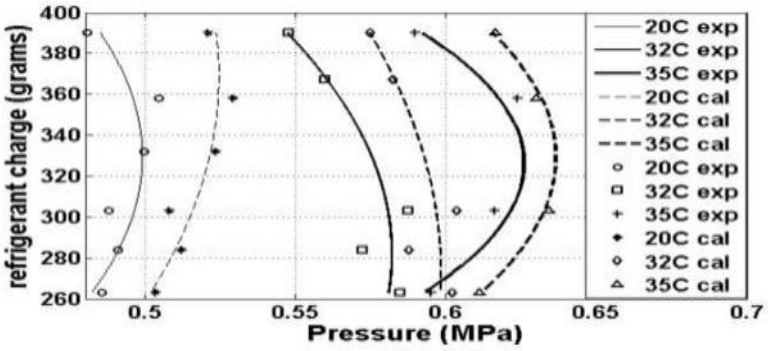

Figure 4-3. Comparison of measured and calculated outlet pressure of evaporator

Figure 4-4 shows the comparison of data measured and calculated cooling capacity at 20°C, 32°C and 35°C room temperature. The Figure shows that at 20°C and 261g charge, the cooling capacity from calculation is 0.1% higher than the cooling capacity from data measured however, at 20°C and 390g charge, the Figure shows the calculated results is 6.3% lower than the cooling capacity from data measured. At 32°C room temperature and 261g charge, the calculated cooling capacity is 12.4% higher than the measured cooling capacity, the difference of calculation and

measured data decreases as the charge increases. It shows the calculation is 6.8% higher than the measured cooling capacity. The calculation cooling capacity is also higher than the cooling capacity at 35°C room temperature. The Figure shows that at 261g charge, the calculation is 15.0% higher and 10.0% higher at 390g charge compared to the experiment results.

The calculation results on the evaporator give the accuracy greater than 9.0%. Compared to the previous research, these results are more accurate than previous work. Nilpueng at al., 2011 reported uncertainty of 13.2% while the present results are less accurate than the accuracy reported by Cheng et al., 2014 (5%) and by Herbert-Raj and Lal, 2011 (2.9 – 3.7%). The uncertainty of mass flow rate was ±0.000138 kg/s, refrigerant pressure was ±25kPa, refrigerant temperature was ±1°C, room temperature was ±0.5°C and air speed was ±0.09 m/s.

4.5.2 Full Air conditioner

The calculation work of this research also can be compared to the calculation work of one full cycle of the air conditioner system. Figure 4-5 shows a T – s diagram of experimental data and computational work. From the Figure, it can be seen that the T – s diagram of computational work is close to the real data from measurement.

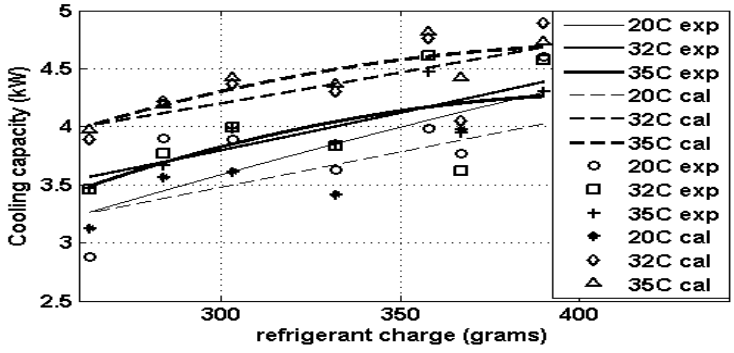

Figure 4-4 Comparison of measured and calculated cooling capacity

Table 4-1 shows the deviation of calculated results from the measured data. At the capillary tube inlet, the calculated temperature and pressure deviate 1.42°C and −0.007 MPa (−0.6% deviation), respectively. Deviation temperature and pressure at evaporator inlet is −2.36°C and 0.02 MPa (−4.0% deviation), respectively. Temperature and pressure deviation at the compressor inlet are 0.20°C and −0.005 MPa (−1.0% deviation), respectively.

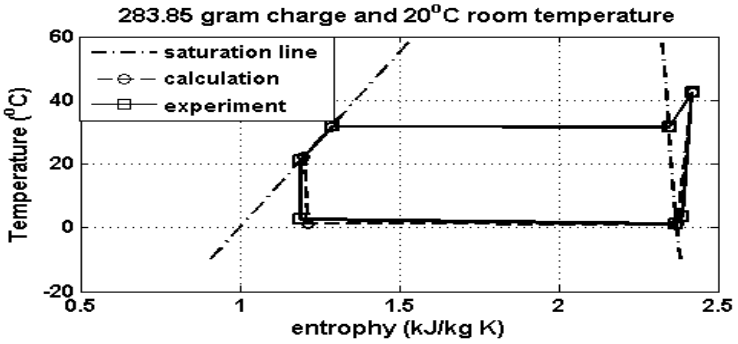

Figure 4-5: T - s diagram for full cycle at 283.85g charge and 20°C room temperature

Table 4-1: Inlet temperature and pressure of four main parts of the air conditioner by measurement and computational work

	Cond. Inlet		CT inlet		Evap. Inlet		Comp. inlet	
	T (°C)	P (MPa)	T (°C)	P (MPa)	T (°C)	P (MPa)	T (°C)	P (MPa)
E	42.4	1.13	20.98	1.133	3.67	0.514	3.65	0.491
C	42.4	1.13	22.41	1.126	1.31	0.494	3.86	0.486
D	0	0	1.42	-0.007	-2.36	-0.02	0.20	-0.005

E: Experimental result
C: Calculated results
D: Deviation of calculation from the experimental result

As the uncertainty of measurement is in the range of the uncertainty of measurement of the previous studies, the result can be used to estimate the performance of the air conditioner.

4.6 Results and discussion

4.6.1. Results

4.6.1.1. Effect of inlet pressure

The evaporator inlet pressure produces a significant contribution in amount of mass accumulated within the evaporator. Figure 4-6a shows that the mass accumulated within the evaporator increases when the inlet pressure to evaporator increases. With total mass accumulated within the evaporator at 0.4 MPa inlet pressure is 67.77g refrigerant. Figure 4-6a shows accumulated refrigerant mass within the evaporator at 0.8 MPa is 176.85g. The change of accumulated heat transfer rate can be observed from Figure 4-6b. The accumulated heat transfer rate decreases when the inlet pressure increases. At 0.4 MPa, the accumulated heat transfer rate is 4.32 kW, and it decreases at 0.8 MPa inlet pressure to 0.96 kW.

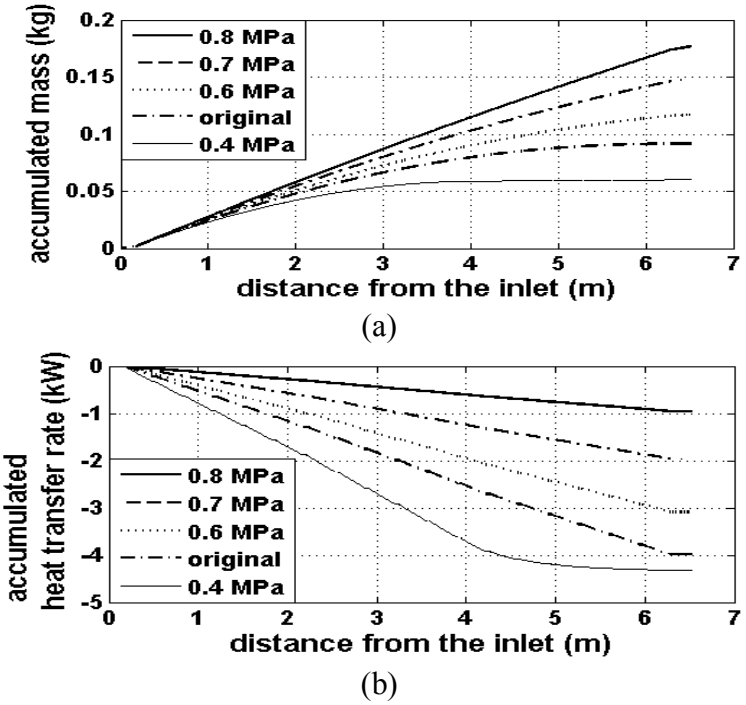

Figure 4-6 a) Effect of evaporator inlet pressure on accumulated mass, b) effect of evaporator inlet pressure on accumulated heat transfer in evaporator

The specific heat transfer rate is the heat transfer rate divided by the total mass of refrigerant within the evaporator pipe from the inlet of the evaporator to a specific point. A specific point refers to the length of the pipe from the inlet of the evaporator until a point along the evaporator pipe. Figure 4-7 shows the variation of specific heat transfer rate by the change of evaporator inlet pressure. The highest specific heat transfer rate is at evaporator inlet's lowest pressure. From the Figure, it can be seen that the specific heat transfer rate at 0.4 MPa inlet pressure is 71.9 kW/kg and decreases to 5.4 kW/kg when the evaporator inlet pressure is increased to 0.8 MPa.

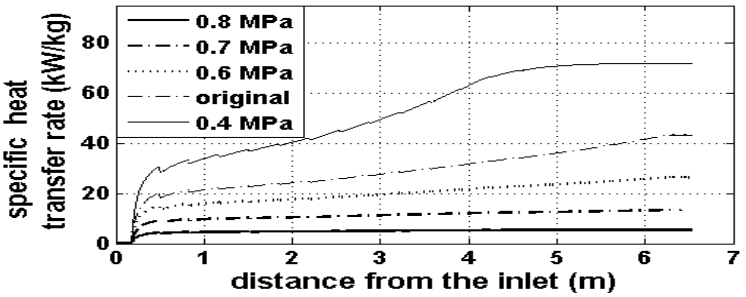

Figure 4-7 Effect of inlet pressure change on specific heat transfer raate

Based on the results of accumulated mass, accumulated heat transferred and specific heat transfer rate in Figure 4-6a, Figure 4-6b and Figure 4-7, it can be seen that decreasing the evaporator pressure gives the better result. Accumulated mass, accumulated heat transfer and specific heat transfer rate remain constant at the outlet of the evaporator and lower pressure (Figure 4-6a, 4-6b and 4-7). However, it should be noted that at lower pressure, the evaporator temperature is low which easily causes the evaporator coil to be covered by the ice layer (frosting) (Teng et al., 2012) particularly at evaporator temperature lower than 0°C.

4.6.1.2. Effect of shortening evaporator

The evaporator with pressure below the original condition is effectively shortened, because the degree of superheat refrigerant at evaporator outlet condition is more than at original. Table 4-2 presents the results of shortening the evaporator pipe.

From the Table, it can be seen that the cooling capacity of the system decreases if the evaporator pipe is shortened. At 0.2 MPa, 0.3 MPa and 0.4 MPa evaporator inlet pressure, the cooling capacity decreases 5.6%, 2.9% and 0.91%, respectively. The mass of refrigerant also decreases when the evaporator pipe is shortened. The percentage of refrigerant mass reduction is by 63.0%, 48.4% and 27.8% at evaporator inlet pressure of 0.2 MPa, 0.3 MPa and 0.4 MPa, respectively.

Table 4-2: Results of shortened evaporator

Pin (MPa)	Cooling capacity (kW)	COP	Mass (kg)	Evap. Length (m)
0.2000	3.6125	3.8029	0.0340	5.1943
0.3000	3.7146	4.7142	0.0475	6.6800
0.4000	3.7924	5.6114	0.0664	9.4633
0.4940	3.8272	6.5937	0.0920	12.6000

4.6.1.3. Effect of wind speed

The effect of evaporator air speed on accumulated refrigerant mass within the evaporator is presented in Figure 4-8a. From the Figure, it can be seen that accumulated mass within the evaporator decreases with the increase in air speed. Accumulated mass decreases from 110. 307g of refrigerant at 1 m/s air speed to 68.03g of refrigerant at 3.0 m/s air speed.

The accumulated heat transfer rate is also affected by the air speed over the evaporator. The accumulated heat transfer rate increases with the decrease in air speed over the evaporator (Figure 4-8b). The heat transfer rate in the evaporator changes from 3.21 kW at air speed of 1.0 m/s to 4.28 kW at 3.0 m/s air speed.

The specific heat transfer rate increases with an increase in air speed over the evaporator. The highest specific heat transfer rate (62.84 kW/kg) is at 3.0 m/s air speed and the lowest heat transfer rate (29.08 kW/kg) is at 1.0 m/s air speed.

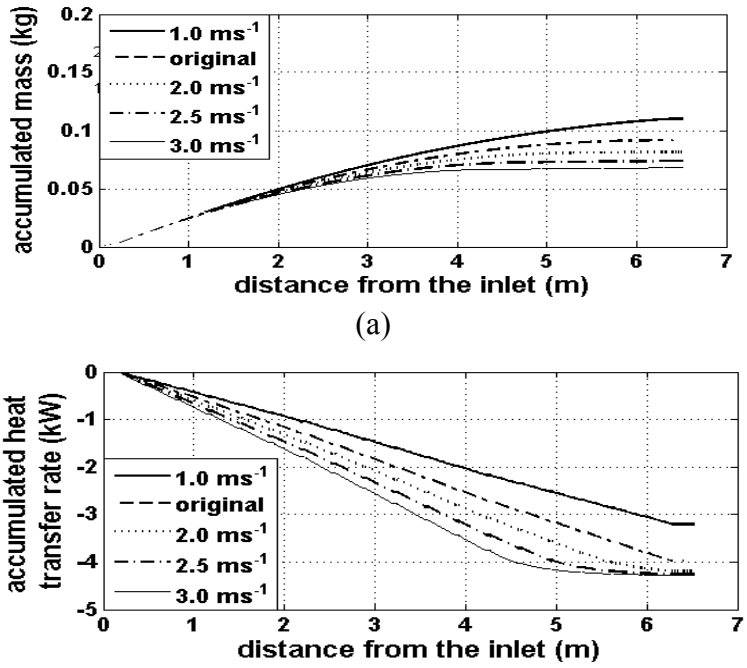

Figure 4-8 Effect of wind speed on accumulated mass (a) and accumulated heat transfer rate (b) of refrigerant in evaporator

It can be seen from Figure 4-8a, 4-8b, 4-9a and 4-9b, accumulated mass and heat transfer, specific heat transfer rate remain constant at the outlet of the evaporator.

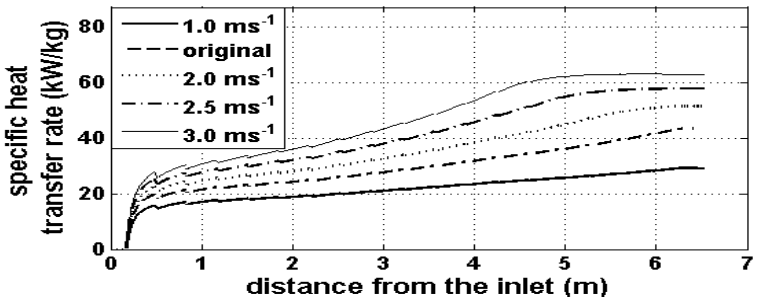

(a)

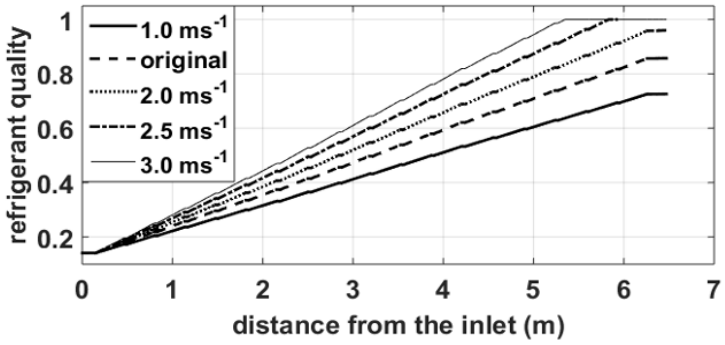

(b)

Figure 4-9Effect of velocity change on specific heat transfer rate (a) and refrigerant quality (b)

4.6.2. Discussion

In this work, the cooling capacity of a single duct portable propane air conditioner has been assessed by a simulation tool. The inlet pressure of the evaporator was varied by assuming the capillary tube of the air conditioner was in adiabatic condition. The calculated results were compared to the experimental work with the accuracy in the range of the accuracies of previous work.

The results show that the lower pressure of the evaporator gives a higher cooling capacity of the evaporator. At 0.4 MPa evaporator inlet pressure, the cooling capacity is 4.32 kW. This result is in agreement with previous studies (Jain et al., 2011; Mastrullo et al., 2014; and Cheng et al., 2014). However, it should be noted that at lower evaporator pressure, frost readily appears at the evaporator (Teng et al., 2010).

The amount of refrigerant mass within the evaporator decreases with a decrease in evaporator pressure. The present research shows the lowest mass of refrigerant within the evaporator is 67.77 g at 0.4 MPa evaporator inlet pressure.

The cooling capacity of the air conditioner increases with an increase in air speed over the evaporator. The highest cooling capacity is 4.28 kW at 3.0 m/s. This result is in agreement with the previous study by Fatouh et al., 2010.

The mass of refrigerant within the evaporator decreases with an increase in air speed over the evaporator. The lowest mass of refrigerant within the evaporator is 68.03g at 3.0 m/s.

It was found that lower inlet pressure of the evaporator and higher speed of air over the evaporator have significantly reduce the mass of refrigerant within the evaporator and increase the cooling capacity of the air conditioner. Also, the heat transfer rate is low near the outlet of the evaporator due to the refrigerant has all evaporated. The above discussion shows; the mass of refrigerant and cooling capacity increase when the inlet pressure of the evaporator decreases and speed of air over the evaporator increases.

Decreasing the refrigerant within the evaporator is important for a propane air conditioning system. One way to decrease the refrigerant mass is to shorten the evaporator pipe (Table 2-5). The evaporator pipe with inlet pressure lower than the original pressure can be shortened due to the ineffective heat transfer at the evaporator outlet. Shortening the evaporator pipe results in lower accumulated refrigerant mass, lower accumulated heat transfer rate, and lower COP (Table 2-5). Lower COP and less refrigerant charge in a shorter evaporator were also found by Zhou and Gan (2019). The percentage of decrease in cooling capacity is much lower

than the reduction in accumulated refrigerant mass. Changing the speed of air over the evaporator changes the performance of the air conditioning system. Increasing the speed of air over the evaporator from the original speed improves the performance of the air conditioning system. The mass accumulated within the evaporator decreases with an increase in airspeed over the evaporator. The accumulated heat transfer rate and specific heat transfer rate increase with an increase in airspeed over the evaporator (Table 2-5).

The research also analysed the performance of the portable propane air conditioning system under different evaporator inlet pressures, different wind speeds, and different evaporator sizes. The outputs of the research are cooling capacity, COP, refrigerant mass, and the specific heat transfer rate of the air conditioning system. The first step was to analyse the effect of different evaporator inlet pressures. Decreasing the evaporator inlet pressure resulted in a higher evaporator heat transfer rate, an increase in the specific heat transfer rate and a decrease in the accumulated refrigerant mass within the evaporator compared to the original (Table 2-5). However, by decreasing the evaporator pressure it is more likely easier for frost to form around the evaporator coil due to the low temperature of the evaporator. Increasing the evaporator's inlet pressure causes a lower heat transfer rate, lower specific heat transfer rate, higher accumulated refrigerant mass, and evaporator temperature.

4.7 Conclusions

As the limit of charge of propane within the air conditioner is important, the evaporator inlet pressure should be designed at low level. The lower evaporator inlet

pressure leads to a smaller mass charge within the evaporator. However, the problem is frost easily appears at lower pressure.

Another alternative for keeping the evaporator charge low is increasing the air speed over the evaporator. Also, with a higher air speed, the risk of frost appearing at the evaporator coil can be minimized.

Another heat exchanger in an air conditioning system is the condenser. The condenser contains the highest refrigerant mass as some refrigerant is in a sub-cooled condition. The next chapter discusses the technique for reducing the refrigerant charge within the condenser.

CHAPTER 5 EFFECT OF INLET PRESSURE ON THE PERFORMANCE AND SIZE OF THE CONDENSER OF THE PORTABLE PROPANE AIR CONDITIONER

This chapter provides the technique for reducing the refrigerant mass within the condenser. Refrigerant within the condenser changes from a superheated vapor to a sub-cooled condition. Most of the refrigerant in the air conditioning system accumulates within the condenser. Finding ways to reduce the refrigerant mass within the condenser is important for safety as refrigerant is flammable. The technique provided in this chapter involves computational work to change the condenser's inlet pressure, thus allowing minimum refrigerant within the condenser without sacrificing air conditioning system performance. This Chapter was adopted from the article that was submitted to the Journal of Thermal Science and Technology.

5.1 Introduction

Refrigerants are used to transfer heat from and to the surrounding environment. They absorb and release heat during evaporation and condensation. They can be divided into two groups of substances: natural and synthetic. Most synthetic refrigerants have a negative impact on the environment, contribute to global warming and ozone depletion (Gartshore, 1997), and have been linked to the appearance of some new diseases (Houhton et al., 2001). The use of synthetic refrigerants is being phased out and is scheduled to be completely banned by 2030 (Teng et al., 2012).

Of all the components in its system, the condenser of an air-conditioner contains the maximum mass of refrigerant (Corberan et al., 2008). No substantial reduction of the

refrigerant mass can be achieved without a significant reduction to the refrigerant mass inside the condenser (Fernando et al., 2004). Fernando et al., 2007 found that by increasing the condensing temperature, the required charge of the refrigerant decreases without changing the size of the condenser. It was also found that increasing the condensing pressure increases sub-cooling (Martinez-Galvan., 2011). The optimum Coefficient Of Performance (COP) of the air-conditioning system depends on the sub-cooling temperature ranging from approximately 7°C to 10°C (Martinez-Galvan., 2011). In another work it was stated that, based on ARI standard calculation cycle, 8.3°C sub-cooling gives the best results (Chen et al., 2011).

Joo et al., 2011 analysed the effect of changing the condenser inlet pressure on cooling capacity. They found that the cooling capacity of the air-conditioner increases by increasing the condenser pressure. This result also agrees with other research results (Kim et al., 2014). However, by changing the condenser pressure, the COP of the air conditioner decreases (Joo et al., 2011; Corberan et al., 2011; Padmanabhan and Palanisamy, 2013). An increase in the inlet pressure of the condenser also affects the degree of sub-cooling. Kim et al., 2014 found that the degree of sub-cooling increased with an increase in the condenser pressure.

This study aims to assess and quantify the effect of increasing inlet pressure on the capacity of the condenser (heat rejected by the condenser) and on the required mass of refrigerant within the condenser of a single-duct portable air-conditioner. The amount of charge within the system is significant as each country has its own safety protocols and legislation. In the EU, the 150g charge limit recommendation is set forth by the International Electro technical Commission's (IEC) while the U.K has a more flexible stance toward R-290 and approves charges up to 500g (Wicher, 2017). During this research, it appeared the US was going to adopt a maximum of 300g

propane charge. However, the EPA did not approve the use of propane refrigerant in any type of air conditioner, even warning it poses a potential fire or explosion hazard (AHRI, 2017).

A single-duct portable air conditioner is an air conditioner system in which all parts of the system are in one package. Portable air conditioners are placed inside the conditioned room which indicates, that contrary to split systems, the air temperature blowing over evaporator and condenser are the same. In this work, a script has been developed to assess the performance of a condenser under different inlet pressures. The results of the script were validated using the experimental results on a portable propane air-conditioner.

5.2 Apparatus

The air conditioner used in this research is a portable air conditioner with a cooling capacity of 2.85 kW and a compressor that runs on an electric power of 0.90 kW. The evaporator of this system has two sets of coils. The condenser of the propane air-conditioner has four sets of coils and is shown in Figure 5-1. The first and second sets are connected in parallel, and the combination is connected in series with the third and fourth sets.

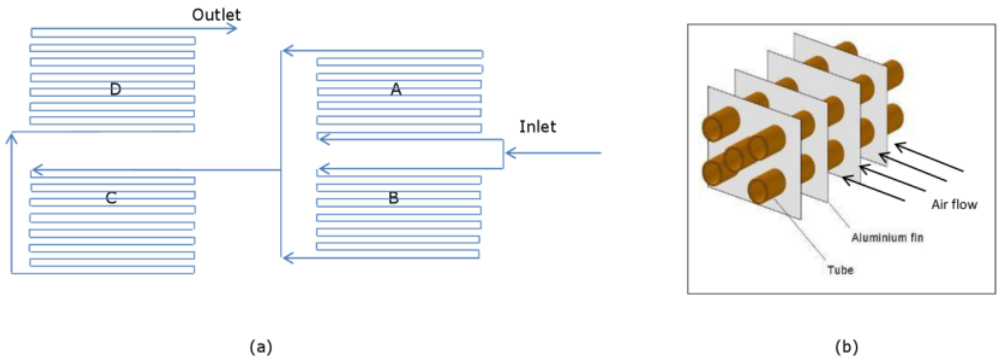

Figure 5-1 Detail arrangement of the condenser and cross flow arrangement used in the air-conditioning system, a)pipe work of condenser b) cross flow used in the

condenser

The coils are made of copper, and their inside and outside diameters are 6.43 mm and 7.14 mm, respectively. The total length of the coils is 17.28 m. The straight sections of the coils have a length of 0.28 m, and the diameter of the curved corners is 0.02 m. The first and second sets of coils include six full coils and the third and fourth sets have seven full coils. The straight sections of coils include six fins per centimeter, but no fins are deployed at the corners. The width of fins is 3 cm, 1.3 cm, 1.35 cm, and 2.85 cm in order of the set numbers. All fins are made of aluminum and their thickness and height are 0.15 mm and 22 mm, respectively. The refrigerant enters from the top and exits at the bottom, the height difference is about 30 cm.

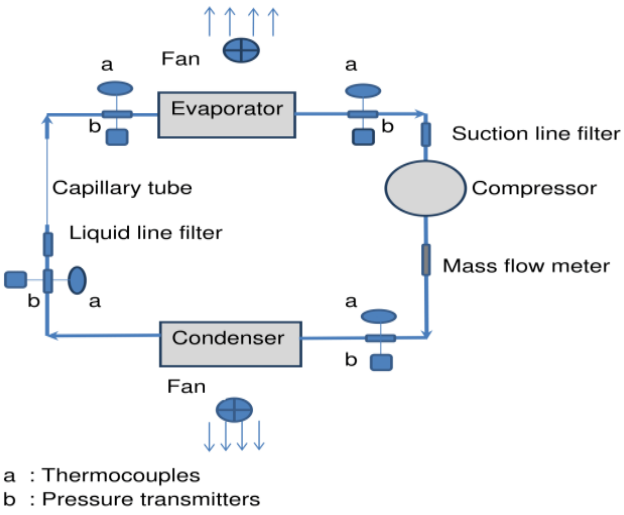

Figure 5-2 A schematic diagram of air conditioning system and layout of instrumentation

The capillary tube of the system is a straight 0.47 m brass capillary tube with 1.62 mm inside diameter and 3.00 mm outside diameter. The evaporator dimension is 0.25 m × 0.32 m × 0.04 m (height × length × width). The evaporator consists of two parallel small fin and tube heat exchangers, with total length of pipe being 12.6 m. The material of evaporator and its fins are made of the same material of the condenser and its fins.

The experimental instruments include a Coriolis mass flow meter (Siemens SITRANS FC430) located at the inlet of the condenser, four J-type thermocouples and four piezoresistive pressure transmitters (Wika type A-10) at the inlet and outlet of the condenser, an anemometer (Lutron LM-8000) to measure air flow speed passing across the condenser, and two K-type thermocouples to measure the ambient temperature. All of the instruments, except for the anemometer, are connected to the data logger (LabVIEW version 12) and all data are recorded by the computer. Figure 5-2 shows a schematic diagram of the air-conditioning system and layout of instrumentation.

5.3 Heat Transfer Model

The heat transfered from the coils (q) at the sections including fins are calculated using the following formula (Incropera, 1996):

$$q = (T - T_{amb}) * (h_{air} + h_r) * A_t * \left(1 - \frac{(N * A_f)}{A_t * (1 - \eta_f)}\right) \quad (5.1)$$

Where T represents propane temperature (°C), T_{amb} is ambient temperature (°C), h_{air} shows convective heat transfer coefficient of air (W/m^2K), h_r is radiative heat transfer coefficient (W/m^2K), A_t stands for total area of fins and pipes (m^2), N is number of fins, A_f denotes area of one fin (m^2), and η_f represents fin efficiency. The convective heat transfer coefficient is determined as follows (Incropera, 1996):

$$h_{air} = \frac{Nu_{air} * k_{air}}{H_f} \quad (5.2)$$

Where Nu_{air} represents Nusselt number of air, k_{air} is thermal conductivity of air (W/m K), and H_f denotes height of fin (m). In the case of turbulent flow, Nusselt number is calculated as (Incropera, 1996):

$$Nu_{air} = (0.037 * Re^{0.8} - 871) * Pr^{(1/3)} \quad (5.3)$$

and in the case of laminar flow, Nusselt number is calculated as (Incropera, 1996),

$$Nu_{air} = 0.664 * Re^{0.5} * Pr^{(1/3)} \quad (5.4)$$

Where Pr represents the Prandtl number of air, and the Reynolds number of air (Re) blowing on the condenser is based on the fin width (Incropera, 1996). The fin efficiency is calculated as,

$$\eta_f = \frac{tanh\, m\, L_c}{m\, L_c} \quad (5.5)$$

Where L_c is the corrected fin length and can be calculated as,

$$L_c = H_f + \frac{t_f}{2} \quad (5.6)$$

Where t_f represents the thickness of the fin. The parameter *m* in Formula 5.5 can be calculated as,

$$m = \left(\frac{h_{air} P}{k_{air} A_f}\right)^{1/2} \quad (5.7)$$

Where, *P* represents the perimeter of the fin (m). The convective heat transfer coefficient, fin perimeter, and fin area can be calculated as,

$$h_{air} = \frac{Nu_{air}\, k}{w_f} \quad (5.8)$$

$$P = 2H_f + 2t_f \quad (5.9)$$

$$A_f = 2\, H_f . w_f - \frac{\pi}{4} do^2 \quad (5.10)$$

Where w_f, and d_o represent fin width, and outside diameter of the pipe. There are no fins at the bendings, or at the connecting pipes between the condenser and thermocouples. The natural convection was assumed only at bending and forced convection was assumed for the rest of the model. The airflow from the condenser blower does not flow over the pipe bending therefore the heat transfer was assumed

as natural convection condition. At these sections, Nusselt number is calculated as follows (Cengel, 2004),

$$Nu_{air} = \left\{0.6 + \frac{0.387 * Ra^{1/6}}{[1+(0.559/Pr)^{9/16}]^2}\right\}^2 \quad (5.11)$$

Where Rayleigh number (Ra) is defined as follows,

$$Ra = \frac{g * \beta * (T - T_{amb})}{v^2} \quad (5.12)$$

and g and ν represent the gravity (m/s^2) and kinematic viscosity (m^2/s), respectively. The coefficient of volume expansion (β) is,

$$\beta = \frac{1}{T_f} \quad (5.13)$$

T_f is the film temperature and is the average of wall and room temperatures.

The convective heat transfer coefficient of air at the locations where no fins are deployed is defined as (Cengel, 2004),

$$h_{air} = \frac{Nu_{air} * k_{air}}{d_o} \quad (5.14)$$

The radiative heat transfer coefficient (h_r) can be calculated as,

$$h_r = 4 \times \sigma \times \in \times T_m^{\,3} \quad (5.15)$$

Where σ, ε and T_m represent the Stefan-Boltzmann constant (5.6703×10^{-8} W/m^2K^4), emissivity and mean temperature, respectively. The emissivity of copper is assumed to be 0.5 (Incropera, 1996).

The outlet enthalpy (h_{out}) at the steady state is estimated using the energy conservation equation as follows (Cengel, 2004),

$$h_{out} = h_{in} - \frac{q}{\dot{m}} + \left(\frac{V_{in}^{\,2} - V_{out}^{\,2}}{2}\right) \quad (5.16)$$

Where h_{out} represents the outlet enthalpy (J/kg), h_{in} is inlet enthalpy (J/kg), $\dot{m}$ is mass flow rate (kg/s), V_{in} represents inlet velocity of refrigerant (m/s), and V_{out} represents

outlet velocity (m/s) of refrigerant. As the outlet velocity is not known initially, the script uses a loop and reiterates the calculation until the outlet enthalpy and velocity satisfies Formula 5.16.

The pressure losses (ΔP) is calculated as follows (Fox, 2004):

$$\Delta P = h_l * \rho_f \tag{5.17}$$

The density of the refrigerant is represented by ρ_f, and total loss (h_l) is calculated using the following formula (Fox, 2004):

$$h_l = \frac{L * f_{ref} * V_{ave}{}^2}{2 * d_i} \tag{5.18}$$

Where L represents the length of segment (m), f_{ref} friction factor, V_{ave} average velocity of the refrigerant at the inlet and outlet of the segment (m/s), and d_i the inside diameter of the segment (m). The friction factor (f_{ref}) is calculated based on Colebrook equation. The equivalent lengths of minor loss of 180-degree bends and T-junctions are assumed to be 14 and 20 times of the pipe diameter (Fox, 2004). Properties of fluid is calculated based on Refprop 6.0 (McLinden et al., 1998).

The condenser was divided into 150 segments in bending and 168 segments in the straight section of each coil. The inlet of each segment was assumed to be the outlet of the previous segment. For the calculation of each segment, the average properties of refrigerant at each segment were used. In the first iteration, the outlet properties are as the same properties of inlet, but the script iterates the calculation until the change of outlet properties becomes negligible (in order of 10^{-14}).

The evaporator was calculated using the same formula as that used for the condenser. The number of segments for bending pipe is the same with the number of segments of condenser (150 segments and 215 segments in the straight section). The number

of segments of the evaporator is more than that in the condenser because the length of evaporator is longer than the length of the condenser.

Pressure drop and thermodynamic process within capillary tube were calculated using the same formula as that used for the condenser and evaporator. In calculating pressure drop and outlet thermodynamic properties, the capillary tube was divided into 700 segments however, the heat transfer process was calculated using the free convection heat transfer process. The speed of air around the capillary tube was assumed to be zero (the capillary tube is covered by a transparent hose and is not affected by wind flow of condenser and evaporator fans). The same with the pipe bend in the condenser and evaporator which are designed outside of air flow from the fans of evaporator and the condenser. Enthalpy difference between inlet and outlet of the compressor and mass flow rate of the refrigerant were used to calculate the compressor work using the following equation:

$$w_{comp} = \dot{m}\left(h_{out\_comp} - h_{in\_comp}\right) \tag{5.19}$$

Enthalpy inlet of the compressor is the same as the enthalpy outlet of the evaporator while the outlet enthalpy of the compressor is the same with the inlet enthalpy of the condenser. The compressor work was calculated as an isentropic compressor.

5.4 Uncertainty of Measurements

In this research, the uncertainties of measurements were categorised in three groups. The first group includes the directly-measured data such as room temperature, mass flow rate of the refrigerant, charge of the system, and pressures and temperatures at the inlet of all four main components of the air conditioner. Two main causes of the uncertainty of the first category were the effect of noise and drift. The maximum uncertainty of mass flow rate was ±0.00138 kg/s (11.94%), charge was ±0.01g

(0.003%), refrigerant pressure was ±25kPa (4.4%), refrigerant temperature was ±1°C (1.64%), and room temperature was ±0.5°C. Variation of room temperature was from 20°C to 35°C, as the result the relative uncertainty was 3.3% ((0.5÷15) ×100).

The second type of data such as density, enthalpy, and sub-cooling are those obtained from the table of properties. Therefore, the uncertainty of the data depends on the uncertainty of measured pressures and temperatures. For example, the maximum uncertainty of density of the refrigerant was determined by comparing the density at the measured pressure and temperature (P, T) with those obtained at four points of (P+25kPa, T), (P-25kPa, T), (T+1°C), (T-1°C). The same approach was applied to estimate the uncertainty of enthalpy and sub-cooling. The maximum uncertainty of density is 0.62 kg/m^3 (16.8%), uncertainty of enthalpy is 3.24 kJ/kg (7.1%), and uncertainty of sub-cooling is 1.4°C (15.24%).

The last category of data was obtained from calculation using the two previous types of data. Those data are velocity, cooling capacity, useful work of compressor, specific cooling capacity, and coefficient of performance. To estimate the maximum uncertainty of this type of data, the square root of the sum of the square uncertainties is applied. The results show a maximum uncertainty of refrigerant velocity is 7.65 m/s (20.61%), the cooling capacity is 0.45 kW (12.48%), the useful work of compressor is 73.6 W (13.89%), the specific charge is 0.0013 kW/kg (13.89%), and COP is 1.299 (18.38%). The uncertainties of measurement are within the range of previous studies. The cooling capacity uncertainty is lower than 13.2% reported by Nilpueng et al., 2011 but higher than 5% and 2.9% - 3.7% which were reported by Cheng et al., 2014 and by Herbert-Raj and Lal, 2011, respectively. Mass flow rate uncertainty of this work is lower than 0.0018 kg/s reported by Da Riva and Del Col, 2011. Temperature measurement uncertainty performed by Padalkar et al., 2014 is

±0.5°C which is comparable with the present work temperature measurement uncertainty.

5.5 Model Validation

The accuracy of the model was validated through the comparison of calculated and measured values at an ambient temperature of 20°C, with the air conditioner in 283.85g charge (a 5.4% undercharged condition), and the inlet propane in superheated state with a pressure and temperature of 1128.45 kPa and 42.4°C. The mass flow rate of propane was measured to be 0.01188 kg/s. Table 5-1 shows the measured and calculated values of inlet and outlet pressure, temperature, enthalpy, capacity of the condenser, specific capacity of the condenser and COP.

In Table 5-1, the measured value of temperature difference between the inlet and the outlet is 21.42°C, which is 6.6% greater than the calculated value of 20°C. The measured pressure along the condenser increases 4.9 kPa while the calculated value decreases by 2.4 kPa. The increase of measured pressure along the condenser is consistent with a previous study (Bell and Mueller, 2001) which states that the pressure rise due to the decrease of momentum can be greater than the decrease of pressure due to friction. However, the variation of measured pressure along the condenser is relatively small and less than the uncertainty of measurement (± 25 kPa) and can be ignored. The differences between the calculated values of enthalpy drop and capacity of the condenser and those calculated directly from the measured values are -3.82 kJ/kg (1.02%) and 0.04 kW (1.01%), respectively. In this case, calculated values of the total heat transfer from the condenser to the ambient, total mass within the condenser, and specific capacity of the condenser are 4.41 kW, 142.7g, and 30.89 W/g, respectively. In addition, the outlet refrigerant is determined

to be in a sub-cooling state, 9.33°C below the saturation temperature while the measured value is 14.8˚C. The calculated COP is 6.59 which is 0.7% lower than the COP that is calculated from measured values (6.64). Taking into account the uncertainty associated with the roughness of the pipes and effects of inflow of compressor oil into the condenser, this level of error is considered acceptable for the purpose of this study.

Table 5-1: Comparison between measured and calculated results at 283.85g charge and 20ºC ambient temperature

	measurement	**Calculation**
mass flow rate (g/s)	11.8	11.8[a]
T_{in} (°C)	42.40	42.40[a]
T_{out} (°C)	20.98	22.40
ΔT(°C)	21.42	20
P_{in} (MPa)	1.12845	1.12845[a]
P_{out} (MPa)	1.13335	1.1260
ΔP (kPa)	-4.9	2.4
h_{in} (kJ/kg)	629.618[b]	629.618[b]
h_{out} (kJ/kg)	254.689[b]	258.510[b]
Δh (kJ/kg)	374.929	371.425
Capacity of the condenser (kW)	4.4533	4.4084
Mass within condenser (g)	N/A	142.7
Outlet condition	14.8˚C sub-cooled	9.33˚C sub-cooled
Specific capacity of the condenser (W/g)	N/A	30.8928
COP	6.6433	6.5948

[a] : Measured values

[b] : The values are from table of properties of propane

5.6 Results

5.6.1 Increase in inlet pressure of the fixed size condenser

After determining the accuracy of the model, it was run for a range of inlet pressures from 1.3 MPa to 2 MPa at the ambient temperature of 27°C. The inlet entropy of the condenser in all cases were assumed to be equal to the outlet entropy of the evaporator (saturated vapour at 0.5 MPa) assuming an isentropic compressor. The inlet temperatures of the condenser are determined based on inlet entropy and pressure. In all cases at this stage, the condenser had the same geometries as described in the previous section, and the inlet mass flow rate was 0.0143 kg/s. However, the script shows that by increasing the inlet pressure of the condenser, the outlet condition of the evaporator changes, therefore the length of the evaporator was accordingly changed to prevent such variations among different cases. The results including the inlet and outlet pressures and temperatures, capacity of the condenser, the mass of propane in the condenser and evaporator, specific charge, and outlet state of refrigerant for different inlet pressures are presented in Table 5-2.

The outlet temperature is expected to increase as the inlet pressure increases. Table 5-2 indicates that this is the case only when the outlet refrigerant is in a saturated state (P_{in}<1.35 MPa). At the inlet pressure of 1.30 MPa, the inlet temperature is 41.23˚C, but the temperature along the condenser decreases due to heat transfer, but the outlet condition is still in saturated state and outlet temperature is 37.69°C. The outlet temperature is 38.33°C at the inlet pressure of 1.32 MPa which shows an increase of 0.64°C compared to the inlet pressure of 1.3 MPa. The outlet condition changes from a saturated state at 1.32 MPa to a sub-cooled state at the inlet pressures of 1.35 MPa and above. In those cases, the outlet temperature actually decreases with increasing pressure. This is due to the lower specific heat and enthalpy of

evaporation of propane at higher pressures. For example, at two pressures of 1.10 MPa and 2.10 MPa, evaporation enthalpies are 324.72 kJ/kg and 259.45 kJ/kg, respectively (McLinden et al., 1998). A lower enthalpy of evaporation is expected to reduce the outlet temperature because the refrigerant temperature only slightly decreases in a saturated state. In addition, it can be demonstrated from the data in (McLinden et al., 1998) that the specific heat of sub-cooled liquid propane decreases with increasing pressure. For example, the specific heat of propane at the pressure of 1.1 MPa is 2.74 kJ/kg K between two temperatures of 20°C and 30°C. This value decreases to 2.71 kJ/kg K at the pressure of 2.10 MPa over the same temperature range.

Table 5-2: Performance of the condenser at an ambient temperature of 27ºC

P_{in} (MPa)	P_{out} (MPa)	ΔP (kPa)	T_{in} (˚C)	T_{out} (˚C)	Cond. Cap. (kW)	Cond. charge (g)	Cond. Spec. capacity (W/g)	L_{evap} (m)	Evap. charge (g)	Total spec cap. (W/g)	Cool. Cap. (kW)	COP	Outlet state
1.3000	1.2973	2.7	41.23	37.69	4.234	119.4	35.461	9.378	55.1	19.887	3.612	5.752	Str
1.3200	1.3175	2.5	41.95	38.33	4.489	126.3	35.553	9.823	62.2	20.285	3.822	5.743	Str
1.3500	1.3477	2.3	43.21	33.24	4.774	136.0	35.103	10.492	70.7	20.687	4.110	6.151	Sc 6.06˚C
1.4000	1.3981	1.9	44.75	29.01	4.957	149.9	33.069	10.886	76.2	18.911	4.276	6.270	Sc 11.60˚C
1.5000	1.4985	1.5	47.98	27.52	5.068	171.3	29.586	11.023	78.3	17.409	4.345	6.007	Sc 16.45˚C
1.6000	1.5988	1.2	51.15	27.21	5.126	186.6	27.471	11.058	78.7	16.429	4.360	5.689	Sc 19.65˚C
1.7000	1.6989	1.1	54.11	27.12	5.169	197.8	26.132	11.075	79.0	15.767	4.364	5.420	Sc 22.51˚C
1.8000	1.7990	1.0	57.03	27.07	5.210	206.2	25.267	11.075	79.0	15.316	4.368	5.183	Sc 25.20˚C
1.9000	1.8990	1.0	59.76	27.05	5.245	212.9	24.636	11.075	79.2	14.922	4.359	4.918	Sc 27.76˚C
2.0000	1.9991	0.9	62.45	27.04	5.279	218.3	24.182	11.092	79.2	14.676	4.366	4.776	Sc 30.21˚C

Str : saturated state
Sc : sub-cooled

The capacity of the condenser continuously increases as the inlet pressure increases. For instance, the capacity is 4.23 kW and 5.28 kW at inlet pressure of 1.30 MPa and 2.00 MPa, respectively. However, the rate of increase of the capacity decreases as

the pressure increases. For example, by increasing the inlet pressure from 1.30 MPa to 1.40 MPa, the capacity of the condenser increases from 4.23 kW to 4.96 kW (17.1% increase), but the capacity of the condenser increases only 0.6% by increasing the inlet pressure from 1.90 MPa to 2.00 MPa.

In a similar manner to the capacity of the condenser, the propane charge in the condenser increases with increases of the inlet pressure. By increasing the pressure from 1.30 MPa to 1.40 MPa, the mass of the charge in the condenser increases from 119.4g to 149.9g, which indicates a 25.5% increase. At higher pressures, the mass still increases but the rate of increase becomes smaller. For example, by increasing the pressure from 1.90 MPa to 2.00 MPa, the mass increases from 212.9g to 218.3g, an increase of only 2.5%.

The specific capacity of the condenser decreases with increasing pressure. In the present case study, the minimum specific capacity is 24.18 W/g at the inlet pressure of 2.00 MPa. As was discussed above, the rate of increase of the condenser capacity is 0.6% for a pressure increase from 1.90 MPa to 2.00 MPa, but the rate of increase of the mass is 2.5% for this same pressure interval.

The total increase of the mass is expected to be slightly higher than the calculated value because, at the higher pressure of the condenser, the length of capillary tube should increase to maintain the same inlet conditions to the evaporator. According to Table 5-2, the propane mass within the evaporator also increases from 55.1g at 1.30 MPa and length of 9.38 m to 79.2g at 2.00 MPa and length of 11.09 m. Increase in mass of refrigerant within the evaporator is due to an increase in evaporator pipe length for having the same evaporator outlet condition when the inlet refrigerant quality of evaporator decreases. This will increase both cooling capacity and COP.

Taking into account the increase of mass in the evaporator, the specific capacity of the air conditioner drops from 19.89 W/g at 1.30 MPa to 14.68 W/g at 2.00 MPa (a decrease of 26.2%).

The increase of the inlet pressure of the condenser and corresponding increase of evaporator length increases the cooling capacity of the air-conditioner. The cooling capacity is 3.61 kW at 1.30 MPa and increases to 4.37 kW at the inlet pressure of 2.00 MPa (+20.87%). However, as the work of the compressor increases to produce a higher pressure, the overall coefficient of performance decreases. The COP is 5.75 at 1.30 MPa and drops to 4.78 at 2.00 MPa (-16.97%).

The above results show that increasing the inlet pressure of the condenser does not decrease the mass of propane for a specific cooling capacity but does increase the capacity of the condenser and sub-cooling. However, as a condenser is designed for a specific capacity, shortening the length of the condenser as pressure increases may reduce the mass within the condenser. To investigate this approach, a thorough understanding of the flow within the condenser is necessary.

5.6.2 Increase of the inlet pressure and shortening the condenser

Figure 5-3 presents the change of density, quality, temperature, specific charge, total mass, and condenser capacity at three inlet pressures of 1.30 MPa, 1.60 MPa, and 2.00 MPa. According to Figure 5-3, at the inlet pressure of 1.30 MPa, the quality reduces along the condenser, but the outlet flow is in a saturated state. At the inlet pressure of 1.60 MPa, at the length of 7.224 m, the quality of the refrigerant becomes zero and it will be in a sub-cooled state along the rest of the condenser. A similar trend can be seen for the inlet pressure of 2.00 MPa. In this case, the length at which the quality becomes zero is 3.8 m.

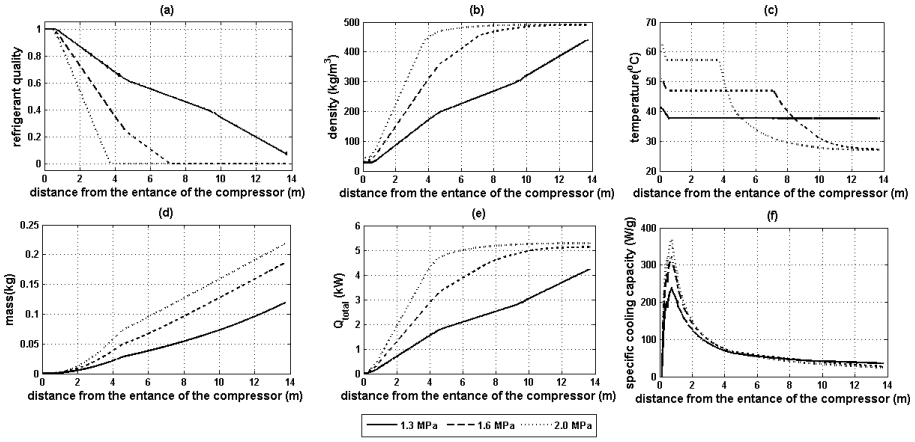

Figure 5-3 Variation of propane properties along the condenser at an ambient temperature of 27ºC, a)quality, b) density, c) temperature, d) mass, e) condenser capacity, and f) specific capacity of the condenser.

Figure 5-3b presents the change of the density. At the inlet pressure of 1.30 MPa, the density increases from 27.91 kg/m^3 at the inlet to about 435.89 kg/m^3 at the outlet of the condenser. The maximum density is 490.80 kg/m^3 for the inlet pressure of 1.60 MPa. The value of maximum density doesn't change significantly for the inlet pressure of 2.00 MPa (492.40 kg/m^3). However, as the refrigerant is in a sub-cooled state along a longer length of the condenser, the overall mass increases.

Figure 5-3c shows the temperature distribution within the condenser. As the inlet pressure increases, the temperature of the refrigerant at the entrance of the condenser increases on the assumption of isentropic compression from constant evaporator outlet conditions. In all cases, the temperature drop in the superheated and liquid state is sharp and is small in the saturated states. In the saturated state, pressure loss the only reason that the temperature falls. The change of temperature in the sub-cooled state is 19.64°C and 30.21°C at the inlet pressures of 1.60 MPa and 2.00 MPa, respectively; far greater than the values recommended in the literature.

Figure 5-3d indicates the accumulated mass of propane from the condenser entrance to specified lengths along the condenser. It should be noted that the coil sets 1 and 2 of the condenser are arranged parallel, thus the length on the Figure only shows the

length of the path of refrigerant particles, but the indicated mass includes the mass within the entrance pipe plus twice of the mass within coil sets 1 or 2. The Figure shows that the increase in mass is very small at the beginning, but its rate increases as the density increases along the condenser.

Figure 5-3e presents the total heat rejected from the condenser from the entrance to the specified length along the condenser in a manner similar to that presented in Figure 5-3d. As was expected, the results show that the rate of heat rejection decreases along the condenser due to the decrease of refrigerant temperature. The results show that at lengths over 12.65 m and 10.50 m and for the cases of 1.60 MPa and 2.00 MPa, respectively, the condenser malfunctions as the refrigerant temperature almost reaches the room temperature. This shows that shortening of the condenser is possible without reducing its capacity. Taking into account that the propane exists in a sub-cooling state and has the highest density at the outlet, this shortening can significantly reduce the mass within the condenser. This also can be concluded from Figure 5-3f. It shows the change of specific capacity along the condenser. In this Figure, the total heat transfer from the entrance is divided by the total mass from the entrance. According to Figure 5-3f, the specific capacity increases from the inlet of the condenser to a maximum value at the start of condensation, and then decreases toward the end of the condenser for all pressures.

The above discussion indicates that reducing the propane mass within the condenser is possible by shortening the length of the condenser. Figure 5-3e indicates that the total capacity of the condenser at the inlet pressure of 1.30 MPa and ambient temperature of 27°C is about 4.2 kW. This capacity can be achieved at the length of 3.96 m and the inlet pressure 2.00 MPa (see Figure 5-3e). The corresponding mass within the system is 56g (see Figure 5-3d). At that length, the propane outlet state is

saturated with a quality of 8% and sub-cooled at the inlet pressure of 1.30 MPa and 2.00 MPa, respectively (see Figure 5-3a). The corresponding outlet temperature is 37.68°C and 52.90°C at the inlet pressures of 1.30 MPa and 2.00 MPa, respectively (see Figure 5-3c). Table 5-3 lists the results at all inlet pressures investigated at the ambient temperature of 27°C and for the fixed condenser capacity of 4.2 kW.

Results in Table 5-3 indicate that by increasing the inlet pressure and shortening the length of the condenser for the condenser capacity of 4.2 kW (2.85 kW cooling capacity system) at ambient temperature of 27°C, the mass within the condenser and the outlet quality decreases (or sub-cooled increases) but the outlet temperature increases. The maximum reduction of the mass is 50.8%, which occurs at the inlet pressure of 2.00 MPa. In this case, the specific capacity is 73.59 W/g, far greater than the original condenser's specific capacity (35.10 W/g).

Table 5-3: Simulated charcteristic of the shortened condenser with a capacity of 4.2 kW (2.85 kW cooling capacity system) at room temperature of 27ºC

P_{inlet} (MPa)	Length of cond. (m)	Lengt of evap. (m)	Mass in cond. (g)	Mass in evap. (g)	$T_{out\ cond}$ (˚C)	Cooling cap (kW)	COP	Cond. specific capacity (W/g)	Total specific capacity (W/g)	Outlet state	Mass reducti on. (%)
1.3000	17.461	9.378	119.4	55.2	37.68	3.6123	5.7515	35.461	20.699	Tp x= 7.4%	NA
1.3200	17.461	9.823	126.3	62.2	38.33	3.822	5.7431	35.553	20.285	Tp x= 1.3%	NA
1.3500	17.461	10.492	136.0	70.7	33.24	4.1097	6.2286	35.103	19.887	Sc 6.060˚C	NA
1.4000	16.064	10.458	127.8	70.1	33.68	4.0947	6.0275	37.410	20.687	Sc 7.238˚C	-7.0
1.5000	13.931	10.200	115.5	66.4	36.71	3.9735	5.4927	40.686	21.846	Sc 7.265˚C	3.2
1.6000	11.943	9.926	99.4	62.3	39.84	3.8534	5.0198	46.428	23.828	Sc 7.029˚C	16.7
1.7000	10.109	9.667	83.1	59.1	42.34	3.7453	4.6455	54.744	26.347	Sc 7.305˚C	30.4
1.8000	8.980	9.429	73.6	55.7	45.16	3.6308	4.2941	60.703	28.069	Sc 7.137˚C	38.3
1.9000	8.081	9.172	65.1	52.7	47.74	3.5132	3.9935	67.438	29.825	Sc 7.103˚C	45.4
2.0000	7.272	8.949	58.8	49.9	50.06	3.4109	3.7323	73.588	31.377	Sc 7.219˚C	50.7

Tp : two phase
Sc : sub-cooled

Comparing results presented in Tables 5-2 and 5-3 indicates that COP decreases by reducing the length of condenser pipe at the same inlet pressure. At 1.40 MPa the

COP decreases from 6.27 (Table 5-2) to 6.03 (-3.9%), at 1.50 MPa, COP decreases from 6.00 to 5.49 (-8.5%) and it decreases from 4.78 to 3.73 (-21.8%) at 2.00 MPa. Table 5-3 shows that a simultaneous increase of inlet pressure and shortening the length has a significant impact on the decrease of COP. For instance, COP decreases from 6.03 at 1.40 MPa to 3.73 at 2.00 MPa (- 38.1%).

5.7 Discussion

A simulation tool has been developed to assess the charge and capacity of a portable propane condenser at different inlet pressures. The inlet entropy has been assumed to be constant in all cases. In practice, to have the same inlet conditions, the other components of the air-conditioner should be modified accordingly. Furthermore, no stress analysis was performed in this study and the same wall thickness has been assumed for all inlet pressures. It is expected that a thicker wall will be required at higher pressures. However, the thicker wall is not expected to have a major effect on the capacity of the condenser. In an air-conditioner system, oil from the compressor penetrates to all components of the system including the condenser. However, such an effect was also ignored in this study.

The accuracy of the results obtained from the simulations was assessed with experimental results. The comparison shows that the simulation is able to estimate the condenser capacity with an error of 3.6%. Taking into account the uncertainty in roughness parameters and the fact that the presence of oil in the condenser is not treated in the simulation, such a level of error is considered within an acceptable range.

The results show that the increase of the inlet pressure of the condenser has a positive impact on the capacity of the condenser, sub-cooling, and cooling capacity

of the air-conditioner, but the coefficient of performance decreases. The results show that the increase of inlet pressure actually increases the mass within the condenser and this approach cannot be regarded as a potential tool to decrease the mass within the condenser of a portable air-conditioner. However, this result is not in agreement with the work of Fernando et al. (2004) who found that by increasing the condensing temperature (which is almost the same as increasing inlet pressure), the total charge of a non-portable system decreases. As the condenser contains the majority of the refrigerant charge, from the work of Fernando et al., 2004 it can be deduced that the mass within the condenser also decreases with the increasing inlet pressure. This apparent contradictory result can be explained by considering the change of densities of propane at different temperatures. The density of propane in liquid form, both in sub-cooled and saturated cases, decreases by increasing condensing temperature (or pressure), but the density of propane vapour in a saturated state increases. Therefore, depending on the state of propane in the condenser, increasing the inlet pressure can either increase or decrease the total mass. If the condenser mainly includes liquid and the outlet is in a sub-cooling state, the total mass within the system tends to decrease. In the Fernando et al. (2004) case, the outlet propane was in a sub-cooled state. If there is less sub-cooling at the outlet of the condenser, or the outlet is in a saturated state, the mass within the condenser will increase with increasing inlet pressure.

Previous studies show that the best performance of condenser occurs at 7°C to 10°C sub-cooled temperature. The level of sub-cooling achieved in the case of a room temperature of 20.0°C is 14.8°C. The results from the present simulations show that, for the condenser in this study with a standard inlet pressure of 1.13 MPa, the optimum level of sub-cooling does not occur at the room temperature of 27°C.

However, the results show that the quality of outlet refrigerant decreases by increasing the inlet pressure and becomes closer to the desired value.

The results of the present simulations show that by increasing the inlet pressure of the condenser, the capacity of the condenser increases but the COP of the system decreases. The results also indicate that a smaller condenser can be used for a certain capacity using a higher inlet pressure of the condenser. The smaller condenser will contain a lower mass of refrigerant. Our results show that by increasing the inlet pressure from 1.30 MPa to 2.00 MPa and shortening the length of the condenser accordingly, the mass of the propane within the condenser can be reduced by 50.7%. In addition, the outlet quality is less than that at 1.30 MPa (for the cases of 1.30 MPa and 1.32 MPa where the outlet state is two phase, outlet quality of refrigerant at 1.30 MPa is 0.07 (see Table 5-3) and 0.01 outlet quality at 1.32 MPa (Table 5-3) which is another advantage for the system. The value of specific capacity of the condenser increases significantly by increasing the inlet pressure and shortening the condenser. In this case, the value increased from 35.46 W/g at 1.3 MPa to 73.59 Watt/g at 2.00 MPa. Also, the total specific capacity of the system **(**cooling capacity/refrigerant mass within condenser and the evaporator) increases from 20.70 W/g at 1.3 MPa to 31.38 W/g at 2.0 MPa.

The above results are focused on the mass of refrigerant in the condenser and evaporator. However, it should be noted that increasing the inlet pressure requires a compressor with a higher compression ratio, resulting in a slight increase in the mass of the refrigerant in the system due to a larger volume of the compressor. Nevertheless, the increase in refrigerant mass is marginal because the refrigerant exists in a superheated condition with a corresponding low density throughout the compressor. In addition, a higher outlet pressure and temperature requires a longer

capillary tube. The mass of refrigerant within the capillary tube is small, and for the air-conditioner considered in this work, it is estimated to be in order of a fraction of a gram (Siang and Sharifian, 2013). Therefore, it is still correct to state that increasing inlet pressure and shortening the condenser simultaneously significantly reduces the mass of propane.

Changing the condenser's inlet pressure can also change the refrigerant mass within the condenser (Table 2-3). Increasing the inlet pressure of the condenser has the benefit of increasing the entire system's performance. However, the consequence of increasing the condenser's inlet pressure is an increase in the accumulated sub-cooled mass within the condenser's outlet (Table 2-5). This is not a potential tool for decreasing the refrigerant charge within the air conditioning system. As the condenser's outlet fills with more liquid refrigerant at a high condenser pressure, the outlet pipe can be shortened to reduce the liquid refrigerant within the condenser. The shortened condenser succeeds in decreasing the mass within the condenser even though there are sacrafices in the cooling capacity and COP of the air conditioning system (Table 2-5).

This research discussed the effect of the condenser's inlet pressure on the condenser's performance and size. The research shows that the outlet temperature of the condenser increases as the inlet pressure increases when the outlet refrigerant is in a two-phase condition. However, the outlet temperature decreases as the inlet pressure increases when the outlet refrigerant is in the sub-cooled state (Table 2-3). This is due to the evaporation (condensation) enthalpy decreasing with an increase in saturation pressure. Condenser capacity increases with an increase in the inlet pressure as well as the refrigerant mass within the condenser (Table 2-5). The mass of refrigerant increases as the condenser outlet is filled with more refrigerant in

liquid form. Increasing the mass of refrigerant simultaneously decreases the specific capacity of the condenser. Increasing the inlet pressure of the condenser decreases the COP of the air conditioning system due to the increase in pressure ratio and condenser work. The refrigerant mass within the condenser continues to increase with the increase in the inlet pressure, with more liquid in the outlet of the condenser (Table 2-5). The outlet can be shortened to reduce the liquid refrigerant within the condenser. The shortened condenser decreases the mass within the condenser however, the cooling capacity and COP of the air conditioning system decreases. The decrease in cooling capacity from the shorter condenser agrees well with research by Zhou and Gan (2019) and Ribeiro and Barbosa (2018).

5.8 Conclusion

The results show that increasing the inlet pressure of the condenser of a commercially available portable propane air-conditioner increases the capacity of the condenser and decreases the outlet temperature. This shows that the recommended sub-cooled value of 7°C to 10°C can be easily achieved at higher inlet pressure and all room temperatures. However, increasing the inlet pressure can increase propane charge in the condenser depending on the outlet conditions. There is an optimum value of inlet pressure for a minimum specific charge.

A significant reduction of the refrigerant mass within the condenser for a certain capacity is achievable by reducing the length of condenser and increasing the inlet pressure. For the air-conditioner under investigation in this work, by increasing the inlet pressure from 1.30 MPa to 2.00 MPa at the room temperature of 27°C, the validated simulation tool indicated that a 50.7% reduction of propane in the

condenser could be achieved without sacrificing the condenser capacity. However, this will reduce COP from 5.75 to 3.73.

The next chapter discusses the performance of the air conditioning system under different room temperatures. After discussing how to reduce the refrigerant mass within the air conditioning system, the thesis discusses the performance of the air conditioning system. The comparison of the performance of a portable propane air conditioning system with a non-portable air conditioning system is also provided. The next chapter is the discussion of the effect of room temperature on the performance of the portable air conditioning system.

CHAPTER 6 IMPACTS OF ROOM TEMPERATURE ON THE PERFORMANCE OF THE PORTABLE PROPANE AIR CONDITIONER

Room temperature is an important variable for an air conditioning system's performance. The change in room temperature influences the difference in temperature between the evaporator and the conditioned room, and the temperature of the condenser and air temperature around the condenser. In the single-duct portable propane air conditioning system, air temperature around the condenser is the air temperature of the conditioned room. This chapter discusses the effect of room temperature on the performance of the portable propane air conditioning system. This Chapter was adopted from the article that was published in the International Journal of Air Conditioning and Refrigeration, Volume 23, no 02, 1550015, 2015.

6.1 Introduction

One of the focus areas of these studies is the assessment of the performance of different systems at different ambient temperatures. Previous studies have not addressed the effect of ambient temperature on portable air conditioners in which the temperature of air surrounding the condenser and evaporator are the same. This research aims to narrow the gap in the literature with an empirical approach. It should be noted that in the case of portable air conditioners, the condenser and evaporator are both located in the room subject to cooling. Therefore, the term of "room temperature" refers to the temperature of air entering the condenser and evaporator, and differs from the outside temperature. The room temperature depends on the cooling capacity of the air conditioner, ambient temperature, size of the room, wall thickness and material type, and many other parameters affecting heat transfer. In this research, the effect of room temperature on the temperature and density of the

refrigerant, the degree of sub-cooling, the maximum velocity of the refrigerant, the mass flow rate of refrigerant, the cooling capacity of the air conditioner, the specific cooling capacity, the work of the compressor, the coefficient of performance (COP) and the maximum pressure of refrigerant have been assessed.

6.2 Literature Review

Previous studies show that a change in ambient temperature has a significant impact on the performance of refrigeration and air conditioning systems. It was found that an increase in temperature of the air adjacent to the evaporator, not only increases the refrigerant temperature in evaporator (Fatouh et al., 2010), but also increasing the condensing temperature (Fernando et al., 2004). Corberan et al., 2011 in their research with propane as the lower the source temperature (evaporator temperature), the lower the density of the refrigerant in the evaporator under the same refrigerant charge. The increase in density at higher ambient temperatures is due to the increase in condensing and evaporating pressure (Herbert-Raj and Lal, 2011; Teng et al., 2012; Kim and Braun, 2012; Kim at al., 2014). Choi and Kim., 2002 using R22 in their research, showed that the degree of sub-cooling decreases with the increase in ambient temperature. Nilpueng et al., 2011 reported that increasing ambient temperature and keeping the evaporator temperature constant, increases the pressure difference across the short capillary tube, which in turn increases the velocity of the refrigerant.

The rise in ambient temperature has a significant impact on the refrigerant mass flow rate. Fatouh et al., 2010 found that, as the temperature of the air surrounding the evaporator increases, the condenser temperature and the mass flow rate increase. They concluded that the increase in the mass flow rate is due to the increase in

vapour density of the refrigerant. Choi and Kim., 2002 reported that the mass flow rate of the refrigerant increases with the increasing temperature of water used to cool the condenser. The increase in the mass flow rate is mainly due to the increase in the pressure difference across the capillary tube. Two separate studies by Rodrigez, 1995 and Farzad, 1990 also concluded that the increase in ambient temperature increases the mass flow rate. The drop of heat source temperature and maintaining the condenser temperature decrease the evaporation pressure, which results in an increase in the pressure difference across the short tube orifice and leads to an increase in the refrigerant mass flow rate (Nilpueng et al., 2011).

The cooling capacity of non-portable systems is affected by ambient temperature. Farzad, 1990 in research using an air conditioner filled with R22, found that at full charge and overcharge conditions, the cooling capacity of his air conditioning system decreased with the increase in ambient temperature which contrasted with the undercharge condition.

Rodriguez, 1995 in research using R22 refrigerant, found that the cooling capacity of the system is highest when the outdoor temperature is the lowest. Choi and Kim., 2002 using a 3.5 kW heat pump filled with R22, found a similar result. In their research, the temperature of water entering the evaporator was maintained at a constant temperature of 24°C, while the temperature of condenser cooling water was raised from 30°C to 42°C with an interval of 4°C. Martinez-Galvan et al., 2011 in a research using a 16 kW propane chiller prototype found a decrease in the cooling capacity with the increase in ambient temperature. They maintained the temperature of water entering the evaporator at 12°C, and raised the temperature of cooling water entering the condenser from 25°C to 40°C with an interval of 5°C. A similar result was found by Corberan et al., 2011 who used a 16 kW propane chiller prototype and

the same temperature range as in the work of Martinez-Galvan et al., 2011. Similar results were also found by Palmiter et al., 2011.

Two studies by Choi and Kim., 2002 and Wu et al., 2012 concluded that the increase in the compressor power is due to the rise in outdoor temperature. Farzad, 1990 found that the increment of power at a lower refrigerant charge is higher than that at a higher refrigerant charge.

Many studies reported the decrease of COP with the increase in ambient temperature, regardless of the refrigerant charge level (Corberan et al., 2011; Kim and Braun, 2012; Kim et al., 2014; Choi and Kim, 2002; Martinez-Galvan et al., 2011). This result can be explained by the decrease in the cooling capacity and the increase in the compressor work as ambient temperature increases. However, Kim et al., 2014 found that the COP increases with the increase in source temperature while maintaining the condenser temperature.

6.3 Methodology and Instrumentation

This study experimentally investigates the effect of ambient temperature on the performance of a portable propane air conditioner. The normal charge of the system is 300g of propane. Previous studies show that the impact of ambient temperature could be different at different refrigerant charge levels. Therefore, the experiments were carried out at three refrigerant charge levels of 263.10g (−12.3%, undercharge), 302.93g (+0.98% overcharge, assumed to be normal charge), and 390g (+30%, overcharge). The experiments were performed at six ambient temperatures ranging from 20°C to 35°C with an interval of 3°C. The air conditioner was placed in a tent, and air temperature was controlled within ±0.5°C of the desired value using an electrical heater. The air conditioner is supplied by a flexible duct which vents the

warm air from the condenser to the outside. The time required to reach a steady state condition in each experiment depended on the room temperature and desired temperature but was usually in the order of two hours. However, due to unavoidable changes of ambient temperature during the experiments, it was necessary to open/close the tent windows to approach or maintain the desired temperature. The whole process was recorded, and the results were selected for further analysis when the room temperature, with an accuracy of ±0.5°C, was maintained at least for 10 min.

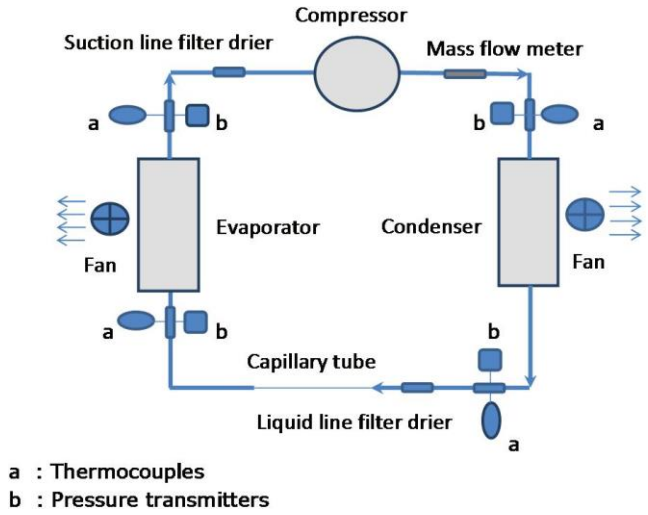

Figure 6-1 Schematic diagram of the portable air conditioner and instrumentation

A Coriolis mass flow meter was installed at the compressor outlet to measure the mass flow rate of the refrigerant. The Coriolis mass flow meter is able to accurately measure the mass flow rate regardless of the fluid state (gas or liquid). Pressures and temperatures were measured using four J-type thermocouples and four piezoresistive pressure transducers at the compressor, condenser, evaporator, and capillary tube inlets. Wind speed over the evaporator and condenser coils was measured using a digital vane anemometer (Lutron LM – 8000). A schematic diagram of the instrumentation is shown in Figure 6-1. The cooling capacity of the air conditioner,

heat dissipation of the condenser and work of compressor were calculated by the energy conservation equation, assuming an adiabatic compressor.

6.4 The Uncertainties of the Presented Values

Three types of quantities are presented in this paper. The first category includes those that have been measured directly. The direct measured values are room temperature, mass flow rate of refrigerant, charge of the system and pressures and temperatures at the inlet of all four main components of the air conditioner. The main uncertainty in the experiments is due to the cumulative effect of noise and drift. The maximum uncertainty in measuring the refrigerant temperature is ±1°C (1.64%), refrigerant pressures is ±25 kPa (14.4%), mass flow rate is ±0.00138 kg/s (+11.94%), charge is ±0.01g (+0.003%), and ambient temperature is 0.5°C (+3.3%). Taking into account the variation of room temperature from 20°C to 35°C in the present work, the relative uncertainty for room temperature was 3.3% ((0.5:15)×100).

The second type of data is that obtained from the table of properties. The uncertainty of these value (density, enthalpy, and sub-cooling) caused by the uncertainty of measured values (pressure and temperature). The maximum uncertainty in the density of the refrigerant was calculated by comparing the density at the measured pressure and temperature (P, T) with those obtained at four points of (P+25kPa, T), (P−25kPa, T), (P, T+1°C), (P, T−1°C). A similar approach was used to estimate the uncertainty in the enthalpy of the refrigerant and sub-cooling. The results show maximum uncertainty of 0.62 kg/m^3 (±16.8%) for density, 4.19 kJ/kg (±1.4%) in the refrigerant enthalpy at the evaporator, 3.24 kJ/kg (±7.1%) in the enthalpy at the compressor, and 1.4°C (±15.24%) in sub-cooling.

The third category includes velocity, cooling capacity, useful work of the compressor, specific cooling capacity, and COP, all of which were calculated using the above-mentioned quantities and the square root of sum of sum of squares formula. They were calculated using the following formulas:

$$vel = \frac{\dot{m}_r}{\rho A_p}, \tag{6.1}$$

$$\dot{Q}_{cool} = \dot{m}_r(h_4 - h_1) + \dot{m}_r\left(\frac{vel_4^{\,2}}{2000} - \frac{vel_1^{\,2}}{2000}\right), \tag{6.2}$$

$$\dot{W}_{comp} = \dot{m}_r(h_1 - h_2) + \dot{m}_r\left(\frac{vel_1^{\,2}}{2000} - \frac{vel_2^{\,2}}{2000}\right), \tag{6.3}$$

$$COP = \frac{Q_{cool}}{W_{comp}}, \tag{6.4}$$

$$SC = \frac{Q_{cool} \times 1000}{charge} \tag{6.5}$$

The maximum uncertainties are estimated to be 7.65 m/s (±20.61%) for the refrigerant velocity, 0.45 kW (±12.48%) for the cooling capacity, 0.07 kW (±13.89%) for the useful work of the compressor, 1.30 (±18.38%) for the COP, and 0.0013 W/g (±12.48%) for the specific cooling capacity.

6.5 Results and Discussion

Some results presented in this paper are only indicative since their variations were less than the experimental uncertainties. Some results were also identified as outliers and were removed prior to curve fitting. The maximum standard deviations of the results are presented in the beginning of each section.

6.5.1 Effect of room temperature on refrigerant temperature

The uncertainty of the experimental data (presented in Figure 6-2) is determined to be 1.1°C based on 1°C and 0.5°C uncertainties of the refrigerant temperature and room temperature, respectively. The maximum standard deviation of the fitted curve is 0.7°C.

Figure 6-2 shows the temperature of the refrigerant at the inlet of four main parts of the air conditioner versus room temperatures at the three different charges. The results show that the refrigerant temperature increases approximately linearly with the increase in room temperature. In Figure 6-2, the temperature of the refrigerant at the evaporator inlet ($T_{in\text{-}evap}$) and compressor inlet ($T_{in\text{-}comp}$) are almost identical and cannot be clearly discerned from each other. The rise in room temperature shows a minor influence on the $T_{in\text{-}evap}$, and $T_{in\text{-}comp}$ compared with other components. For example, at the refrigerant charge of 263.10g and room temperature of 20°C, $T_{in\text{-}evap}$ and $T_{in\text{-}comp}$ are 3.2°C and 2.8°C, respectively. At 35°C, these values increase to $T_{in\text{-}evap}$ of 10.9°C and $T_{in\text{-}comp}$ of 11.0°C, which represent temperature rises of $\Delta T_{in\text{-}evap}$ of 7.7°C and $\Delta T_{in\text{-}comp}$ of 8.2°C, while room temperature rises by 15°C.

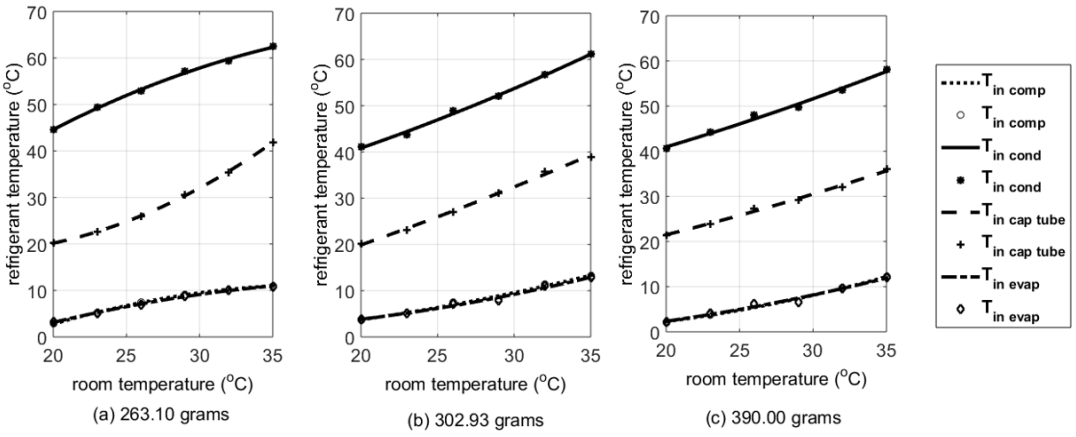

Figure 6-2 Refrigerant temperature versus room temperature at different charge levels

The effect of room temperature (T_{room}) on the temperature of the refrigerant at the capillary tube inlet ($T_{in\text{-}cap\text{-}tube}$) is greater than that of $T_{in\text{-}evap}$ and $T_{in\text{-}comp}$. The maximum effect of T_{room} on $T_{in\text{-}cap\text{-}tube}$ occurs at the charge of 263.10g. At this charge $T_{in\text{-}cap\text{-}tube}$ is 20.2°C at T_{room} of 20°C and is 41.9°C at room temperature of 35°C. This shows a temperature rise of 21.8°C while room temperature increases only 15°C.

Room temperature also has a major impact on the refrigerant temperature at the condenser inlet ($T_{in\text{-}cond}$). For example, at 390.00g charge, $T_{in\text{-}cond}$ at 20°C and 35°C room temperature is 40.6°C and 58.1°C, respectively. This shows an increase of 17.5°C in refrigerant temperature while room temperature increases by 15°C. The same trend can be observed at 302.93g charge. The temperature at the condenser inlet increases from 40.8°C to 61.1°C, which represents an increase in 20.3°C over the same room temperature range. In the case of 263.10g charge, the temperature increases from 44.6°C to 62.3°C, which represents a 17.7°C temperature increase.

The experimental results show that the rise in room temperature increases the refrigerant temperature at the inlet of all main components of the air conditioner. The results were expected and are in agreement with previous studies (e.g., Fatouh et al., 2010 and Fernando et al., 2004). Initially the difference between the refrigerant temperature in the evaporator and room temperature increases, it corresponds to a higher cooling capacity. In a steady state operation, the total heat rejected by a condenser is equal to the sum of the heat absorbed by evaporator and the useful work of the compressor, therefore the heat discharged by the condenser increasing according to energy conservation law. Consequently, the refrigerant temperature in the condenser increases more than room temperature to enable the dissipation of more heat. This increase raises the refrigerant temperature in the evaporator, thus the temperature difference in the evaporator drops, and consequently the cooling capacity decreases in comparison with the initial sharp increase. This analysis is supported by the experimental results indicating that the effect of room temperature is more significant at the inlet and outlet of the condenser as compared to the inlet and outlet of the evaporator. As the refrigerant exists in saturated state in the condenser, the increase in temperature leads to a corresponding increase in pressure.

The results also show that a rise in pressure occurs, which is in line with the previous work on non-portable air conditioners (e.g., Herbert-Raj and Lal, 2011).

6.5.2 Influence of room temperature on density of refrigerant

The room temperature has an effect the density of the refrigerant at different parts of the air conditioner. Density has been estimated using the table of propane properties Refprop 6.1 (NIST, 1998) based on the measured pressures and temperatures. The maximum uncertainties of the results in Figure 6-3 are estimated to be 17.1%. The maximum standard deviation of fitted curves is 0.0287 kg/m^3.

The results show that the density of the refrigerant at the compressor inlet increases as room temperature increases. For example, at 263.10g charge, the density increases from 10.46 kg/m^3 at 20°C to 12.68 kg/m^3 at 35°C (+21.2%). At 390.00g charge, the density at 20°C is 10.38 kg/m^3 and increases to 12.46 kg/m^3 at 35°C (20.0%). The relative increase (20.0%) is more than the relative uncertainty of the experiment (17.1%). The increase in the density at the compressor outlet (inlet of the condenser) is more significant. For instance, the density at the charge of 263.10g increases from 21.25 kg/m^3 at 20°C to 31.35 kg/m^3 at 35°C (+47.6%). The density increases by 50.0% and 19.1% at the charge of 302.93g and 390.00g, respectively, for the same range of temperature.

At the capillary tube and evaporator inlets, the density decreases as the temperature increases. At the inlet of the capillary tube, the density decreases by 7.1%, 6.3% and 4.7% at the charges of 263.10g, 302.93g and 390.00g, respectively. At the inlet of the evaporator, as the room temperature increases, the density decreases by 13.7%, 11.5% and 8.6% at the charges of 263.10g, 302.93g and 390.00g, respectively. It should be noted that the relative decrease in the density at the inlets of capillary tube

and evaporator is less than the relative uncertainty of the experiment, so inconclusive.

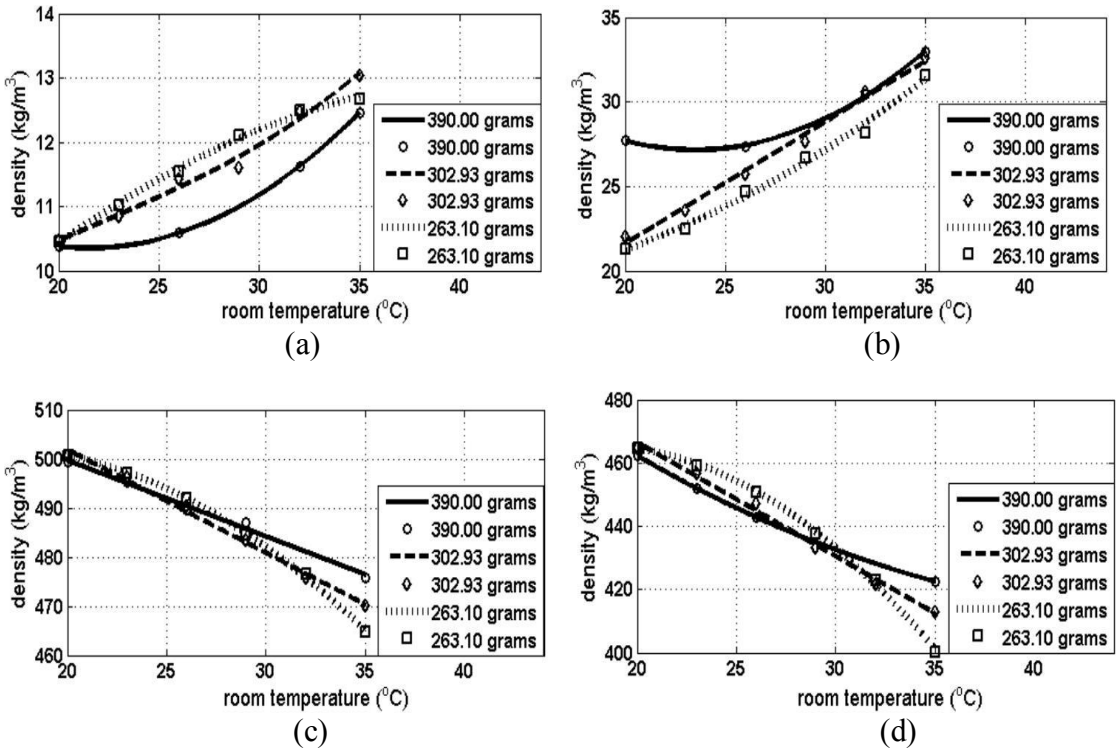

Figure 6-3 Refrigerant density versus room temperature at different refrigerant charge levels: (a) inlet of compressor, (b) inlet of condenser, (c) inlet of capillary tube and (d) inlet of evaporator.

The rise in room temperature increases the density at the inlet of the compressor and condenser. It was shown in Sec. 6.5.1 that the temperature and pressure of the refrigerant at the inlet of the compressor and condenser simultaneously increase with the rise in room temperature. The increase in temperature and increase in pressure have opposite impacts on the density, but overall, the density increases for superheated propane and decreases for liquid or saturated propane. For instance, at 263.93g charge and pressure and temperature of 1.0686 MPa and 44.57°C (the inlet condition of compressor at 20°C room temperature), propane density is 21.26 kg/m3 which is less than the density of 31.60 kg/m^3 at pressure and temperature of 1.58 MPa and 62.43°C (the inlet condition of compressor at 35°C room temperature). The density is 500.75 kg/m^3 at the temperature and pressure of 20.16°C and 1.11 MPa

(the inlet of the capillary tube at 20°C room temperature) which is 7.18% higher than the density of 464.81 kg/m^3 in pressure and temperature of 1.65 MPa and 41.91°C.

The distribution of the refrigerant within the air conditioner could not be directly measured in our experimental setups. In the absence of density distribution, the change of the refrigerant distribution can only be deduced based on the density variation at the inlet and outlet of the components. The results show that the density increases at the inlet and outlet of the compressor as room temperature increases. This indicates that the mass of the refrigerant within the compressor more likely to increase. The density at the inlet and outlet of the capillary tube decreases as the room temperature increases. This shows that the mass within the capillary tube probably decreases. However, the refrigerant mass within the capillary tube is small when compared with the mass within the other components and cannot compensate for the increase in the mass in the compressor. The results for the condenser and evaporator are not quite as decisive. At the inlet of the condenser, the density increases; but it decreases at the outlet. At the inlet of the evaporator, the density decreases; but it increases at its outlet. As the value of the density at the outlet of the condenser is greater than that at its inlet, the results show that the mass within the condenser probably decreases. A similar result can be drawn for the evaporator. The value of the density at its inlet is greater than at its outlet, thus the refrigerant mass within the evaporator possibly decreases as room temperature increases. The above results are only suggestive, not conclusive.

6.5.3 Effect of room temperature on sub-cooling

Figure 6-4 shows that the refrigerant sub-cooling at the outlet of the condenser decreases with the increase in room temperature for all the charges measured. From Figure 6-4 the maximum impact was observed at the lowest charge of 263.10g. At

this charge, the degree of sub-cooling decreased from 11.0°C to 6.5°C (−4.5°C), while at the highest charge of 390.00g, the sub-cooling decreased from 12.3°C at 20°C to 10.9°C at 35°C room temperature (−1.4°C). These results are in agreement with the previous work of Choi and Kim, 2002. As discussed in Sec. 6.5.1, the increase of refrigerant temperature in the condenser is more than the increase of room temperature, which result in a higher heat transfer rate in the condenser. However, as it will be shown in Sec. 6.5.1, the mass flow rate increases more than that of the heat transfer, pointing to a less severe decrease of specific enthalpy, thus less sub-cooling. For instance, at a refrigerant charge of 263.93g and room temperature of 20°C, the heat rejected by the condenser is 3.47 kW which increases to 4.32 kW at the room temperature of 35°C, representing an increase of 24.56%. At the same time, the mass flow rate increases from 0.0088 kg/s at 20°C room temperature to 0.0123 kg/s at 35°C room temperature which shows an increase of 40.07%. The comparison between the increase of heat rejected by the condenser (24.56%) and the rise of the mass flow rate (40.07%) shows that the change of the specific enthalpy in the condenser actually decreases leading to the reduction of sub-cooling.

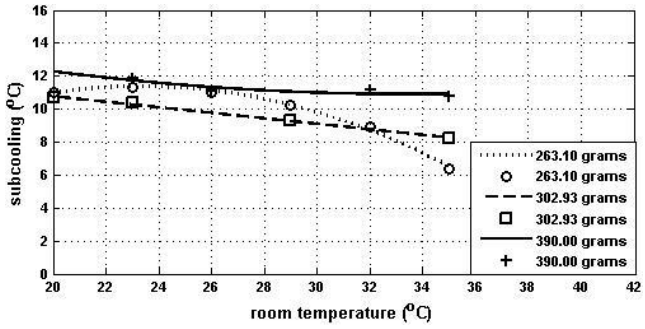

Figure 6-4 Degree of sub-cooling versus room temperature at different charge levels

6.5.4 Influence of room temperature on maximum velocity

The maximum uncertainty of the results presented in this section is expected to be 20.88% based on 20.61% uncertainty of the velocity and 3.3% uncertainty associated with the room temperature. The fitted curve has a maximum standard deviation of 2.4 m/s.

Figure 6-5 shows the effect of room temperature on the maximum velocity of the refrigerant. The effect of room temperature on the maximum velocity at low and moderate charge (263.10g and 302.93g charge) is less than the maximum uncertainty of the experiment. At the charge of 263.10g, the velocity increases from 25.8 m/s at 20°C to 29.7 m/s at 35°C room temperature (+15.2%). These values become 34.6 m/s and 32.1 m/s (−7.3%) respectively at the charge of 302.93g. However, at the highest charge of 390.00g, the maximum velocity decreases from 50.6 m/s at 20°C to 36.3 m/s at 35°C room temperature (−28.3%).

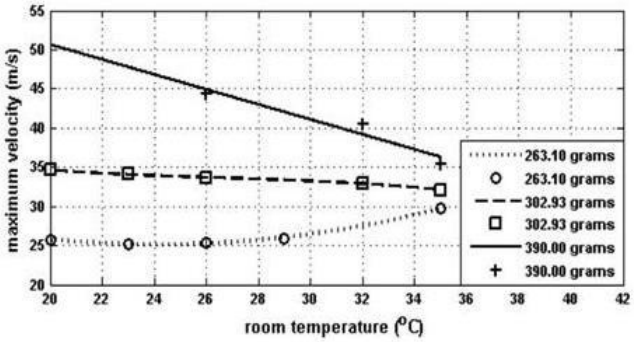

Figure 6-5 Maximum velocity versus room temperature at different charge levels

The results for the maximum velocity of the refrigerant within the air conditioner at undercharge and standard charge are not conclusive. The results at the overcharge condition show that the maximum velocity decreases by the increase in room temperature. This result can be explained based on the increase in density. Velocity increases if the rate of increase in mass flow rate surpasses that of density (see Eq.

(6.1)). For example, in 302.93g refrigerant charge, the mass flow rate increases from 0.011775 kg/s at 20°C to 0.01360694 kg/s at 35°C (15.56% increase), and the density at the inlet of the compressor increases from 10.47 kg/m^3 at 20°C to 13.05 kg/m^3 at 35°C (24.62% increase). As the rate of increase in the mass flow rate is smaller than that of the density, the velocity decreases. On the contrary, in the case of 263.10g refrigerant charge, the velocity increases with the increase of room temperature. In that case, the mass flow rate increases from 0.00875 kg/s at 20°C to 0.01226 kg/s at 35°C (40.07% increase), while the density increases only 20.0%, from 10.38 kg/m^3 at 20°C to 12.46 kg/m^3 at 35°C. It should be noted that the maximum velocity occurs at the outlet of the evaporator where the density is at minimum. This result shows that the outlet diameter of the evaporator can be increased to reduce the maximum velocity. In contrast, a previous work (Nilpueng et al., 2011) shows that the refrigerant velocity slightly increases as room temperature increases.

6.5.5 Influence of room temperature on mass flow rate

The presented results are expected to have a maximum uncertainty of 12.40% based on 11.94% uncertainty of mass flow rate and 3.33% uncertainty of room temperature. The maximum standard deviation of the fitted curves is 0.8392×10^{-3} kg/s.

Figure 6-6 shows the effect of room temperature on the mass flow rate of the refrigerant. The mass flow rate increases with increase in room temperature except at 390.00g charge. For instance, at the charge of 263.10g, the mass flow rate increases from 0.0084 kg/s at 20°C to 0.0121 kg/s at 35°C room temperature (+44.0%). The same pattern can be observed at the charges of 302.93g (+15.7%). The only exception occurs at the charge of 390.00g where the mass flow rate shows a peak at

around 27.2°C room temperature. In this charge and at the room temperature of 20°C, the mass flow rate is 0.0145 kg/s, and increase as the temperature increases until it reaches a value of 0.0158 (+9.0%) at room temperature of 27.2°C. With further increases in room temperature, the mass flow rate decreases and reaches a value of 0.0143 kg/s at a room temperature of 35°C, representing a 9.5% decrease with respect to the peak value.

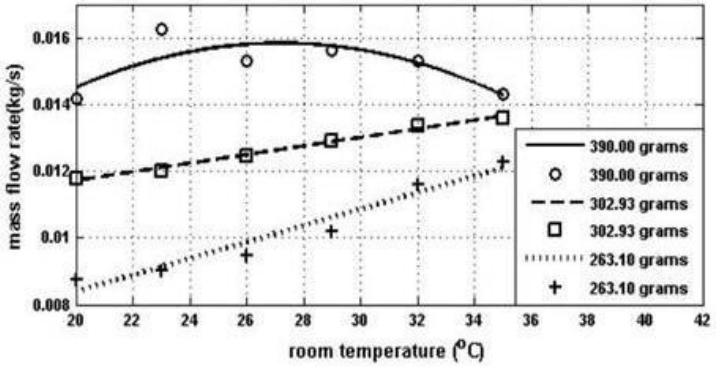

Figure 6-6 Mass flow rate versus room temperature at different charge levels

The increase in mass flow rate due to the increase in room temperature is in agreement with previous studies by Farzad, 1990; Rodrigez, 1995; Choi and Kim, 2002; and Fatouh et al., 2010. The mass flow rate increases with T_{room} due to the increase in the density of the refrigerant (see Sec. 6.5.2). However, at the highest charge, some decrease can be seen. This could be ascribed to a possible increase in internal leaks of the compressor. In Sec. 6.5.2, it was shown that the rise of room temperature increases the refrigerant temperature and hence, the viscosity of oil in the mixture with the refrigerant decrease. The poor viscosity of oil increases the internal leakage (Evan, 2013). However, it should be noted that the decrease in the mass flow rate at the highest charge is less than the uncertainty of the experiment and the results are not conclusive.

6.5.6 Effect of room temperature on cooling capacity

The cooling capacity of the air conditioner has been calculated using the experimental data. Some typical results are presented in Figure 6-7. The uncertainty of the results presented in this section is 12.48% based on 12.03% uncertainty in the calculated cooling capacity and 3.33% uncertainty of room temperature. The maximum standard deviation is 0.03 kW.

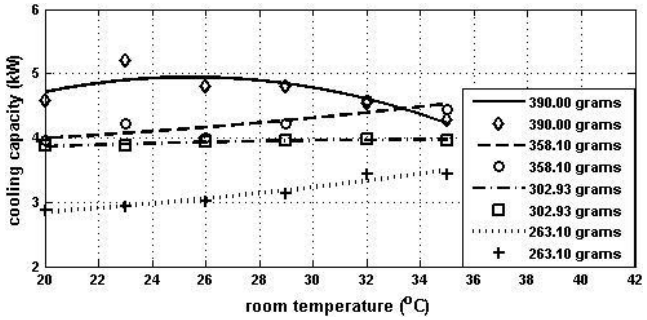

Figure 6-7 Cooling capacity versus room temperature at different charge levels

The results show that the cooling capacity of the portable propane air conditioner increases as room temperature increases, with the exception of the overcharged condition. According to Figure 6-7, in the case of 12.3% undercharge (263.10g), the cooling capacity increases from 2.86 kW at 20°C room temperature to 3.52 kW at 35°C room temperature (+23%). The increase is only 2.7% (0.11 kW) in the case of 302.93g charge (0.98% overcharge) over the same room temperature range. In the case of 30% overcharge (390.00g), the cooling capacity initially increases from 4.74 kW at 20°C to 4.98 kW at 27°C (4.9%), and then decreases to 4.25 kW at a room temperature of 35°C. In this case, the cooling capacity at 35°C is 10.45% and 14.65% less than those at 20°C and 27°C, respectively. Taking into account the uncertainty of the experiment (12.48%), the change of cooling capacity at 20°C and 27°C (+4.9%) is not conclusive. The cooling capacity decreases from 27°C to 35°C (−14.65%) and the results are conclusive.

Equation (6.2) shows that the cooling capacity of an air conditioner is a function of the mass flow rate. A comparison between the experimental results of cooling capacity and mass flow rate (Figures 6-6 and 6-7) shows that their changes are extremely similar.

The results obtained are not fully consistent with previous studies. Farzad, 1990 commented that, in an undercharged condition, the cooling capacity increases with room temperature, but it decreases under full and overcharged conditions. The results presented by other researchers are partially different from those obtained by Farzad. Choi and Kim, 2002 found that the cooling capacity decreases as condenser temperature increases, but the rate of decrease is higher at undercharged condition. Rodrigez, 1995; Martinez−Galvan et al., 2011; and Corberan et al., 2011 obtained similar results. It should be noted that, in the previous studies, the increase in ambient temperature refers to the increase in air temperature refers to the increase in air temperature surrounding the condenser, while the air temperature around the evaporator remains unchanged. In this work, the contrary is found. The increase in refrigerant temperature in the evaporator is less than that of the room temperature (see Sec. 6.5.1), thus the temperature difference increases, resulting in an increase in the cooling capacity.

6.5.7 Effect of room temperature on specific cooling capacity

The uncertainty of the specific cooling capacity (SC) is 12.48% based on the uncertainty of the cooling capacity and uncertainty of mass measurement. The maximum standard deviation of fitted curves is 0.7441 W/g

Figure 6-8 shows that, at the undercharge condition, the SC increase from 10.83 W/g at T_{room} = 20°C to 13.30 W/g at T_{room} = 35°C (+20.8%). At the standard charge, the

change of SC is less than the maximum uncertainty of the experiment. It increases from 12.76 W/g at T_{room} = 20°C to 13.11 W/g at T_{room} = 35°C (2.74%). Therefore, there is no conclusive result. At the overcharged condition, the SC first increases from 12.13 W/g at 20°C to 12.68 W/g at 25.4°C (+4.56%), and then decreases to 10.78 W/g (−14.96%) at 35°C. In the absence of the previous studies, the only conclusive result that can be obtained is the reduction of the specific cooling capacity at overcharged condition and at higher room temperature. The specific cooling capacity is defined as cooling capacity per mass of refrigerant (Eq. (6.5)). Thus, for a certain mass of refrigerant in the system, its change with room temperature is expected to be similar to that of the cooling capacity, which is confirmed to be the current experimental results.

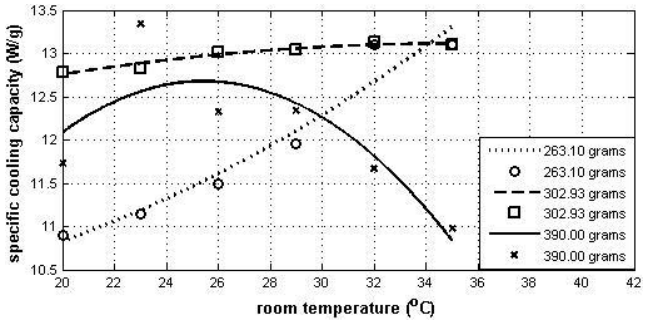

Figure 6-8 SC versus room temperature at different refrigerant charge levels

6.5.8 Effect of room temperature on useful work of the compressor

Figure 6-9 indicates the useful work of the compressor versus room temperature. The maximum uncertainty of the results is expected to be 14.28% and the maximum standard deviation is 0.02 kW. The Figure shows that the useful work of the compressor increases with the increase in room temperature in all the cases. However, the impact of room temperature on the work is greater at lower charges. The useful work of the compressor at 263.10g charge is 0.49 kW at 20°C and 0.84 kW at 35°C, representing an increase of 69.9%. At 302.93g and 390.00g charges, the

rate of the increase in the useful work of the compressor over the full room temperature range decreases to +46.17% and 32.31%, respectively. It should be noted that the useful work of the compressor decreases by 3.7% at the highest charge as room temperature increases from 31.2°C to 35°C. As the value of the decrease is less than the relative uncertainty of the experiment, the result is not conclusive. There are two reasons for the increase of the work of the compressor. The first is the increase in mass flow rate, discussed in Sec. 6.5.5, the second is the increase in the specific work of the compressor, defined as follows:

$$\omega_s = \frac{k \times R \times T_1}{k-1}\left[\left(\frac{P_2}{P_1}\right)^{k-1/k} - 1\right] \qquad (6.6)$$

The above formula shows that the specific work of a compressor increases by the increase in pressure ratio or inlet temperature. The increase of inlet temperature with room temperature was discussed in Sec. 6.5.1. In addition, the pressure ratio increases with the rise of room temperature. For example, at 263.10g charge, P_2 increases from 1.65 MPa at 20°C room temperature to 1.65 MPa at 35°C room temperature (48.23% increase), but P_1 increases only 22.60% from 0.49 MPa at 20°C room temperature to 0.60 MPa at 35°C room temperature. This shows that the pressure ratio increases from 2.20 at 20°C to 2.77 at 35°C.

The results are in agreement with the previous work by Farzad, 1990. The work of the compressor is expected to increase as the room temperature increases, mainly due to the increase in mass flow rate which was discussed in Sec. 6.5.5.

6.5.9 Effect of room temperature on COP

Figure 6-10 shows the COP of the portable air conditioner (used in this work) versus room temperature. The maximum uncertainty of the results is expected to be

18.68%, and fitted curve has a maximum standard deviation of 0.4784. The COP of the air conditioner is calculated based on the cooling capacity and the useful work of the compressor which were calculated in previous sections (see Secs 6.5.6 and 6.5.8).

The results show that the COP of the air conditioner decreases with increase in room temperature. For example, at 12.30% undercharge condition (263.10g charge), COP decreases from 5.83 at room temperature of 20°C to 4.26 at room temperature of 35°C (−26.9%). The effect of room temperature on COP is slightly stronger as the charge increases. At 302.93g charge, the COP decreases from 6.78 at 20°C to 4.92 at 35°C (−27.4%). The COP decreases from 7.83 to 5.49 (−29.9%) at the charge of 390.00g as room temperature increases from 20°C to 35°C, respectively.

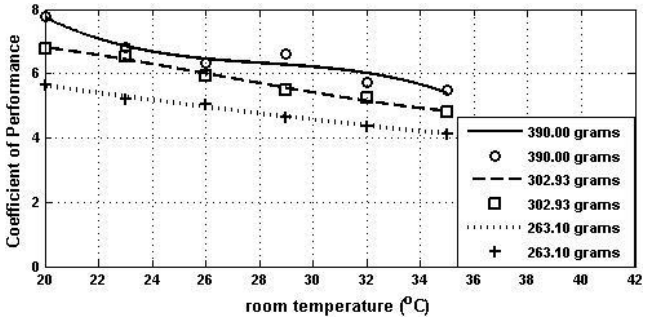

Figure 6-9 COP versus room temperature at different charge levels

The results are similar to the previous results for non-portable air conditioners. Choi and Kim, 2002 found that the COP decreases with an increase in room temperature at all charge levels. They found that the decrease of the COP is due to the increase in power consumption and the decrease in cooling capacity due to the rise of room temperature. Recent studies also show similar results (e.g., Refs. Corberan et al., 2011 and Martinez-Galvan et al., 2011). However, it should be noted that in this portable air conditioner, the cooling capacity increases with the increase in room

temperature (Figure 6-7), therefore the decrease of the COP is less severe than that of non-portable air conditioners.

It should be noted that the COP is the ratio of cooling capacity to useful work of compressor (see Eq. (6.4)). Therefore, the decrease in COP with the rise of room temperature reflects the fact that the increase in the cooling capacity is less than the increase of useful work of the compressor (see Secs. 6.5.6 and 6.5.8). For example, at 263.10g charge, the cooling capacity increases 23% from 2.86 kW at 20°C room temperature to 3.52 kW at 35°C room temperature while the useful work of the compressor increases 69.9% from 0.49 kW at 20°C to 0.84 kW at 35°C.

6.5.10 Effect of room temperature on maximum pressure of air conditioner

The maximum uncertainty of the results presented in this section is 5.5% based on 25 kPa (4.4%) and 0.5°C (3.3%) uncertainties associated with pressure and temperature readings, respectively.

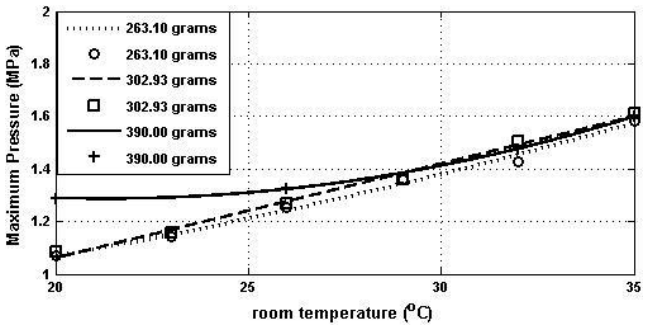

Figure 6-10 Maximum pressure versus room temperature at different refrigerant charge levels

Figure 6-11 shows a significant increase in the maximum pressure versus room temperature. The maximum pressure is reached at the compressor outlet. According to Figure 6-11, at the charge of 263.10g, the maximum pressure increases from 1.07 MPa at 20°C to 1.57 MPa at 35°C (+47.47%). The maximum pressure increases by

50.75% and 23.98% at the charges of 302.93g and 390.00g, respectively, over the same room temperature range.

The results of the present work are similar to the results of previous studies. The maximum pressure occurs at the outlet of the compressor and increases due to the increase in refrigerant temperature at the compressor outlet as room temperature increases (as discussed in Sec. 6.5.1). The process is usually assumed to be adiabatic or isentropic in a compressor. The relationship between pressure and temperature for an adiabatic process is

$$P_2 = P_1(T_2/T_1)^{k/k-1} \quad (6.7)$$

The above formula shows that the outlet pressure of the compressor increases as T_2/T_1 ratio or P_1 increases. It was shown (Sec. 6.5.1) that at a room temperature of 20°C and refrigerant charge of 263.10g, the inlet pressure is 0.4854 MPa and the inlet and outlet temperatures are 275.93 K and 317.72 K, respectively. At the room temperature of 35°C, the inlet pressure is 0.5951 MPa and the inlet and outlet temperatures are 284.19 K and 335.58 K, respectively. This shows not only the inlet pressure increases, but also the temperature ratio increases from 1.15 at 20°C to 1.18 at 35°C room temperature.

All the previous work found that the pressure of refrigerant increases with an increase in room temperature (Herbert-Raj and Lal, 2011; Teng et al., 2012; Kim and Braun, 2012; Kim et al., 2014).

6.6 Summary and further discussion

The results show many similarities and some differences between the performance of portable propane air conditioners and non-portable air conditioners and refrigeration systems. The refrigerant temperatures increase as room temperature increases. The

increase in refrigerant temperature at the inlet and outlet of the condenser is higher than the increase in room temperature, whereas the increase in the refrigerant temperature at the inlet and outlet of the evaporator is less than the increase in room temperature. This is the key point to the discussion of portable air conditioners' performance. As the refrigerant in the evaporator and condenser is in a saturated state, the increase in temperature leads to an increase in pressure. Therefore, the pressure ratio and pressure difference increase at both sides of the capillary tube and compressor, leading to an increase in the mass flow rate and useful work of the compressor. The increase in the difference between the refrigerant temperature at the condenser and room temperature leads to a better discharge of heat from the condenser. However, as the mass flow rate increases, the degree of sub-cooling decreases slightly. A greater difference between the refrigerant temperature at the evaporator and room temperature increases the cooling capacity of the air conditioner. However, the COP decreases. The main difference between the performance of portable air conditioners and others is related to cooling capacity. The effect of room temperature rises is significant for the increase in the specific cooling capacity at lower charge but is insignificant at the standard charge. At overcharge condition, the specific cooling capacity increases at lower room temperatures, but decreases at higher room temperatures.

The next important variable in the air conditioning system is the room temperature. Variations in room temperature change the performance of the air conditioning system. An increase in room temperature increases the refrigerant temperature in all inlets of the main parts of the air conditioning system (Table 2-3). Research by Choudhari and Sapali (2018) found that an increase in room temperature has negligible effect on the discharge temperature of the compressor. Jawale and Keche

(2018) and Liu et al. (2018) found the opposite result to the present research. The important result of the effect of room temperature on refrigerant temperature is that the increase in condenser temperature is more than the increase in evaporator temperature. Therefore, the difference between condenser temperature and room temperature is higher than the difference between the evaporator temperature and room temperature. As a result, the increase in heat dissipation in the condenser is more than the heat absorbed by the evaporator.

An increase in room temperature changes the density of the refrigerant at the inlet of the main parts of the air conditioning system (Table 2-4). The density of the refrigerant at the compressor inlet and condenser increases, while the density of the refrigerant at the capillary tube inlet and the evaporator decreases (Table 2-4). This situation shows the migration of refrigerant mass when the room temperature changes. As the density at the compressor increases, it more likely that the mass of refrigerant within the compressor increases when the room temperature increases but, the mass of refrigerant within the capillary tube decreases. Furthermore, the degree of sub-cooling decreases as the room temperature increases (Table 2-5). An increase in room temperature increases the heat transfer in the condenser and, at the same time, the mass flow rate increases. Because the increase in mass flow rate is more than the increase in heat transfer, the sub-cooling decreases.

An increase in room temperature increases the mass flow rate of the refrigerant at undercharge and standard charge. In an overcharged condition, the mass flow rate increases to a maximum value, and then decreases as the room temperature increases (Table 2-5). An increase in mass flow rate with an increase in the room temperature gives the opposite result (Ramesha et al., 2016). An increase in room temperature is a benefit for cooling capacity. As explained before, the increase in room temperature

increases the temperature difference between the evaporator and room temperature, and the cooling capacity also increases which agrees well with Liu et al. (2018). An increase in mass flow rate also indicates an increase in cooling capacity as the room temperature increases. The present research confirms the research by Choudhari and Sapali (2018). They analysed the effect of variation in indoor temperature at the same outdoor temperature. The other research changing the outdoor temperature found that, increasing outdoor temperature decreases cooling capacity (Shen and Fricke, 2020; Yusof et al., 2018).

The specific cooling capacity (SC) of the air conditioning system can be detected at undercharged and overcharged conditions. SC at undercharged condition increases with an increase in room temperature, while SC decreases at the overcharged condition and high room temperature (Table 2-5). The useful work of the compressor increases as the room temperature increases (Table 2-4). The reasons for the increase in the useful work of the compressor are the increase in mass flow rate and the increase in the specific work of the compressor.

The COP of the air conditioning system decreases with an increase in room temperature in all cases of refrigerant charge. In this research, the COP is the ratio of cooling capacity to useful work of compressor. As explained previously, cooling capacity and useful work of compressor increase with the increase in room temperature however, the increase in cooling capacity being less than the increase in useful work of the compressor, causes the COP to decrease. The present research agrees with the research by Yusof et al. (2018), Ramesha et al. (2018) and Shen and Fricke (2020). The other research by Jawale and Keche (2018) and Choudhari and Sapali (2018) found the opposite result. An increase in room temperature increases the maximum pressure of the air conditioning system. The maximum pressure

increases as the room temperature increases. As the room temperature increases, condenser temperature, evaporator pressure and temperature also increase. The increase in maximum pressure with an increase in room temperature can be explained by the formula:

$$P_2 = P_1\left(T_2/T_1\right)^{k/k-1}$$

The experiment's result shows that the evaporator pressure and ratio of outlet temperature to inlet temperature increases with an increase in room temperature. The increase in evaporator pressure and the ratio of inlet to outlet temperature is the reason for the increase in the maximum pressure of the air conditioning system. The same result was found in the research by Jawale and Keche (2018).

6.7 Conclusion

The performance of a portable propane air conditioner at different room temperatures shows many similarities and a few significant differences with those of non-portable air conditioner and refrigeration systems. Similar to non-portable systems, as room temperature increases, the refrigerant temperature in all parts of the system, the refrigerant mass flow rate, work of the compressor and maximum pressure of the system increases, and the level of refrigerant sub-cooling and COP of the system decreases. The results also suggest that, as room temperature increases, the refrigerant accumulates more in the compressor and less in other parts of the system.

The main differences between portable and non-portable systems are the change of the maximum velocity of the refrigerant and cooling capacity with the increase in room temperature. Unlike non-portable systems, the maximum velocity of the

refrigerant at the overcharge condition decreases with the increase in room temperature. The results in undercharge condition are not conclusive, but they suggest an increase in maximum velocity with temperature, similar to non-portable systems.

Similar to non-portable systems, the results obtained show that the cooling capacity of an undercharge system increases with an increase in room temperature. Unlike a non-portable system, the results indicate a slight increase in cooling capacity for a full charge portable air conditioner. In addition, the cooling capacity of an overcharge and portable air conditioner initially increases and then decreases with the increase in room temperature.

The performance of an air conditioning system also depends on the amount of refrigerant charge within the system. The next chapter presents the discussion on the effect of refrigerant charge levels on the portable propane air conditioning system.

CHAPTER 7 PERFORMANCE OF A SINGLE-DUCT PORTABLE PROPANE AIR CONDITIONING SYSTEM UNDER DIFFERENT CHARGE LEVELS

The next important variable, besides room temperature, which affects the performance of the portable propane air conditioning system is the refrigerant charge level. This chapter discusses the performance of the portable propane air conditioning system under different refrigerant charge levels. The charge level was varied from 263.09g – 300g charge (12.1% undercharged – 30% overcharged). The normal charge of the system is 300g. This article was published in the Heat Transfer – Asian Research, volume 46, issue 8, pages 1246 – 1261.

7.1 Introduction

Previous studies show that the amount of refrigerant charge has a significant effect on the performance of heat pumps (Choi and Kim, 2002; Corberan et al., 2011). Previous works have been carried out on heat pumps and split or window type air conditioners in which the surrounding temperatures of the evaporator and condenser are different. In contrast, the surrounding temperatures of the condenser and evaporator of a portable air conditioner are the same and equal to the room temperature. This study does not cover the performance of double-duct portable air conditioners in the market, which use outside air for cooling of the condenser. To avoid the hot air flow from the condenser to the room, a duct is used to direct the hot air from the condenser to the outside. Portable air conditioners are expected to have a high coefficient of performance (COP) due to a higher temperature different between the refrigerant and the surrounding air in both the condenser and evaporator. Recent research (Sharifian and Siang, 2015) shows a different response to the change of

room temperature in comparison to that of non-portable systems. As a result, the change of the charge may impact its performance compared with other heat pumps and air conditioners.

This research aims to fill the research gap for portable air conditioners by investigating the effect of refrigerant charge on important parameters at different room temperatures ranging from 20°C to 35°C. The investigated parameters are cooling capacity, specific cooling capacity, work of compressor, COP, maximum pressure of refrigerant (significant for safety), maximum velocity (important for noise and vibration assessment and system life), and degree of sub-cooling (important for robust stability and performance). In addition, the effects of the charge on some other parameters are included for a better understanding of the system. They are refrigerant mass flow rate, temperature, and density. Such information is essential for the design of portable air conditioners to achieve higher performance, lower noise, less vibration, longer service life, and lower energy consumption. The experimental results are compared with those of non-portable systems.

7.2 Literature review

Goswami et al. (2001) analysed the effect of refrigerant charge on refrigerant temperatures at the inlet of the main components of a propane air conditioner working in a vapour–compression refrigeration cycle. They found that the refrigerant temperature at the inlet to the condenser, compressor, and evaporator decreases with the increase in refrigerant charge but remains constant at the inlet of the expansion valve. Mastrullo et al. (2014) determined the effect of charge on refrigerant temperature in the condenser and evaporator. They found that the increase in refrigerant charge always increases both refrigerant temperature at the condenser and

evaporator, and decreases the quality of steam at the evaporator outlet. Cheng and colleagues (Cheng et al., 2014) found that the suction and discharge temperatures of the compressor decrease with the increase in refrigerant charge.

The effect of charge on the density of refrigerant was investigated by Herbert-Raj and Lal (2011). They found that the inlet pressure of the condenser and evaporator increases with the increase in refrigerant charge, leading to an increase in density of refrigerant. Kim et al. (2014) mentioned that the increase in refrigerant charge increases the condensing pressure and so does the density of refrigerant in the condenser (Kim et al., 2014). Another recent study found a similar result (Mastrullo et al., 2014).

The degree of sub-cooling has a significant effect on the performance of the system and its stability (Martinez-Galvan et al., 2011). Previous studies show that the increase in refrigerant charge increases the degree of sub-cooling (Choi and Kim, 2002; Mastrullo et al., 2014; Kim et al., 2014; Chen et al., 2012). Farzad (1990); Rodriguez (1995) and Grace et al. (2005) investigated the effect of the charge on the refrigerant mass flow rate. They found that the mass flow rate of refrigerant increases with the increase in refrigerant charge, however, two other studies by Martinez-Galvan et al. (2011) and Chen et al. (2012) show somewhat different results. Chen et al. (2012) found that the mass flow rate increases until around full charge and then decreases at additional charge. The full charge refers to the originally designed charge of the system specified by the manufacturer and in most cases determined for highest COP. Martinez-Galvan et al. (2011) found that after an optimal charge, the mass flow rate of refrigerant decreases due to an increase in pressure ratio.

Farzad (1990) found that cooling capacity increases sharply with an increase in refrigerant charge until full charge, and then it decreases slightly. The range of charge in his work was from 20% undercharge to 20% overcharge. Martinez-Galvan and colleagues[10] found results similar to Farzad (1990); Choi and Kim (2002) found slightly different results. They found that maximum cooling capacity occurs at 7.5% overcharge. However, Corberán et al. (2008) found that the cooling capacity of heat pumps first increases until an optimal charge is determined for the maximum COP and then remains constant with additional charge. Research by Corberán et al. (2011) showed the same results.

Farzad (1990); Goswami et al. (2001); and Choi and Kim (2002) found that the power input of the compressor increases with the increase in refrigerant charge. Choi and Kim (2002) pointed out that the increase is due to an increase in mass flow rate and compression ratio. Goswami et al. (2001) found a similar result and showed that the work of the compressor increases sharply in an undercharged condition, but only moderately around the full charge level.

The effect of refrigerant charge on the COP of the system has been investigated by many researchers including Choi and Kim (2002), Martinez-Galvan et al. (2011), and Corberán et al. (2011). They found that COP increases until the optimum charge, and then decreases. Choi and Kim (2002) reported a sharp increase from undercharge to full charge, and then a moderate decrease from the full charge to overcharge condition.

Research carried out by Herbert-Raj and Lal (2011) showed that the inlet pressure of condenser and evaporator increases with an increase in charge. Chen et al., 2012 found similar results. They reported that the increase in refrigerant charge increases

the discharge pressure of the compressor but that the effect on suction pressure is different. Suction pressure increases with an increase in refrigerant charge until full charge but remains constant at the overcharge condition. However, a recent study shows that an overcharge of refrigerant leads to an increase in evaporating pressure (Kim et al., 2014). Another recent study showed that an increase in the refrigerant charge increases the condensation pressure (Mastrullo et al., 2014).

7.3 Methodology and Instrumentation

This research was primarily carried out experimentally. A portable propane air conditioning system with a standard charge of 300g propane was used. The system was filled with a 260g charge (12.3% undercharged) to a 390g charge (30% overcharged), and the experiments were carried out at different room temperatures. Further charges were not followed up in this work due to safety concerns as specified by the manufacturer. A Coriolis mass flow meter was installed at the compressor outlet to measure the mass flow rate of the refrigerant. The Coriolis mass flow meter is capable of measuring the fluid in one phase (liquid or vapour state). A power meter, four thermocouples (J type), and four piezoresistive pressure transducers were used to measure the temperature and pressure of the refrigerant at the inlet of the main components of the system, respectively. The position of the instruments can be seen in Figure 7-1.

The cooling capacity, condenser capacity, and useful work of the compressor were calculated using the energy conservation equation based on the measured data. The air conditioning system was placed inside a tent for easier room temperature control. Room temperature was regulated by zipping and unzipping the tent door or with an electric heater placed inside the tent.

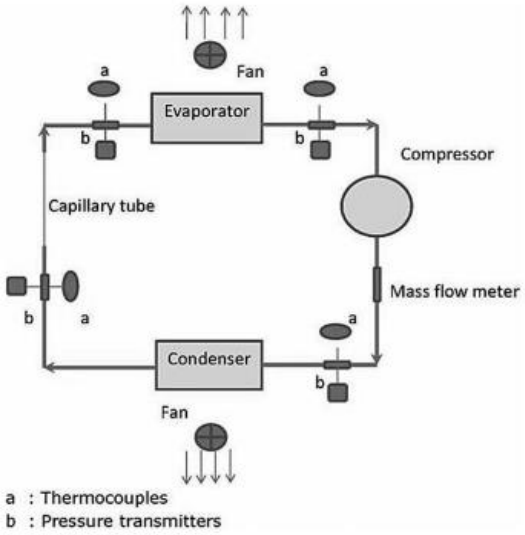

Figure 7-1 Schematic diagram of the portable air conditioner system with instrumentation

7.4 Uncertainty Measurement

Three types of quantities are presented. The first category includes those quantities that have been directly measured; including room temperature, mass flow rate of refrigerant, charge of the system, and pressures and temperatures at the inlet of all four main components of the air conditioner. The main uncertainty in the experiments was due to the cumulative effect of noise and drift. The maximum uncertainty in measuring the refrigerant temperature was ± 1°C (1.64%), refrigerant pressure was ±25 kPa (4.4%), mass flow rate was ±0.00138 kg/s (11.94%), charge was ±0.01g (0.003%), and room temperature was ±0.5°C (3.33%). It should be noted that room temperature varied from 20°C to 35°C; therefore, the relative uncertainty was 3.3% ((0.5 ÷ 15) × 100). In some cases, where the room temperatures of two different experiments are compared, the uncertainty is assumed to be ±1°C, or 6.7% ((1 ÷ 15) × 100).

The second types of data are those obtained from the table of properties. The uncertainty of these values (density, enthalpy, and sub-cooling) is caused by the uncertainty of the measured values (pressure and temperature). The maximum

uncertainty in the density of the refrigerant was determined by comparing the density at the measured pressure and temperature (P, T) with those obtained at four points of (P + 25 kPa, T), (P − 25k Pa, T), (P, T + 1°C), and (P, T − 1°C). A similar approach was used to estimate the uncertainty in the enthalpy of the refrigerant and sub-cooling. The results show a maximum uncertainty of 0.61 kg/m^3 (16.8%) for density, 1.4°C (15.24%) for sub-cooling, 4.91 kJ/kg (1.4%) for the enthalpy of refrigerant at the evaporator, and 3.24 kJ/kg (7.1%) for the enthalpy of refrigerant at the compressor.

The third category includes velocity, cooling capacity, useful work of compressor, specific cooling capacity, and COP, all of which were calculated using two previous quantities. The uncertainties were estimated using the one-word approach and the square root of the sum of the square of uncertainties. The results show a maximum uncertainty of 7.65 m/s (20.61%) for the refrigerant velocity, 0.45 kW (12.48%) for cooling capacity, 73.6 W (13.89%) for useful work of the compressor, 0.0013 W/g (13.89%) for specific charge, and 1.30 (18.38%) for COP.

The estimated uncertainty of the results in this work is within an acceptable range compared to previous studies. The cooling capacity has an uncertainty of 12.48%, which is less than the 13.2% reported by Nilpueng et al. (2011) but more than the uncertainty of 5% reported by Cheng et al. (2014), 2.9% to 3.7%, stated by Herbert-Raj and Lal (2011) and 3.76% to 4.47% determined by Padalkar et al. (2014). Uncertainty of the mass flow rate is 0.00138 kg/s, which was less than 0.0018 kg/s determined by Da Riva and Del Col (2011). The uncertainty of the temperature measurement performed by Padalkar et al. (2014) was ±0.5 °C and this is comparable to the measurement obtained in this work.

Some results presented in this article are only indicative, as their variation is less than the uncertainty of the experiments. Some results have also been identified as outliers and have been removed prior to curve fitting.

7.5 Results and Discussion

7.5.1 Effect of refrigerant charge on refrigerant temperature

The maximum uncertainty of the results presented in this section is 6.67% (1°C), and the maximum standard deviation of the fitted curves is 1.9°C. Figure 7-2 illustrates the impact of the charge on refrigerant temperature at different room temperatures. From Figure 7-2, temperature at the condenser inlet ($T_{in\text{-}cond}$) decreases slightly with the increase in charge regardless of room temperature. The maximum decrease is 5.5°C, which occurs at a room temperature of 23°C as the charge increases from 263.10g to 347.8g.

At the capillary tube inlet with low room temperatures (T_{room}) of 20°C, 23°C, and 26°C, the change in temperature at the capillary tube inlet ($T_{in\text{-}cap}$) is less than the uncertainty of the experiment and can be regarded as insignificant. However, at higher room temperatures, $T_{in\text{-}cap}$ decreases with the increase in charge. The decrease in refrigerant temperature from minimum charge to maximum charge is approximately 2.5°C at T_{room} of 29°C, 4°C at T_{room} of 32°C, and 5.5°C at T_{room} of 35°C. The effect of the charge on the inlet temperatures of the evaporator ($T_{in\text{-}evap.}$) and compressor ($T_{in\text{-}comp.}$) is negligible. However, at a room temperature of 35°C, the increase in $T_{in\text{-}evap}$ and $T_{in\text{-}comp}$ is about 1.4°C, which is slightly greater than the uncertainty of the experiment.

The literature reports inconsistent results regarding the effect of charge on refrigerant temperature. The results presented here are in good agreement with most of the

results described in the literature. Our results show that the inlet temperature of the condenser decreases by the increase in charge, which is similar to the results found by Goswami et al. (2001) and Cheng et al. (2014), but contrary to the results of Mastrullo et al. (2014). The insignificant impact of the charge on the inlet temperature of the capillary tube is consistent with the results reported by Goswami et al. (2001). However, our results show that, at high room temperature, $T_{in\text{-}cap}$ decreases, which has not been reported previously in the literature. The insignificant effect of the charge on the inlet temperature of the evaporator is inconsistent with all previous studies. Goswami et al. (2001) and Cheng et al. (2014) reported that $T_{in\text{-}evap}$ decreases as charge increases, while Mastrullo et al. (2014) reported that it increases, which is only in partial agreement with our results. The results presented in this section show an insignificant effect of the charge on the inlet temperature of the compressor except for a room temperature of 35°C, while Goswami et al. (2001) and Cheng et al. (2014) reported otherwise.

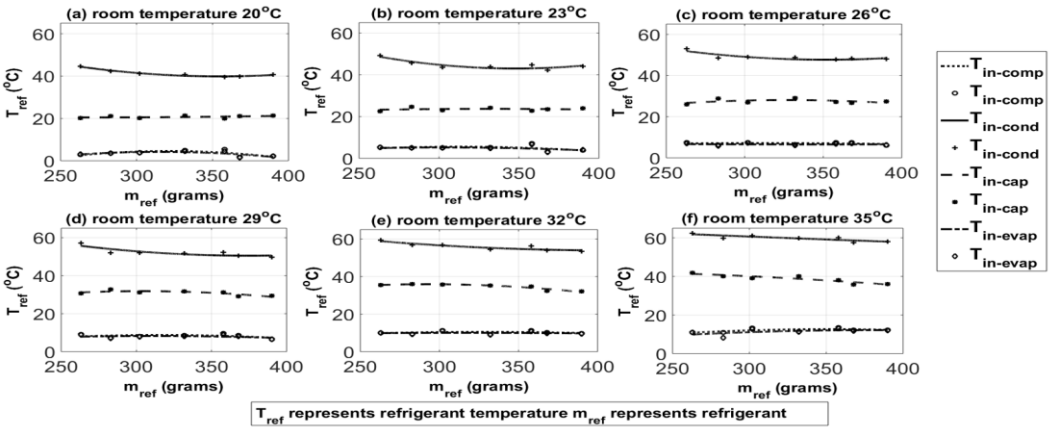

Figure 7-2 Refrigerant temperature versus refrigerant charge at different room temperatures

7.5.2 Effect of refrigerant charge on density of refrigerant

Figure 7-3 presents the effect of the refrigerant charge on the density of the refrigerant. The variation of the density can be used to estimate where the added charge accumulates. The uncertainty of the results presented in Figure 7-3 was

estimated to be 17.1%. The maximum standard deviation of the curves in the Figure is 1.9 kg/m^3. Figure 7-3 shows that the change of density at the inlet of the compressor for all room temperatures is less than the accuracy of the experiment and is regarded as negligible. As shown in Figure 7-3, the density variation is −0.95% at 20°C, −5.79% at 29°C, and −2.96% at 35°C room temperature. The increase in density at the inlet of the condenser and lower room temperatures is significant. The density variation is +23.18% at 20°C and +24% at 29°C as the charge increases from 263.10g to 390g. However, the increase in density at 35°C room temperature is only 7.9%, which is considered to be negligible.

The change in density at the capillary tube inlet is −0.3% at 20 °C, −0.4% at 23 °C, +0.6% at 29°C, and +2.4% at 35°C. At the evaporator inlet, the change in the density is −0.6% at 20°C, +1.2% at 29°C, and +5.6% at 35°C, as the charge increases from 263.10g to 390g. As these changes are less than the uncertainty of the results, they are regarded as inconclusive.

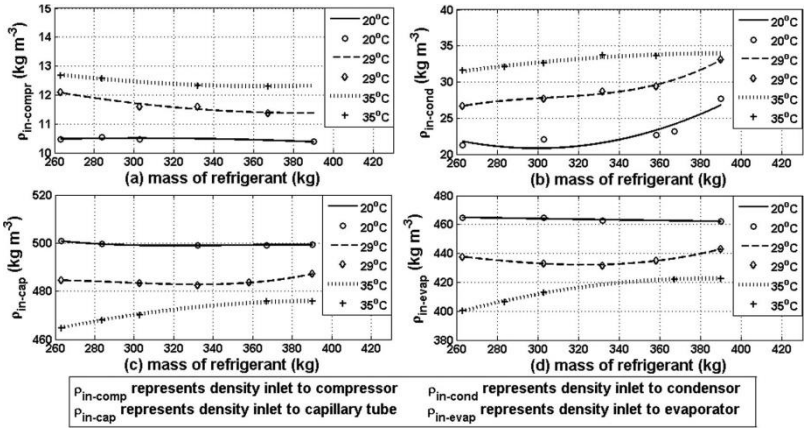

Figure 7-3 Refrigerant density versus refrigerant mass at different room temperatures

The only conclusive result is the increase in density at the condenser inlet by the increase in charge, which is consistent with previous work by Kim et al. (2014).

7.5.3 Effect of refrigerant charge on degree of sub-cooling

The maximum uncertainty associated with sub-cooling is 1.4°C, and the maximum standard deviation in Figure 7-4 is 0.3°C. Figure 7-4 shows the increase in the degree of sub-cooling with the increase in charge. The result shows that, at an average room temperature (26°C), the charge does not have a significant impact on the degree of sub-cooling but that its effect is sizeable at low and high room temperatures. According to Figure 7-4, at the room temperature of 20°C, the degree of sub-cooling increased from 11.1°C at 263.10g charge to 15.5°C at 390g charge (+4.4°C). The degree of sub-cooling increased by 0.9% (+0.1°C) at 26°C and 71.42% (+4.5°C) at 35°C room temperature. These results are in agreement with the previous results reported in the literature (Choi and Kim, 2002; Mastrullo et al., 2014; Kim et al., 2014).

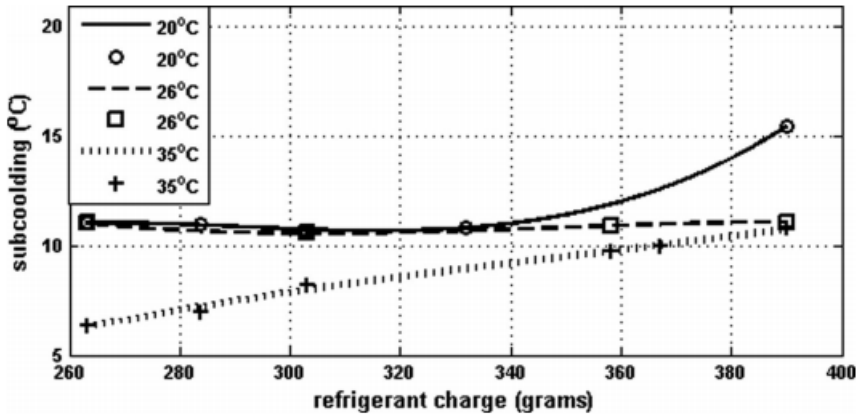

Figure 7-4 Degree of sub-cooling versus refrigerant mass at different room temperatures

7.5.4 Effect of refrigerant charge on maximum velocity

Figure 7-5 presents the maximum velocity of the refrigerant with a maximum uncertainty of 20.61% and maximum standard deviation of 1.466 m/s. The calculation shows that the refrigerant velocity reaches a maximum at the evaporator outlet where the density is at a minimum. Figure 7-5 shows an increase in the maximum velocity with the increase in charge. According to the Figure, the effect of

refrigerant charge on the maximum velocity is more significant at lower room temperatures. At 20°C room temperature, the maximum velocity increased from 25.7 m/s at 263.10g charge to 42.1 m/s at 390g charge (+63.4%), while the increase is 75.9% at 26°C room temperature. The effect of refrigerant charge is the increase in maximum velocity by 18.5% at room temperature of 35°C.

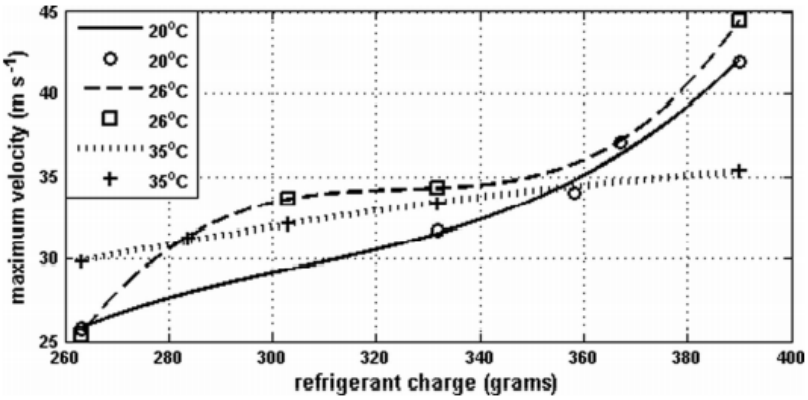

Figure 7-5 Maximumvelocity versus refrigerant mass at different room temperatures

7.5.5 Effect of refrigerant charge on mass flow rate

The mass flow rate was measured at the compressor outlet with a maximum uncertainty of 0.00138 kg/s (11.94%). The fitted curves in Figure 7-6 have a maximum standard deviation of 0.00085 kg/s. Figure 7-6 shows that, with the increase in refrigerant charge, the mass flow rate increases for all room temperatures. At 20°C room temperature, the mass flow rate increases from 0.00999 kg/s at 263.10g charge to 0.01320 kg/s at 390g charge (+32%). The increase rate decreases by the rise in room temperature. The increase in mass flow rate is 28.7% at 26°C and 14.4% at 35°C room temperature.

Most of the previous studies are consistent with these results. The previous studies concluded that, with the increase in charge, mass flow rate increases (Choi and Kim, 2002; Farzad, 1990; Rodriguez, 1995; Grace et al., 2005). However, according to two separate research reports published by Corberan et al., 2011; and Chen et al.,

2012, the mass flow rate reaches a maximum value at a certain charge and then decreases with further increases in charge. The present results suggest such a trend may only be the case at a high room temperature of 35°C.

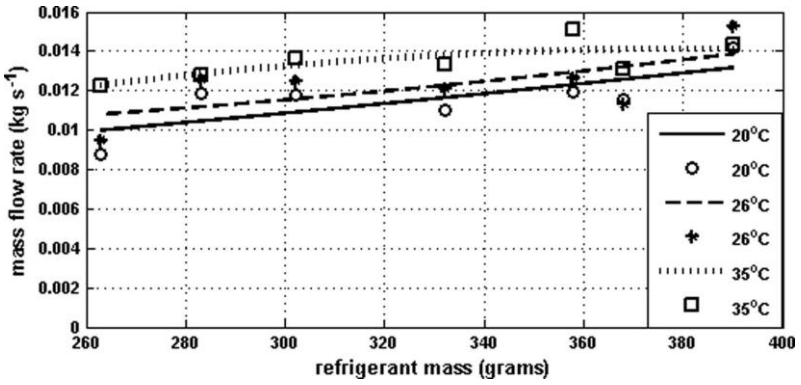

Figure 7-6 Mass flow rate versus refrigerant mass at different room temperatures

7.5.6 Effect of refrigerant charge on cooling capacity

The calculated values of cooling capacity versus the refrigerant charge at two room temperatures of 20°C and 35°C are presented in Figure 7-7. The maximum uncertainty was estimated to be 11.95%, and the fitted curves have a maximum standard deviation of 0.09 kW.

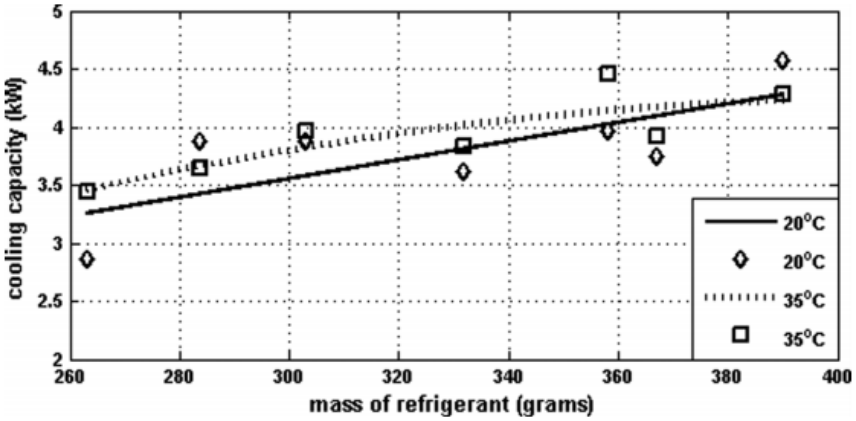

Figure 7-7 Cooling capacity versus mass of refrigerant at different room temperatures

Figure 7-7 shows that the cooling capacity increases significantly with the increase in charge at both room temperatures of 20°C and 35°C. The cooling capacity increases from 3.29 kW to 4.31 kW at 20°C (+30.9%), and from 3.49 kW to 4.25

kW at 35°C (+21.9%). These results are not consistent with the previous studies on non-portable air conditioners. Corberán et al. (2008) and Corberán et al. (2011) found that the cooling capacity reaches a maximum value with the increase in charge, but then remains unchanged with a further increase. Other researchers reported that the cooling capacity slightly decreases with the increase in charge after the peak value, which occurs close to full charge (Choi and Kim, 2002; Corberan et al., 2011; Farzad, 1990). Our results show the contrary. At a room temperature of 20°C, the cooling capacity always increases. However, the results at a room temperature of 35°C appear to show a later peak at a charge above 30% overcharge, which is in partial agreement with the previous studies.

7.5.7 Effect of refrigerant charge on specific cooling capacity

The uncertainty of the cooling capacity is 12.48%. Taking into account the reading uncertainty of the weighing scale (0.003%), the maximum uncertainty of the specific cooling capacity (the cooling capacity divided by refrigerant charge) remains 12.48%. The maximum standard deviation of the fitted curve is 0.18 W/g.

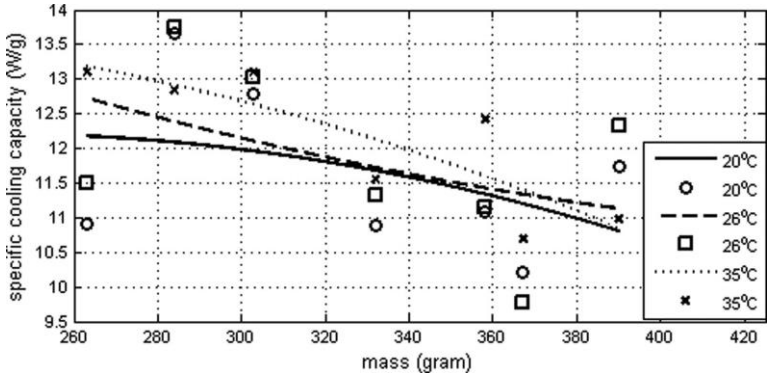

Figure 7-8 Specific cooling capacity versus mass of refrigerant at different room temperatures

Figure 7-8 shows that the specific cooling capacity decreases with the increase in refrigerant charge. At 20°C room temperature, the specific cooling capacity decreases from 12.31 W/g at 263.10g charge to 10.91 W/g at 390g charge, which

indicates an 11.38% decrease. At 26°C, the decrease in specific cooling capacity is from 12.73 W/g to 11.30 W/g (−11.23%). At 35°C, the specific cooling capacity decreases 18.18% from 13.19 W/g at 263.10g charge to 10.79 W/g at 390g charge. There is no conclusive result at low and moderate room temperatures (20°C and 26°C) because the change of specific cooling capacity (−11.38% and −11.23%) is less than the maximum uncertainty of the experiment (12.48%).

7.5.8 Effect of refrigerant charge on compressor work

The useful work of the compressor of the air conditioner versus refrigerant charge is presented in Figure 7-9. The results have a maximum uncertainty of 13.89%, and the fitted curves have a maximum standard deviation of 0.07 kW.

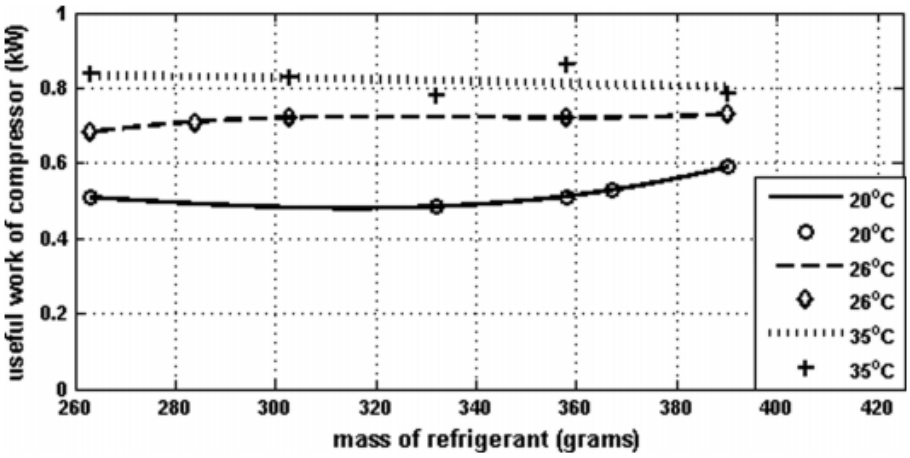

Figure 7-9 Work of compressor versus mass of refrigerant at different room temperatures

Figure 7-9 shows that, at a room temperature of 20°C, the useful work of the compressor increases from 0.51 kW at the charge of 269.1g to 0.59 kW at the charge of 390g (+15.9%). The results also show that at lower charge from 263.10g to 315.1g, the useful work of the compressor decreases slightly from 0.51 kW to 0.48 kW (−5.5%). The drop of the work is less than the maximum uncertainty of the experiment and is not conclusive. At 26°C room temperature, the work of the compressor increases from 0.63 kW at 263.10g charge to 0.73 kW at 390g charge

(+15.53%). At 35°C room temperature, the work of the compressor decreases from 0.83 kW at 263.10g charge to 0.80 kW at 390g charge (−3.67%). The result at the room temperature of 35°C is not conclusive. The increase in the useful work of the compressor with the increase in the charge is in full agreement with previous studies (Choi and Kim, 2002; Goswami et al., 2001; Farzad, 1990).

7.5.9 Effect of refrigerant charge on COP

Figure 7-10 shows the calculated COP versus the refrigerant charge at four room temperatures of 20°C, 26°C, 32°C, and 35°C. The maximum uncertainty of the results was estimated to be 18.38%, and the fitted curves have a maximum standard deviation of 0.42.

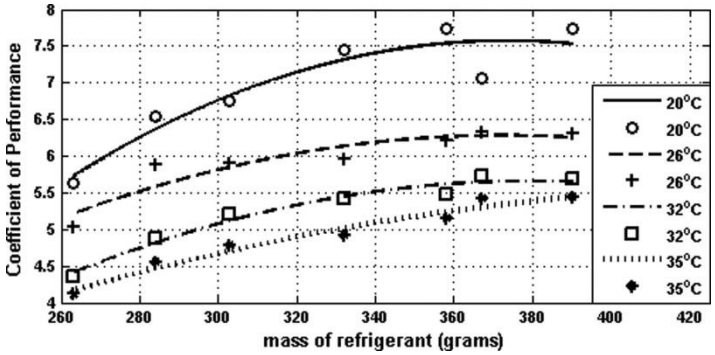

Figure 7-10 COP versus mass of refrigerant at different room temperatures

The results show that the COP continuously increases by the increase in charge in all room temperatures. The increase is 32.4% at 20°C, 20.6% at 26°C, 28.6% at 32°C, and 30.3% at 35°C room temperatures. It is notable that the rate of increase declines as the refrigerant charge increases except for the room temperature of 35°C. These results are not consistent with the results in the literature. According to previous studies, the coefficient of the performance reaches a peak at a specific charge, and then decreases thereafter (Choi and Kim, 2002; Corberan et al., 2011; Martinez-Galvan., 2011). It should be noted that the rate of increase in COP decreases with the

increasing charge. This implies that a maximum COP may be reached at further charges.

7.5.10 Effect of refrigerant charge on maximum pressure

The maximum pressure of the refrigerant at the compressor outlet versus the refrigerant charges is presented in Figure 7-11. The maximum uncertainty of the results is 5.5% and the maximum standard deviation of the curves is 54.1 kPa.

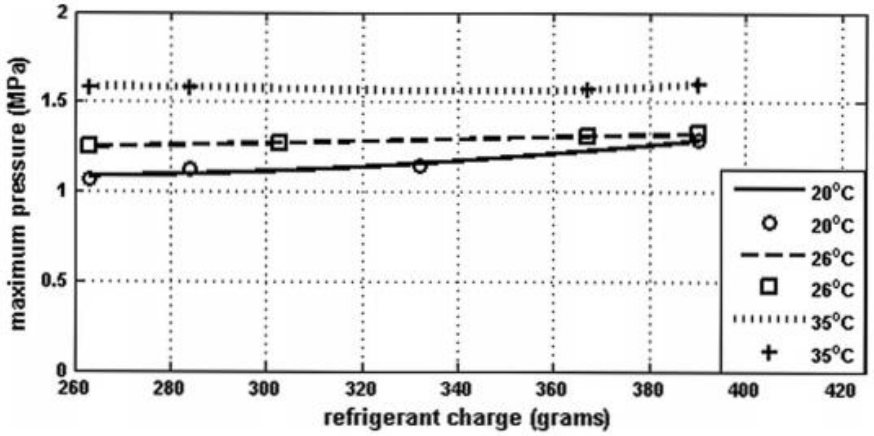

Figure 7-11 Maximum pressure versus mass of refrigerant at different room temperatures

Figure 7-11 shows a significant effect of the charge on the maximum pressure of the air conditioner at lower room temperatures. At a room temperature of 20°C, the maximum pressure increases from 1085.9 kPa to 1285.2 kPa (+18.4%) as the charge increases from 263.10g to 390g. At a room temperature of 26°C, the effect is moderate (+5.87%). As room temperature increases, the effect of the charge on the maximum pressure decreases and becomes insignificant. For example, at a room temperature of 35°C, the maximum pressure increases from 1584 kPa to 1601 kPa (+1.05%), which is less than the maximum uncertainty of the experiment (5.5%).

The experimental results presented in this section show that the maximum pressure of the system, which occurs at the compressor outlet, increases significantly at lower

room temperatures, but remains fairly constant at higher room temperatures. Previous studies show that the maximum pressure increases with the increase in charge, but there is no mention of room temperature (Mastrullo et al., 2014; Herbert-Raj and Lal, 2011; Kim et al., 2014).

7.5.11 Discussion

In the previous section, the experimental results corresponding to the effects of charge on the performance of the portable air conditioner were reported. The effects are extensive and the links between different aspects are not straightforward. For a better understanding of the cycle, in some cases, it is necessary to consider several effects simultaneously.

The first conclusive results to be discussed are related to the increases in mass flow rate with the increases in refrigerant charge. Once the compressor is switched off and the air conditioner is filled with a higher amount of refrigerant, the density at all points within the air conditioner is expected to be higher. As a result, the refrigerant has a higher density at the inlet of the compressor during the first rotation of the compressor once it is switched on; therefore, the initial mass flow rate is higher for the case with a larger charge (Li et al., 2010). Ignoring the negligible effect of the gravity, a uniform density can be presumed inside the system. Therefore, during the first rotation of the compressor, once it is switched on, the mass flow rate is higher for the case with a larger charge. A higher initial mass flow results in a higher-pressure difference between the two ends of the capillary tube, which requires the compressor to work harder to maintain the new operating condition. At this stage, what actually occurs depends on both the characteristics of the compressor and its operating point with respect to its design point. In addition, the higher initial refrigerant velocity, measured at a point located before the compressor, was

attributed to the increase in mass flow rate. A higher velocity while the static density is nearly constant (Figure 7-3a) leads to a higher stagnation density at the inlet section of the compressor, which is about 0.9 m from the measurement point. Our calculation of the stagnation density shows that the higher velocity contributes 2.9% of the mass flow rate increase at most. Therefore, as already mentioned, different performances of the compressor at different operating points are the main reason behind the change of the mass flow rate and explains the inconsistent results. The increase in mass flow rate with the increase in refrigerant charge agrees with most of the previous studies. There are only two studies (Corberán et al., 2011; and Chen et al., 2012) that show a decrease of mass flow rate when the charge exceeds a certain value.

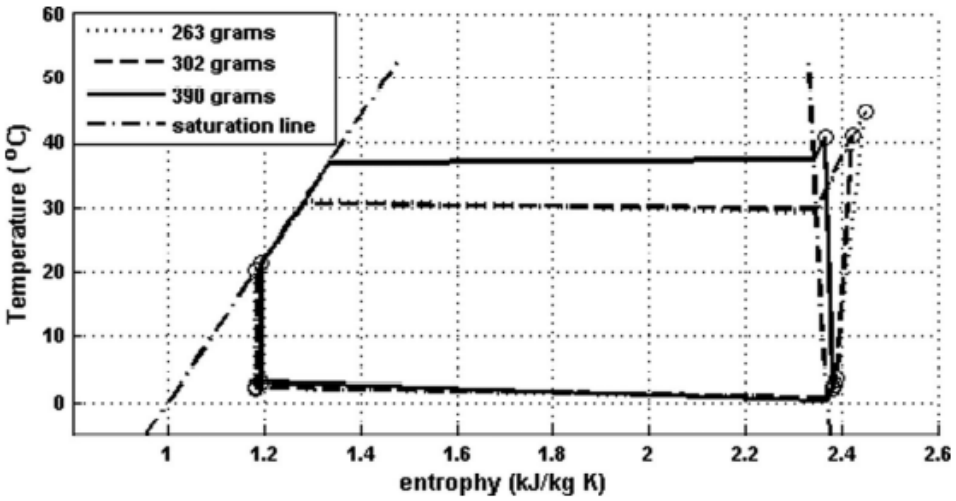

Figure 7-12 Entropy-temperature diagram for the portable propane air-conditioner at room temperature of 20C

The results also show that an increasing charge has no discernible impact on the conditions of the refrigerant at the inlet of the compressor. A noticeable decrease in temperature was detected at its outlet, which was not expected due to the increase in the outlet pressure. To clarify this issue, in Figure 7-12, the conditions of the refrigerant at the exit of the compressor and at a room temperature of 20°C are

shown for different charge levels. According to the Figure, the outlet entropy decreases as charge increases. There are two possibilities explaining the results: (1) a higher heat transfer per mass flow rate of the refrigerant from the compressor and (2) a lower irreversibility rate in the compressor. The first possibility is unfeasible in this case because the inlet temperature of the compressor is unchanged, and the outlet temperature decreases at higher charges. The second possibility was examined by determining the efficiency of the compressor, which is defined as the ratio of useful work of a compressor to inlet electrical power. The results verify a higher efficiency of the compressor at higher charges, up to room temperature of 29°C. For instance, the increase in refrigerant charge from 263.09 g to 390.00 g leads to the increase in efficiency by 4.9% at 20°C, 22.71% at 23°C, 12.23% at 26°C, and 0.5% at 29°C. No increase in the efficiency was detected at room temperatures of 32°C and 35°C.

A higher outlet pressure from the compressor leads to a higher temperature within the condenser even though the outlet temperature of the compressor is lower at a higher charge (Figure 7-12). A higher outlet pressure from the compressor leads to a higher temperature within the condenser even though the outlet temperature of the compressor is lower at a higher charge (Figure 7-12). A higher temperature and mass flow rate yields a greater heat removal from the condenser. The specific latent heat of evaporation at higher temperature decreases and corresponds to a higher sub-cooling at the outlet of the condenser (Figure 7-4) (Herbert-Raj and Lal, 2011). However, as the saturation temperature is higher at the elevated pressures, the temperature at the outlet of the condenser remains nearly the same (Figure 7-2). The sub-cooled liquid flows through a longer length of the capillary tube in this situation; this contributes to lowering the noise level (Martinez-Ballester et al., 2014). As the mass flow rate increases the total head loss in the capillary tube increases and

leading to the outlet pressure of the capillary tube remaining nearly unchanged and subsequently, the inlet pressure and temperature of the evaporator does not significantly change. The cooling capacity of the air conditioner at higher charge increases due to the increase in the convective heat transfer coefficient inside the evaporator tube caused by a higher mass flow rate and lower quality of the inlet refrigerant to the evaporator (see Figure 7-4 for higher sub-cooling and Figure 7-3 for lower quality). However, the specific cooling capacity at higher charge level decreases (Figure 7-9) showing a higher increase in mass flow rate compared to cooling capacity. An identical wind speed over the evaporator and approximately the same temperature difference for all cases do not offer a proportional correlation between cooling capacity and mass flow rate.

The experimental set up cannot exactly identify where the extra charge goes while the air conditioner is on. One way to assess this is to look for the change in density. The experimental results showed that the increase in charge causes only small changes in the density of the working fluid except at the compressor's outlet. The evaporator does not greatly accommodate the extra charge as the results show relatively small density variation at two ends of the evaporator in all cases. The capillary tube con-tributes a very small density fraction of the refrigerant. The inlet of the compressor also does not show a big variation and its outlet is in superheat conditions and does not greatly contribute to accommodating the extra charge. However, the increase in density at the inlet of the condenser and the sub-cooling proves that most of the added charge is accommodated by the condenser. This is in agreement with previous studies (Kim et al., 2014). Unfortunately, the measured density cannot be reliably used to locate the extra charge. The density variations are negligible except at the compressor outlet. However, as the refrigerant is at superheat

state and thus low density at that point, this variation cannot explain where the added charge is. The only way to explain where the added charge has been accumulated is to note the increase of sub-cooling at a higher charge. The increase of sub-cooling reveals that the added charge piles up as liquid within a longer length of the condenser. The insignificant variation of the density at that point can be justified by considering the liquid state of the refrigerant at the end of the condenser.

The increase in COP with charge is an important result. Due to the increase in mass flow rate and outlet pressure of the compressor at higher charge, both the cooling capacity of the system and the useful work of the compressor increase. Previous studies on non-portable air conditioners show that the COP increases up to a certain charge but then decreases. Unlike previous studies, the results obtained in this work do not indicate any decrease of COP up to 30% overcharge case. These results suggest that portable air conditioners have a greater capacity to realize a higher performance than others by adding the charge. The increase in COP cannot mainly be attributed to the increase in mass flow rate, since it leads to the increase in both cooling capacity and useful work of the compressor. Taking into account that the cooling capacity is approximately the difference between heat discharged from the condenser and useful work of the compressor, the increase in refrigerant temperature at the condenser plays a major role in the increase in COP at higher charges. In addition, the decrease of entropy at the outlet of the compressor, which decreases its required work, can partially contribute to increase in COP.

Care should be taken in generalizing the findings of this study to other portable air conditioners. The decrease of outlet entropy of the compressor at higher charge had a positive impact in reducing the required useful work of the compressor. Such a decrease may not occur in other air conditioners. In this study, the useful work of the

compressor was considered in defining the COP, and the compressor demonstrated a higher efficiency at higher charge. This may lead to an even greater increase in COP at higher charge if the efficiency was defined based on the inlet electrical power. With this definition, however, the COP may decrease at the higher charge if the compressor operates at a lower efficiency part of its performance characteristic curve.

This research aims to fill the research gap for portable air conditioners by investigating the effect of refrigerant charge on important parameters at different room temperatures ranging from 20°C to 35°C. The amount of charge is particularly important for hydrocarbon refrigerants as they are explosive. Therefore, many countries have adopted their own safety protocols and legislation regarding the maximum amount of hydrocarbon in HVAC appliances.

7.6 Summary and Further Discussion

The effects of increasing charge on the performance of a portable propane air conditioner were assessed and compared with those of non-portable refrigeration and air conditioners. There are more similarities than differences between the performances of the two systems. The main similarities are the increase in density at the outlet of the compressor, sub-cooling, mass flow rate, and work of the compressor with the increase in charge. Taking into account some inconsistencies in the literature, some similarities in the variation of refrigerant temperatures in the different parts of the air conditioner with the increase in the charge exist between the two systems. However, most of the previous studies on the non-portable systems reported a temperature drop at the evaporator inlet, while our results show an insignificant change in the temperature. This demonstrates some significant

dissimilarities between the performance of portable and non-portable air conditioners.

The increase in mass flow rate and insignificant change of the evaporator temperature increases the cooling capacity of the evaporator. Unlike the non-portable systems, the cooling capacity of the portable systems continues to rise and does not reach a maximum value at around the full charge of the system. The COP also does not reach a maximum value due to the negligible increase in the work of the compressor. The simultaneous and continuous increase in the cooling capacity and COP is a significant advantage of portable propane air conditioners over non-portable systems. However, it should be noted that the results of this study are only valid for an up to 30% overcharge condition.

The increase in charge has some negative impacts on the performance of portable systems, which can be somewhat controlled. These impacts include the increase in the maximum velocity as well as the maximum pressure of the refrigerant. The increase in the maximum velocity results in a higher noise level and shorter system life and occurs between the outlet of the evaporator and the inlet of the compressor. The velocity can be reduced by a larger diameter tubing of the evaporator and suction line, and if necessary, by a suitable choice of compressor. The rise in the maximum pressure is also hazardous and should be controlled. All air conditioners are designed for safe operation at high room temperatures, and fortunately, the results indicate that the increase in the maximum pressure at the compressor outlet and high room temperature is not too significant.

The major negative impact of the increase in the charge is the decline of the specific cooling capacity. The results show that the propane required for a given cooling

capacity increases if a portable over-charge propane air conditioners is used. Taking into account the increase in the COP and noting that the green and renewable energy currently does not contribute to a large portion of the energy production, the use of an overcharged portable propane air conditioner is good for the environment but poses some safety risks.

7.7 Conclusion

The performance of a portable propane air conditioner at different refrigerant charge levels from 12.1% undercharge to 30% overcharge has been experimentally assessed and compared with that of non-portable air conditioners. The results show many similarities and some key differences between the two systems as the refrigerant charge increases. The similarities include the increase in density, sub-cooling, mass flow rate, and useful work of the compressor, and the differences are the continuing increase in cooling capacity and COP from 12.1% undercharge to 30% overcharge for the tested portable propane air conditioner. The main disadvantage of increasing refrigerant charge is the decrease of specific cooling capacity.

CHAPTER 8 CONCLUSION

8.1 Introduction

This chapter begins with a summary of the results of the six computational and experimental studies presented in the previous chapters. A summary of outcomes and suggested strategies for reducing the total charge within the portable single-duct propane air-conditioners is presented. At the chapter's end, two new studies are suggested as further works.

8.2 Summary of the results

This work attempts to provide a better understanding of the performance of single-duct portable propane air conditioners and identify their performance similarities and differences compared with those of non-portable air conditioners. These findings can assist with the design of this type of air conditioner, focusing on possible ways of reducing the amount of charge within the system (Chapters 2 – 5). In the first step, to weigh the design process, a pilot experimental study was conducted to assess the impacts of room temperature on the performance of a portable propane air conditioner and compare it with those of non-portable air-conditioners (Chapter 6). The experimental results identified a few significant differences and many similarities between the performances of the two systems (Section 6.7). Similar to non-portable systems, the refrigerant temperature in all parts of the system (refrigerant mass flow rate, work of the compressor, and maximum pressure of the portable system) increases as room temperature increases, and the level of refrigerant sub-cooling and COP of the system decreases. The results also suggested that, as room temperature increases, the refrigerant accumulates more in the compressor and less in other parts of the system.

The main identified differences between the two systems were the change in the maximum velocity of the refrigerant and cooling capacity with the increase in room temperature (Chapter 7). Unlike non-portable systems, the maximum velocity of the refrigerant at the overcharge condition decreases with the increase in room temperature. In addition, a slight increase in cooling capacity for a full charge portable air conditioner was observed (Section 7.6). For an overcharged portable air conditioner, the cooling capacity initially increases and then decreases with the increase in room temperature. For non-portable air-conditioners, the cooling capacity decreases with an increase in room temperature regardless of the level of charge.

The results of the first experimental work (Chapter 6) clarified several important differences between the impacts of room temperature on the performance of portable and non-portable air-conditioners. In the second experimental work (Chapter 7), the impacts of different charge levels on the performance of the two types of air-conditioners were assessed. The results again showed many similarities and some key differences between the performances of the two systems as the refrigerant charge increases (Section 7.6). The similarities include the increase in density, sub-cooling, mass flow rate, and useful work of the compressor. The differences are the continuing increase in cooling capacity and COP for the 12.1% undercharged condition to 30% for the overcharged condition for the tested portable propane air conditioner. The main disadvantage of increasing refrigerant charge was the decrease in specific cooling capacity. However, it should be noted that the results of the study are only valid for an up to 30% overcharge condition.

The study led to a better understanding of the performance of single-duct portable propane air conditioners and suggested some ways of decreasing the charge. A list of similarities and differences between the performance of portable and non-portable air

conditioners and some suggested strategies in reducing total charge within portable air-conditioners are as follows.

Similarities between the performance of portable and non-portable air conditioners are:

i. Increase in room temperature increases the refrigerant temperature at all parts

ii. Increase in room temperature increases the mass flow rate of refrigerant

iii. Increase in room temperature increases the work of compressor

iv. Increase in room temperature increases maximum pressure

v. Increase in room temperature decreases sub-cooling

vi. Increase in room temperature decreases the COP

vii. Increase in the air temperature around the evaporator and condenser decreases the specific heat transfer

viii. Increase in refrigerant charge increases the density of refrigerant at the outlet of the compressor.

ix. Increase in refrigerant charge increases sub-cooling

x. Increase in refrigerant charge increases the mass flow rate

xi. Increase in refrigerant charge increases the work of compressor.

The main differences in performance of portable air-conditioners compared to non-portable air conditioners are:

i. Increase in room temperature slightly increases the cooling capacity at full charge

ii. Increase in room temperature decreases the maximum velocity

iii. At 30% overcharged condition, an increase in room temperature increases the cooling capacity which then decreases with a further increase in room temperature

iv. Increase in refrigerant charge continues to increase the cooling capacity (up to 30% overcharged)

v. Increase in refrigerant charge continues to increase the COP (up to 30% overcharged).

A study on the effects of inlet pressure on the performance and size of the condenser of the portable propane air conditioner was conducted to assess the impact of alternative designs (Chapter 5). The results indicate that increasing the inlet pressure of the condenser increases the capacity of the condenser and decreases the outlet temperature; and the recommended sub-cooled value of 7°C to 10°C can be easily achieved at higher inlet pressure and at all room temperatures (Section 5.8). However, increasing the inlet pressure can increase propane charge in the condenser depending on the outlet conditions. There is an optimum value of inlet pressure for a minimum specific charge. The study also showed that a significant reduction in the refrigerant mass within the condenser for a certain capacity is achievable by reducing the length of the condenser and increasing the inlet pressure simultaneously (Section 5.8). For the air-conditioner under investigation, by increasing the inlet pressure from 1.30 MPa to 2.00 MPa at a room temperature of 27°C, the study estimated that

a 50.7% reduction of propane in the condenser could be achieved without sacrificing the condenser capacity. However, this will reduce COP from 5.75 to 3.73.

In the next step, a computational study was conducted to identify the effects of inlet pressure, size, and wind speed of an evaporator on the amount of refrigerant charge and to assess inlet pressure, size and wind speed over the evaporator effects on the overall performance of portable propane air conditioners (Chapter 4). The study shows that a lower evaporator inlet pressure leads to a smaller charge within the evaporator. However, this technique causes frost to appear on the evaporator coils. This risk can be minimized by increasing the air speed over the coils (Section 4.7).

Two studies were completed to find the best way to reduce the mass of refrigerant in the capillary tube (Chapters 2 and 3). In the first study, two potential designs were investigated to reduce the inner diameter of the capillary tube and reduce the coil diameter (Chapter 2). The results show that both designs are effective and capable of reducing the required refrigerant by 1.098 g and 0.981 g that corresponds to 91.5% and 81.8% of the mass within the capillary tube, respectively. The first design has the disadvantage of increasing the refrigerant velocity speed to a level that may exceed the recommended value and consequently reduce the life of the tube (Section 2.5). It also produces excessive noise, which is particularly important for portable air-conditioners that are located inside the room. In addition, these designs are not applicable if the distance between condenser and evaporator cannot be bridged by the new short capillary tube or small coil diameter.

The mass of refrigerant in the capillary tube is around 0.1% of the total mass of refrigerant within the usual air-conditioners. Therefore, despite the high reduction of

mass within the capillary tube, the advantage of utilising the suggested techniques is very limited.

A second study was completed to estimate the impact of the integration of the capillary tube and liquid line which usually contains about 1% to 2% of total refrigerant (Chapter 3). The computational results support the concept of substituting the capillary tube and liquid line of propane air-conditioners with a larger diameter and longer capillary tube (Section 3.5). The results show that a 64% reduction of the refrigerant within the combined capillary tube/liquid line is achievable and has the advantage of a reasonable reduction in the maximum velocity of refrigerant.

8.3 Cost Analysis

Another benefit of decreasing the diameter of the capillary tube is that the price of a smaller and shorter capillary tube is expected to be cheaper compared to the existing capillary tube. The cost of modifying the air conditioner with a new capillary tube is only the replacement cost. As the inlet and outlet conditions of the capillary tube for existing and new capillary tubes are similar, the energy used remains constant.

The cost effect of replacing the existing capillary tube and liquid line with a new extended capillary tube is positive. The new capillary tube has considerably less copper material compared to the existing liquid line which has a larger diameter. The material of the new larger capillary tube is slightly more compared to the existing capillary tube. However, the total material of the new design is expected to be less than the existing system. The replacement cost of the existing capillary tube and liquid line by the new extended capillary tube is expected to be low. There is no change in energy used before and after modification because the inlet and outlet pressures and temperatures remain constant.

Decreasing the evaporator pressure and increasing the airspeed over the evaporator is not a low-cost modification. The compressor of the air conditioner must be replaced with a compressor with a higher-pressure ratio and a higher volume capacity of evaporator blower is required, therefore the modification is a high cost.

The implication of increasing the inlet pressure of the condenser is to change the compressor size, select a new smaller condenser, and a new longer capillary tube, therefore; the modification needs a high cost. The new condenser is smaller than the existing condenser is less expensive, and a new longer capillary tube is more expensive than the existing system. As the COP of the new system is lower with higher cooling capacity, the system needs more energy to run.

8.4 Conclusion

Based on this study, suggested strategies for reducing the total charge of propane within portable single-duct propane air conditioners are as follows:

1. Increasing the inlet pressure of the condenser and reducing the size of the condenser simultaneously for the desired cooling capacity. The main disadvantage of this technique is the reduction of COP. The estimation of charge reduction within the condenser is around 25% within ACs (as most condensers contain approximately 50% of total charge (Corberan et al., 2008; Jierong et al., 2017)
2. Reduction of evaporator inlet pressure and increasing wind speed on the coils. The estimation of charge reduction within the evaporator is more than 50% or approximately 6% within ACs (as most evaporators contain around 12% of total charge (Corberan et al., 2011)

3. Integrating the capillary tube and liquid line. The percentage of charge reduction within the capillary tube and liquid line is 63.9% or about 0.9% within a typical air conditioner (liquid line and capillary tube contain about 1.4% of total charge within a typical air conditioner). Total charge of liquid line and capillary tube within a non-portable air conditioner is more than 4.39% (Corberan et al., 2008).
4. A slight overcharge design of the portable air conditioners compared to non-portable systems as the cooling capacity and COP still increase at full charge
5. Applying a slightly larger capillary tube diameter with a smaller coil diameter compared to the small diameter of a straight capillary tube. This reduces the refrigerant mass within the capillary tube by more than 50% or 0.05% within the air conditioners.

8.5 Further work

Several strategies for reducing total charge within the portable single-duct propane air conditioner based on the outcomes of this experimental and computation work have been suggested. However, in this work, each strategy has been studied separately and the combined effect of the suggested strategies is unknown. Therefore, it is important to put all suggestions together and study the overall effect.

It was shown that reducing the evaporator pressure increases the frosting risk on the evaporator coil. Two possible solutions are: 1) use of a secondary fluid as the heat absorbent (chiller) for a small air conditioner and 2) add a small percentage of isobutane to the propane to increase the evaporator temperature. A comprehensive study is required to assess the effectiveness of both strategies in terms of performance and cost-effectiveness.

REFERENCES

Accelerate, Australia, New Zealand Adopt IEC's Hydrocarbon Charge Limit for Commercial Cabinets (accessed on 19 October 2020, https://accelerate24.news/refrigeration/australia-new-zealand-adopt-iecs-hydrocarbon-charge-limit-for-commercial-cabinets/2020/)

AHRI Refrigerant Safety., 2017 Available: http://www.ahrinet.org/Contractors-Specifiers/Refrigerant-Safety.aspx [Accessed 5 January 2017].

American Standard Inc, Trane 2002, Refrigerant piping, viewed 7 January 2013, (http://www.njatc.org/downloads/trc006en.pdf&sourceid=ie7&rls=com.microsoft:en-AU:IE-Address&ie=&oe=&gws_rd=cr&redir_esc=&&ei=rxTvUdvUNMf-1AWR4IDQBQ)

Australian Department of Agriculture, Water and the Environment, 2020, Refrigeration and Air conditioning - Consumer, (Accessed on 3rd April 2020, https://www.environment.gov.au/protection/ozone/rac/consumers)

Australian Department of Agriculture, Water and the Environment, 2019, Hydrofluorocarbon phase-down, (Accessed on 19th February 2020, https://www.environment.gov.au/protection/ozone/hfc-phase-down)

Bell, K. J and Mueller, A. C. Wolverine Engineering Book II, Wolverine tube, Inc, Decatur AL, USA. 2001

Blanco Castro J., Urchueguia J. F., Corberan J. M. and Gonsalvez J.,"Optimized design of a heat exchanger for an air-to-water reversible heat pump working with propane (R290) as refrigerant: Modelling analysis and experimental observations." In *Applied Thermal Engineering*, vol 25 (14-15): 2450 – 2462, 2005.

British Refrigeration Assosiation (BRA), Guide to flammable refrigerants (Accessed on 13th July 2020, https://www.refcom.org.uk/media/1157/bra-guide-to-flammable-refrigerants-issue-1-oct-12.pdf)

Cengel, Y. A & Boles, M. A., Thermodynamics, 5edn, McGraw Hill, Boston. 2006

Cengel Y. A.," Heat transfer: a practical approach, New York, McGrawHill, 2004.

Cengel Y. A,"Thermodynamics: an engineering approach. Boston, McGraw-Hill Higher Education, 2006.

Chen, J., Ding, R., Li, Y., Lin, X., Chen, Y., Luo, X. and Yang, Z.,. Application of a vapor–liquid separation heat exchanger to the air conditioning system at cooling and heating modes. *International Journal of Refrigeration*, *100*, pp.27-36. 2019

Chen, J., Min, K., and Li, F. Comparison of performance between R290 and R417A in heat pump air conditioning water heater combination. *1st International Conference on Civil Engineering, Architecture and Building Materials, CEABM* 2011, June 18, 2011 - June 20, 2011, Haikou, China, Trans Tech Publications. 2011

Chen Y, Hua N, Deng L. Performances of a split-type air conditioner employing a condenser with liquid–vapour separation baffles. *International Journal of Refrigeration*. 35:278–289. 2012

Cheng S, Wang S, Liu Z. Cycle performance of alternative refrigerants for domestic air-conditioning system based on a small finned tube heat exchanger. *Applied Thermal Engineering*. 64(1):83–92. 2014

Choi JM and Kim YC. The effects of improper refrigerant charge on the performance of a heat pump with an electronic expansion valve and capillary tube. *Energy*. 27:391–404. 2002

Choudhari, C.S. and Sapali, S.N., Testing of environment friendly refrigerant R290 for water cooler application. *International Journal of Engineering-Transactions A: Basics*, *31*(1), pp.157-163. 2018

Christina Nunez, Causes and Effects of Climate Change, National Geographic. 2019. (Accessed on February 18th 2020, https://www.nationalgeographic.com/environment/global-warming/global-warming overview/)

Cooling Post, Will the US follow Europe with hydrocarbons? (accessed on 19 October 2020, https://www.coolingpost.com/features/will-the-us-follow-europe-with-hydrocarbons/)

Copeland, Refrigerant manual, hvacrinfo, 2000., viewed 7 January 2013 (http://www.hvacrinfo.com/Cope_manuals/AE104_R2.pdf)

Corberán JM, Martínez IO, Gonzálvez J. Charge optimisation study of a reversible water-to-water propane heat pump. *International Journal of Refrigeration*. 31:716–726. 2008

Corberán J-M, Martínez-Galván I, Martínez-Ballester S, Gonzálvez-Maciá J, Royo-Pastor R. Influence of the source and sink temperatures on the optimal refrigerant charge of a water-to-water heat pump. *International Journal of Refrigeration*. 34:881– 892. 2011

Dai, B., Liu, S., Li, H., Sun, Z., Song, M., Yang, Q. and Ma, Y., Energetic performance of transcritical CO_2 refrigeration cycles with mechanical sub-cooling using zeotropic mixture as refrigerant. *Energy*, 150, pp.205-221. 2018

Da Riva E, Del Col D. Performance of a semi-hermetic reciprocating compressor with propane and mineral oil. *International Journal of Refrigeration.* 34(3):752–763. 2011

Department of Agriculture, Water and the Environment Australia, 2020. Climate science (accessed on 3 November 2020, https://www.environment.gov.au/climate-change/climate-science-data/climate-science)

Devecioğlu, A.G. and Oruç, V., Enhancement of Energy Parameters for Refrigerants Used instead of R22 by Arranging Capillary Tube Length. *Journal of Energy Engineering*, *143*(1), p.04016038. 2017

Deymi-Dashtebayaz, M., Farahnak, M., Moraffa, M., Ghalami, A. and Mohammadi, N., Experimental evaluation of refrigerant mass charge and ambient air temperature effects on performance of air-conditioning systems. *Heat and Mass Transfer*, 54(3), pp.803-812. 2018

Doiphode, P., Lakshmanan, V. and Samanta, I., Experimental and Numerical Study of Cooling Performance of Air Conditioner Using R32/CO2 Refrigerant Mixture. International Journal of Air-Conditioning and Refrigeration, 27(02), p.1950019. 2019

Donald Wuibbless, Ozone depletion, Encyclopaedia Britannica. 2020 (Accessed on 19th February 2020, https://www.britannica.com/science/ozone-depletion)

El-Sayed, A.R., El Morsi, M. and Mahmoud, N.A., A review of the potential replacements of HCFC/HFCs using environment-friendly refrigerants. *International Journal of Air-Conditioning and Refrigeration,* 26(03), p.1830002. 2018

Emani, M.S. and Mandal, B.K., June. The use of natural refrigerants in refrigeration and air conditioning systems: a review. In IOP Conference Series: Materials Science and Engineering (Vol. 377, No. 1, p. 012064). IOP Publishing. 2018, June

EPA (United States Environmental Protection Agency), 2018 (Accessed on 3rd May 2020, https://www.epa.gov/ozone-layer-protection/basic-ozone-layer-science)

EPA (United States Environmental Protection Agency), 2018 (Accessed on 6th July 2020, https://www.epa.gov/ozone-layer-protection/health-and-environmental-effects-ozone-layer-depletion)

Evans J. S., Why are there so many oil? 2013, Available at http://www.wearcheck.co.za/downloads/bulletins/bulletin/tech27.pdf (accessed on 27 March 2014).

Farzad M. *Modeling the effects of refrigerant charging on air conditioner performance characteristics for three expansion devices.* PhD Thesis, Texas A&M University; 1990.

Fernando P, Palm B, Lundqvist P, Granryd E. Performance of a Single-Family Heat Pump at Different Working Conditions Using Small Quantity of Propane as Refrigerant. *Experimental Heat Transfer*; vol. 20, no. 1, pp. 57-71. 2007

Fernando P., Palm B., Lundqvist P. and Granryd E., Propane heat pump with low refrigerant charge: Design and laboratory tests, *International Journal of Refrigeration* vol 27 (7), 761–773. 2004

Fernando, P. D., *Experimental Investigation of Refrigerant Charge Minimisation of a Small Capacity Heat Pump*. Department of Energy Technology. Stockholm, Royal Institute of Technology. **Doctoral**: 106. 2007

Fox R. W.,"Introduction to fluid mechanics, Hoboken NJ, John Wiley, 2004.

Fox R. W., Pritchard P. J., McDonald A. T. Introduction to Fluid Mechanics, 7th edn, John Willey & Sons, New Jersey; 2010.

Gartshore, J., "Refrigerations Appliances using Hydrocarbon Refrigerants: Manual for Safe Design, Manufacturing, Servicing and Drop-in Conversion of Commercial and Domestic Refrigeration Appliances," An ECOFRIG, 1995

Goswami D, EK G, Leung M, Jotshi C, Sherif S, Colacino F. Effect of refrigerant charge on the performance of air conditioning systems. *International Journal of Energy Research*. 2001;25:741–750.

Grace I, Datta D, Tassou S. Sensitivity of refrigeration system performance to charge levels and parameters for on-line leak detection. *Applied Thermal Engineering*. 25:557–566. 2005

Greenhouse gas protocol (GHG Protocol), 2014, Global warming potential value, (Accessed 19th February 2020, https://www.ghgprotocol.org/sites/default/files/ghgp/Global-Warming-Potential-Values%20%28Feb%2016%202016%29_1.pdf)

Herbert R M, Mohan L D. Performance variation of an R22 window air conditioner retrofitted with a HFC/HC refrigerant mixture under different ambient conditions over a range of charge quantities. *Heat Trans Asian Research*. 40:246–268. 2011

Hjelle I. A., 2014. When Ammonia becomes toxic, Institute of Basic Medical Sciences (accessed on 10th August 2020, https://www.med.uio.no/imb/english/research/news-and-events/news/2014/when-ammonia-becomes-toxic.html#:~:text=Ammonia%20is%20very%20toxic%20to,to%20remove%20potassium%20is%20perturbed.&text=People%20with%20impaired%20liver%20function,of%20ammonia%20in%20the%20blood)

Houghton, J. T., Ding, Y., Griggs, D. J., Noguer, M., Linden, P. J. V. D., Dai, X., Maskell, K and Johnson, C. A. *Climate Change 2001: The Scientific Basis*. 2001

Hu, X., Zhang, Z., Yao, Y. and Wang, Q., Non-azeotropic refrigerant charge optimization for cold storage unit based on year-round performance evaluation. *Applied Thermal Engineering*, 139, pp.395-401. 2018

Hydrocarbon21, Opportunity seen with higher HC charge limit in U.S. (accessed on 19 October 2020, (https://hydrocarbons21.com/articles/9004/opportunity_seen_with_higher_hc_charge_limit_in_u_s_)

Incropera F. P.,"Introduction to heat transfer."New York, Wiley, 1996.

Intergovernmental Panel on Climate Change (IPCC), Global warming of 1.5ºC, 2018 (Accessed on 3rd May 2020, https://report.ipcc.ch/sr15/pdf/sr15_spm_final.pdf)

IPCC. Intergovernmental Panel on Climate Changes, Radiative Forcing of Climate Change, The 1994 report of the scientific assesment working group of IPCC, summary for policy makers,28 p, 1994.

Jakuboski, S., Baterfly Range shift are a sign of global warming. Green Science, 2012 (Accessed 5th July 2020, https://www.nature.com/scitable/blog/green-science/butterflies/)

Jahn, K., Propane replacing R-22. ASHRAE Journal, 52(4), pp.74-76. 2010

Jain V., Kacchhwaha S. and Mishra R.,'Comparative performance study of vapour compression refrigeration system with R22/R123a/R410A/R407C/M20.' In www.IJEE. IEEFoundation.org. vol 2 (2), pp 297 – 310, 2011.

Jawale, V.S. and Keche, A.J., Experimental performance study of R290 as an alternative to R22 refrigerant in a window air conditioner. In *IOP Conference Series: Materials Science and Engineering* (Vol. 377, No. 1, p. 012046). IOP Publishing. 2018, June

Jierong, L. and Tingxun, L., Detailed dynamic refrigerant migration characteristics in room air-conditioner with R290. *International Journal of Refrigeration*, 88, pp.108-116. 2018

Joo, Y., Kang, H., Ahn, J. H., Lee, M and Kim, Y. Performance characteristics of a simultaneous cooling and heating multi-heat pump at partial load conditions. *International Journal of Refrigeration*, 34(4): 893-901. 2011

Kataoka, Osami. ISO 5149, IEC60335-2-40 Proposed Changes to Incorporate 2L Refrigerants. *ASHRAE Annual Conference*, June 24, 2012.

Kim D. H, Park H. S, Kim M. S. The effect of the refrigerant charge amount on single and cascade cycle heat pump systems. *International Journal of Refrigeration.* 40:254–268. 2014

Kim W. and Braun J. E, Evaluation of the impacts of refrigerant charge on air conditioner and heat pump performance, *Int. J. Refrig*. vol 35, pp 1805–1814. 2012

Li B, Peuker S, Alleyne A, Hrnjak PS. Refrigerant migration modeling during shut-down and start-up cycling transients. *International Refrigeration and Air Conditioning Conference*. Indiana: Purdue; 2010.

Liu, C., Wang, D., Sun, Z., Chen, L., Shi, J. and Chen, J., Effects of charge on the performance of R290 air conditioner with different expansion devices. *Applied Thermal Engineering*, *140*, pp.498-504. 2018

Lu. D and Flavelle. C., Rising Seas Will Erase More Cities by 2050, New Research Shows, 2019. (accessed on 3 November 2020, https://www.nytimes.com/interactive/2019/10/29/climate/coastal-cities-underwater.html)

Ma, Q. and Tipping, R.H., The distribution of density matrices over potential-energy surfaces: Application to the calculation of the far-wing line shapes for CO_2. The Journal of chemical physics, 108(9), pp.3386-3399. 1998

Maclaine-Cross, I.L. and Leonardi, E., Comparative performance of hydrocarbon refrigerants. In Proceedings of IIF-IIR conference (Commissions B2 with B1, E1 and E2), Melbourne, Australia (pp. 1-11). 1996, February

Maclaine-Cross, I.L. and Leonardi, E., 1997. Why hydrocarbons save energy. AIRAH journal, 51, pp.33-38.

Martinez-Ballester S, Bardoulet L, Pisano A, Bordes-Costa JM, Corberán JM. Visualization of the refrigerant flow at the capillary tube inlet of a household refrigeration system. *International Refrigeration and Air Conditioning Conference.* Indiana: Purdue University; 2014.

Martínez-Galván I, Gonzálves-Maciá J, Corberán JM, Royo-Pastor R. Oil type influence on the optimal charge and performance of a propane chiller. *International Journal of Refrigeration.* 34:1000–1007. 2011

Mastrullo R, Mauro A, Menna L, Vanoli G. Replacement of R404A with propane in a light commercial vertical freezer: a parametric study of performances for different system architectures. *Energ Convers Manage.* 82:54–60. 2014

McQuay, Refrigerants, 2013, viewed 7 January 2013 (http://www.mcquay.com/mcquaybiz/literature/lit_ch_wc/AppGuide/AG31-007.pdf)

Fatouh M., Ibrahim T. A. and Mostafa A., Performance assessment of a direct expansion air conditioner working with R407C as an R22 alternative, *Appl. Therm. Eng.* vol 30, pp 127–133. 2010

McLinden M. O., Klein S. A., Lemmon E. W. and Peskin A. P.,"NIST Standard Reference Data Base 23 – Version 6.01, USA, NIST, 1998.

More heating air conditioning, Air conditioning can make you sick: Here's how to avoid it. 2020 (Accessed on 12th July 2020, https://mooreheating.com/air-conditioning-can-make-you-sick-heres-how-to-avoid-it/)

Munson, B. R., Fundamentals of fluid mechanics, 4th ed. Edn, Willey, New York. 2002

National Aeronautics and Space Administration (NASA), What is a Dobson unit? 2018 (Accessed on 19th February 2020, https://ozonewatch.gsfc.nasa.gov/facts/dobson_SH.html)

National Oceanic and Atmospheric Administration (NOAA), Greenhouse gases. 2020 (Accessed on 18th February 2020, https://www.ncdc.noaa.gov/monitoring-references/faq/greenhousegases.php)

National Aeronautics and Space Administration (NOAA), Climate forcing. 2020a (Accessed on 11th March 2020, https://www.climate.gov/maps-data/primer/climate-forcing)

National Geographic, Causes and effects of climate change, 2020, (Accessed on 6th February 2020, http://www.nationalgeographic.com/environment/global-warming/global-warming-effects/)

National Geographic, Carbon dioxide levels are at a record high. Here's what you need to do, 2020, (Accessed on 6th February 2020, http://www.nationalgeographic.com/environment/gglobal-warming/greenhouse-gases/)

Nilpueng K, Supavarasuwat C, Wongwises S. Performance characteristics of HFC-134a and HFC-410A refrigeration system using a short-tube orifice as an expansion device. *Heat Mass Transfer*. 47:1219–1227. 2011

NIST, NIST reference Fluid thermodynamic and transport properties database: Version 6.0 (REFPROP 6.01), NIST. 1998

NIST, NIST reference Fluid thermodynamic and transport properties database: Version 6.0 (REFPROP 6.02), NIST. 2000

Oberthur S. and Ott H. E., *Kyoto Protocol* (Springer, New York, 1997).

Padalkar A. S., Mali KV, Devotta S. Simulated and experimental performance of split packaged air conditioner using refrigerant HC-290 as a substitute for HCFC-22. *Appl Therm Eng.* 2014;62:277–284.

Palmiter L., Kim J. H., Larson B., Francisco P. W., Groll E. A. and Braun J. E., Measured effect of air-flow and refrigerant charge on the seasonal performance of an air-source heat pump using R-410A, *Energy Build.* vol 43, pp 1802–1810. 2011

Padmanabhan, V. M. V and Palanisamy S, K. Exergy efficiency and irreversibility comparison of R22, R134a, R290 and R407C to replace R22 in an air conditioning system. *Journal of Mechanical Science and Technology* 27(3): 917-926. 2013

Park, K. J. & Jung, D., Thermodynamic performance of HCFC22 alternative refrigerants for residential air-conditioning applications, *Energy and Buildings*, vol. 39, no 6, pp. 675-680. 2007

Park K. J., Seo T. and Jung D., "Performance of alternative refrigerants for residential air-conditioning applications," in *Applied Energy*, vol. III (10), pp. 985–991, 2007.

Poggi F., Macchi-Tejeda H., Leducq D and Bontemps A.," Refrigerant charge in refrigerating systems and strategies of charge reduction.' In *International Journal of Refrigeration*, vol 33, pp 353 – 370, 2008.

Pearson, S.F., *Refrigerants past, present and future*. In The International Congress of refrigeration in Washington DC USA.[cited July 22, 2008]. 2003

Ramesha, D. K., Kiran, S. and Kushal, K., An Overview of Propane Based Domestic Refrigeration Systems. *Materials Today: Proceedings*, *5*(1), pp.1599-1606. 2018

Rana Prathap Padappayil and Judith Borger, 2020. Ammonia Toxicity, National Center for Biotechnology Information (Accessed on 10th August 2020, https://www.ncbi.nlm.nih.gov/books/NBK546677/)

Ribeiro, G. B. and Barbosa Jr, J. R., Numerical analysis of R-290/POE ISO 22 condensers based on the second law and SEER rating. *International Journal of Refrigeration*, *88*, pp.441-450. 2018

Rodriguez A. G. *Effect of refrigerant charge, duct leakage, and evaporator air flow on the high temperature performance of air conditioners and heat pumps.* Master's Thesis, Texas A&M University; 1995.

Saravanan, A. L., Lal, D. M. and Selvam, C., Experimental Investigation on the Performance of Condenser for Charge Reduction of HC-290 in a Split Air-Conditioning System. *Heat Transfer Engineering*, 41(17), pp.1499-1511. 2020

Sharifian, A. and Siang, J.T., 2015. Impacts of room temperature on the performance of a portable propane air conditioner. *International Journal of Air-Conditioning and Refrigeration*, *23*(02), p.1550015.

Shen, B. and Fricke, B., Development of high efficiency window air conditioner using propane under limited charge. *Applied Thermal Engineering*, *166*, p.114662. 2020

Siang, J. T. and Sharifian, A., 2013. Reducing the mass of the refrigerant in the capillary tube of a propane air-conditioner. In *Proceedings of the 14th Asian Congress of Fluid Mechanics (14 ACFM)* (Vol. 2, pp. 850-857). Publishing House for Science and Technology.

Storslett, E., Experimental investigation of a heat pump assisted drum drying system using propane (R290) as working fluid (Master's thesis, NTNU). 2018

Tanaka, I. R., Fajar, B., Utomo, T. S. and Yohana, E., Experimental Study Performance R-22 AC Split Retrofitted With Propane. In *MATEC Web of Conferences* (Vol. 159, p. 02021). EDP Sciences. 2018

Tannert, T. and Hesse, U., Noise effects in capillary tubes caused by refrigerant flow. 2016

Teng T. P., Mo H. E., Lin H., Tseng Y. H., Liu R. H. and Long Y. F., Retrofit assessment of window air conditioner, *Applied Thermal Engineering, vol* 32, pp 100–107. 2012

Underwriter Laboratories Inc. (UL), Update — Revisiting Flammable Refrigerants (accessed on 19 October 2020, https://legacy-uploads.ul.com/wp-content/uploads/sites/2/2017/02/UL_WhitePaper_FlammableRefrigerants_final_digital-2.pdf)

UNEP. United Nation Environment Program. Handbook for International treaties for protection of the ozone layers, 6thed. Nairobi, Kenya, 2003.

UNEP Ozone Secretariat. Combating climate change given big confidence boost in Canada, Government agree to accelerated "freeze and phase-out" of ozone and climate damaging chemicals at Montreal Protocol's 20th anniversary celebrations. Canada: Montreal Protocol; 2007

United Nations Industrial Development Organisation (UNIDO), "Preparing for HCFC phased out: Fundamentals of uses, alternatives, implications and funding for article 5 countries, 2009 (Accessed on July 30th 2020, https://www.unido.org/sites/default/files/2009-10/Preparing_for_HCFC_phaseout_0.pdf)

Vaitkus L.,"Low charge transport refrigerator (I). Refrigerant charge and strategies of charge reduction." In *Mechanics*, vol 17 (6), pp 665 – 673, 2012

Welch. C, As the Antarctic Peninsula heats up, the rules of life there are being ripped apart. Alarmed scientists aren't sure what all the change means for the future. National Geographic. 2018 (Accessed on May 16th 2020,

https://www.nationalgeographic.com/magazine/2018/11/antarctica-climate-change-western-peninsula-ice-melt-krill-penguin-leopard-seal/)

West L, The Health Effects of Global Warming, 2019, (accessed on 3 November 2020, http://www.treehugger.com/global-warming-150000-deaths-every-year-1203900)

Wicher, A. Europe's Propane Refrigeration Proliferation. Emerson Climate Technologies. 2017 Available: https://www.emerson.com/documents/commercial-residential/146286.pdf [Accessed 5 January 2017].

Willis K J., Kemp A., Strauss B H, Sea Level Rise, 2018, (Accessed on 16th January 2021, https://ocean.si.edu/through-time/ancient-seas/sea-level-rise)

World Health Organization (WHO), Environmental management of refrigeration equipment. 2015 (Accessed on February 18th 2020, https://public.wmo.int/en/media/press-release/greenhouse-gas-concentrations-atmosphere-reach-yet-another-high)

https://www.who.int/medicines/areas/quality_safety/quality_assurance/supplement_16.pdf?ua=1)

World Meteorological Organization (WMO), Greenhouse gas concentrations in atmosphere reach yet another high, 2019 (Accessed on 19th February 2020,

World Wide Fund for Nature (WWF), 11 Artic Species Affected by Climate Change (Accessed on 5th July 2020, https://www.wwf.org.uk/updates/11-arctic-species-affected-climate-change)

Wuebbles. D, Ozone Depletion, Ensiclopedia Britannica, 2020 (Accessed on 6th July 2020, https://www.britannica.com/science/ozone-depletion/Ozone-layer-recovery

Wu J., Yang L. and Hou J., Experimental performance study of a small wall room air conditioner retrofitted with R290 and R1270, *International Journal of Refrigeration, vol* 35, pp 1860–1868. 2012

Yoon, J. I., Son, C. H., Moon, C. G., Kong, J. Y. and Yoon, J. H., Performance characteristics of portable air conditioner with condensate-water spray. In IOP Conference Series: Materials Science and Engineering (Vol. 675, No. 1, p. 012043). IOP Publishing. 2019, November

Yusof, M. H., Muslim, S. M., Suhaimi, M. F. and Basrawi, M. F., The Effect of Outdoor Temperature on the Performance of a Split-Unit Type Air Conditioner Using R22 Refrigerant. In *MATEC Web of Conferences* (Vol. 225, p. 02012). EDP Sciences. 2018

Zhou, W. and Gan, Z., A potential approach for reducing the R290 charge in air conditioners and heat pumps. *International Journal of Refrigeration*, *101*, pp.47-55. 2019

Zhou G, Zhang Y. Numerical and experimental investigations on the performance of coiled adiabatic capillary tubes. *Applied Thermal Engineering*, vol. 26, no. 11–12, pp. 1106-14. 2006

Zhou, G. and Zhang, Y., Performance of a split-type air conditioner matched with coiled adiabatic capillary tubes using HCFC22 and HC290. *Applied Energy*, 87(5), pp.1522-1528. 2010

APPENDIX

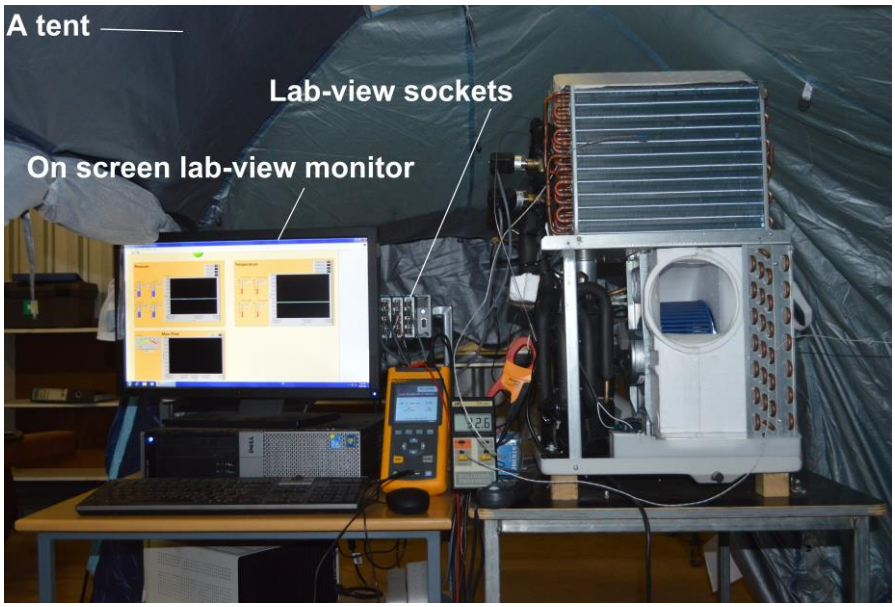

Figure 13 Experimental Setup

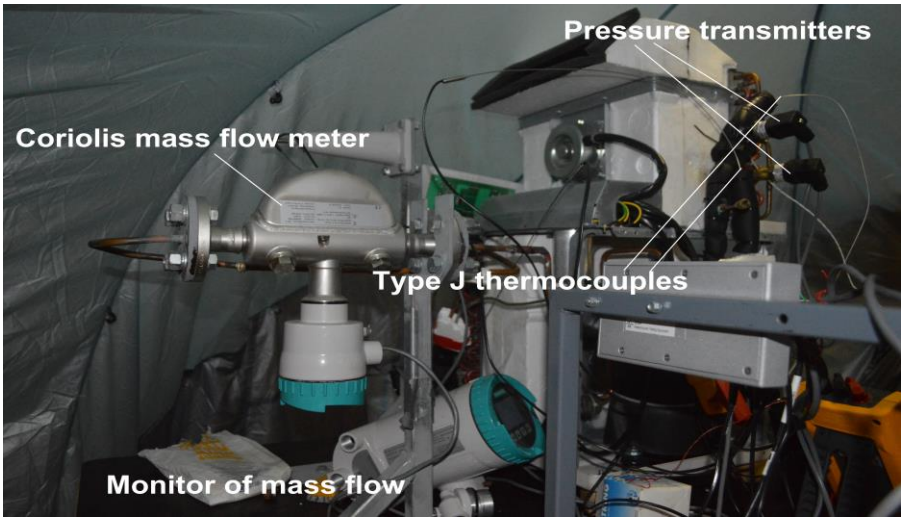

Figure 14 Mass flow meter, thermocouples and pressure transmitters